EVALUATION OF COMBUSTION, PERFORMANCE AND EMISSION OF A DIRECT INJECTION COMPRESSION IGNITION (DICI) ENGINE RUNNING ON A DIESEL-SYNGAS BLEND

JEREMIAH NJERU GATUMU

MASTER OF SCIENCE
(Mechanical Engineering)

JOMO KENYATTA UNIVERSITY OF AGRICULTURE AND TECHNOLOGY

2021

Evaluation of Combustion, Performance and Emission of a Direct Injection Compression Ignition (DICI) Engine Running on a Diesel-Syngas blend

Jeremiah Njeru Gatumu

A Thesis Submitted in Partial Fulfillment of the Requirements of the Degree of Master of Science in Mechanical Engineering of the Jomo Kenyatta University of Agriculture and Technology

2021

DECLARATION

This thesis is my original work and has not been presented for a degree in any other university.

Signature: ..... Date .....

Jeremiah Njeru Gatumu

This thesis has been submitted for examination with our approval as the University Supervisors:

Signature: ..... Date .....

Dr. Eng. Hiram Ndiritu, PhD

JKUAT, Kenya

Signature: ..... Date .....

Dr. Benson Gathitu, PhD

JKUAT, Kenya

DEDICATION

To my family without whose never-failing support and encouragement, this project would not have been completed.

ACKNOWLEDGEMENTS

This project expended a large amount of resources: time, effort and material. Its execution would not have been possible if I did not have the support of many individuals and organizations. Foremost, is my God, Jehovah, who, through His Son, Jesus Christ, graciously gave me the strength, knowledge and understanding required to carry out this project.

Further, I would like to extend my sincere gratitude to my supervisors: Dr. Eng. H. Ndiritu and Dr. B. Gathitu for their guidance and support through their constructive comments and suggestions. In conducting the research work, I received immense technical support and help from Ms. Stellamaris Nzove, JKUAT, who graciously allowed me access to the gasifier she had earlier designed and developed and the staff in the thermodynamic laboratory, JKUAT, Mr. Eric Waiyaki and Mr. Joseph Muigai; they all deserve my greatest gratitude.

The completion of this project would not have been possible without the support of the Technical University of Mombasa, my employer and partial sponsor, and my family members. I would also like to express my sincere gratitude to many others whom I have not mentioned here, but who in one way or the other helped in actualising the project. Our God bless you all mightily.

TABLE OF CONTENTS

LIST OF TABLES

LIST OF FIGURES

LIST OF APPENDICES

LIST OF NOMENCLATURE

Nomenclature

Greek symbols

η	Efficiency
γ	Specific heat ratio
ϕ	Equivalence ratio of air/fuel
ρ	Syngas density
Σ	Total sum
τ	Torque
θ	Crank angle(CA)

Other symbols

a	Crank length
b	Brake
B	Bore diameter
D	Intake valve diameter
G	Number of intake valves per cylinder
m	Mass
n	Mass fraction,
N	Revolutions per minute
p	Pressure
P	Power
Q	Volumetric flowrate
S	Stroke length
T	Temperature
U	Velocity
V	Volume
W	Work per cycle
$\tilde{x}$	Moles fraction
Y	Volume fraction
[ ]	Species concentration in moles per cubic cm

Subscripts

1	Inlet in fluid flow
2	Outlet in fluid flow
b	Brake
f	Fuel
bth	Brake thermal
D	Diesel

s	Syngas
th	Thermal

Abbreviations

ACHE	Air Cooled Heat Exchanger
API	American Petroleum Institute
ASU	Air Separation Unit
BP	Brake Power
BSFC	Brake Specific Fuel Consumption
BTE	Brake Thermal Efficincy
CCS	Carbon Capture and Sequestration.
CI	Compression Ignition
CR	Compression Ratio
CNG	Compressed Natural Gas
DME	Di-methyl Ether
EGR	Exhaust Gas Re-circulation
HC	Hydrocarbons
HHV	Higher Heating Value
ICE	Internal Combustion Engine
ID	Internal Diameter
IGCC	Integrated Gasification Combined Cycle
IMEP	Indicated Mean Effective Pressure
ID	Injection Timing
LHV	Lower Heating Value
MBG	Medium-British thermal unit Gas
MBT	Maximum Brake Torque
MCV	Medium Calorific Value
MFB	Maximum Fuel Burn
NO$_x$	Oxides of Nitrogen
OD	Outer Diameter
PCC	Pulverized Coal Combustion
PM	Particulate Matter
SFC	Specific Fuel Consumption
SVF	Syngas Volume Flowrate
SI	Spark Ignition
SNG	Synthetic Natural Gas
SO$_x$	Oxides of Sulphur
SR	Stoichiometric Ratio
TEMA	Tubular Exchanger Manufacturers Association
THC	Emissions of Total Hydrocarbon

ABSTRACT

The world energy need is primarily met by fossil fuel such as coal and petroleum oil. These are utilised in electricity generation, industrial heating and transportation. However, continued utilisation of fossil fuels such as coal is adversely affected by their depletion and impact on health and the environment. For coal to be a source of clean energy, it need to be gasified to produce syngas which burns with less harmful emission and pollution than solid coal. Studies on syngas from coal and its use as an alternative to petroleum fuels in internal combustion engines are limited. This is possibly due to the reported low power output of engines fuelled by syngas even though it has proved to have high anti-knock property. The present study is therefore an endeavour to provide a solution to this major drawback of dual fuel engines. This research involved study of the performance and emissions parameters of compression ignition engine fuelled by blends of syngas-diesel. Syngas was used as the primary fuel and diesel as the pilot fuel, both applied in varying proportions. Measurement, test and analyses were conducted by varying syngas volume flowrate, compression ratios, the quantity of diesel supplied, ignition timing, engine load and speed. The air intake system of the engine was modified to allow for homogeneous mixing of air and syngas before supplying the mixture to the combustion chamber. Eddy-current dynamometer, engine data acquisition system were used to carry out measurements and the gas analyser to determine emission in the engine exhaust gases. Tests showed that the best results were: brake specific fuel consumption; 0.75 kg/kwh, brake thermal efficiency; 13.05% and emissions of NO_x at 31.8 ppm; CO_2, 0.94% and particulate matter; 4.6%. All realised at the compression ratio of 18, advance injection timing of 27.4° bTDC, at speed of 1500 rpm and syngas volume flowrate of 100%. These results indicate that the fuel consumption improved almost five folds, power output decreased by about 32% and emissions of NO_x, CO_2, particulate matter decreased by 24.3%, 26.5% and 32% respectively and HC emission increased by 31.4% from 58.75% when compared to engine when operated on

single fuel mode of diesel. Overall, the study demonstrated that improvement of performance and reduction of emissions of dual-fuel engines through compression ratios and fuel injection timing adjustments are possible.

CHAPTER ONE
INTRODUCTION

1.1 Background

There exist a direct correlation between energy use and the quality of life and national wealth as measured by Gross Domestic Product. Many countries world over, Kenya included, have increasingly become dependent on imported oil during the last decades. This dependency hurts the Kenya economy and adds about five million U.S dollars per year to country's trade deficit, according to the treasury economic report (Rotich and Muia, 2018; Rotich and Thugge, 2018). Additionally, because of political instability in some of the oil-producing countries, and increasing demand from other developing countries, considerable uncertainty exists for the future supply and price of imported oil.

With the vast natural resources of coal recently discovered in Mui basin, Kitui county and fossil oil in northern regions and remarkable work of installing renewable energy facilities is sustained, Kenya has the potential to become energy independent in one to two decades (Owiro et al., 2015). That would mean, the recent surge in renewable power generation such as geothermal, wind, solar, hydro and nuclear power further strengthens these expectations. In order, to exploit each of the aforementioned energy sources, certain inherent challenges will have to be surmounted. The installation cost of hydro, wind and geothermal projects is very high with solar, hydro and wind requiring huge parcels of land for construction of dam and farms, respectively. In the case of nuclear energy, which had been predicted to provide a third of electric power by 2050, to date, there have been three major accidents at commercial nuclear power plants: Three Mile Island in 1979, Chernobyl in 1986 and Fukushima in March 2011 (Giraldo et al., 2012). The consequences of these accidents and the major challenges posed by nuclear waste disposal have only reaffirmed the long-held uncertainties in nuclear

power as a solution to global energy supply problems.

In the last two decades, there has been focused attention on whether fuel for power production, transportation and feedstock for the chemical industry could be obtained from the gasification of coal. This has assumed greater urgency given challenges associated with renewable energy and the considerable increase in the price of crude oil and natural gas over the past decade. Crude oil prices have quadrupled, which also include concerns about the security of their supply (Fo et al., 2009; Roberts, 2013). Coal has been mined and used as a source of energy for centuries and now accounts for 27% of the world's energy supplies (Alam et al., 2013). The electrical power industry remains significantly coal-based, generating 35% of the world's total electricity production (Shadle et al., 2010). World War II led to the shortage of gasoline and as a result development of syngas-fuelled vehicles expanded all over the world. This saw the production of more than a million such vehicles (Hagos et al., 2014b). Its use is projected to increase by 80% by 2030 (Asaro and Smith, 2013). However, of the three main fossil fuels (coal, fuel oil and natural gas), coal is the most polluting fossil fuel, producing about 1.5 - 2.5 times more than the proposed standard of 450 gm/kWh for CO_2 emissions. A chart showing CO_2 emissions from different fuels is given in Figure 1.1 (Quaschning, 2019). The chart indicate that hard, which is coal in solid form, produces 0.34 kg of CO_2/kWh when natural gas that produces 0.2 kg of CO_2/kWh produces, 70% less CO_2 emission. There this demonstrate the need to devise ways of utilising coal in gaseous form, so as to reduce the uncontrolled release of $CO_2$to the atmosphere (Alvarez-Rodriguez et al., 2012).

1.2 Syngas as an Alternative Fuel for Internal Combustion Engines

The United Nations Committee on Climate Change (UNCCC) set recommendations on the use of coal as a source of energy while mitigating the climate change it is likely to cause. One of the recommendations is to replace most conventional

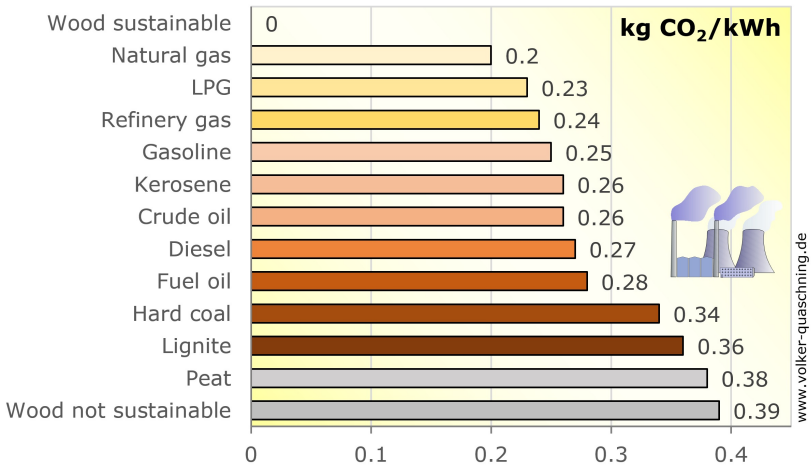

Figure 1.1: CO_2 emission over the life cycle of alternative-fuel production (Quaschning, 2019)

internal combustion engines with syngas or natural gas in direct-fuelled spark ignition (SI) and compression ignition (CI) engines. It is required that these engines use liquid fuels such as methanol and Di-methyl Ether (DME) produced from syngas as the feed-stock (Fallis, 2013). Another requirement is that oil usage should decrease to below 50% of the current production by 2050 to control CO_2 emissions (Roberts, 2013). Besides, conventional coal-fired power generating plants will need to be phased out of service by 2020. From this time onwards, all new fossil fuel (coal and natural gas) plants shall need carbon capture and sequestration capability and older coal-fired plants will need to be retrofitted.

To achieve the foregoing requirement, there will be a need to gasify coal as is now done in the gasifier plant. The performance and costs of coal gasification plants depend largely on the plant design and the final production objectives (Fermoso et al., 2009). A gasification system that is part of an integrated chemical plant producing methanol, ammonia and electricity differs design, complexity and operation requirements from a system whose only purpose is feeding an integrated gasification combined cycle (IGCC) and carbon capture and storage (CCS) facility. Although coal quality is also very important for coal gasification output, syngas with required quality deficiency may be upgraded further to meet specific

demands. The syngas could be converted into synthetic natural gas (SNG) but with the capital cost increased by approximately 25% and the cost of the final product increasing by 40% (Blesl and Bruchof, 2010; Fermoso et al., 2010).

Depending on the type of gasifier and the operating conditions, gasification can be used to produce a fuel gas suitable for any number of applications. A low heating value fuel gas is produced from an air-blown gasifier for use as an industrial fuel and power production. A medium heating value fuel gas is produced from enriched oxygen blown gasification for use as synthesis gas in the production of chemicals such as ammonia, methanol, and transportation fuels. A high heating value gas can be produced from shifting the medium heating value product gas over catalysts to produce a substitute or synthetic natural gas (SNG) that can be used in internal combustion engines (ICEs) (Shadle et al., 2010).

Much of the research currently available in the field of syngas utilization focuses on its use as a direct fuel in IGCC and in production of fuel and chemicals, where syngas is used as an intermediate product (Hagos et al., 2014b). However, internal combustion engine (ICE) is the most important technological equipment, playing a major role in the distributed energy power generation for a variable power output requirement. It has a very flexible application in moving and stationary machinery (Fallis, 2013). Compared to the turbine, power plant or even nuclear fission technologies, ICEs have benefits like low capital cost, reliability, good part-load performance, high operating efficiency, and modularity and are quite safe to use. In this regard, utilization of syngas in engines has very high unexploited commercial benefits and emissions-reduction potential; yet research in which the actual syngas obtained from various methods of reforming and gasification, is used as the second fuel is limited (Hagos et al., 2014b; Kousheshi et al., 2020).

There have been relatively few improvements in gasifier design in the last decade and possibly, due to this, the constituent of syngas that comes from gasification lacks consistency. On power generation application, the data on the existing coal-based IGCC plant show that they have not been able to achieve 85% oper-

ational availability [uptime/(uptime + downtime)] sustainably as was observed in a Ph.D thesis by De Souza-Santos (Fernando, 2014). Researchers have observed that these operational problems are not all caused by the gasifier itself but are frequently related to the more conventional plant. Nevertheless, studies have shown that the gasifier as a significant source of operational challenges such as frequent breakdown and high maintenance requirements. For syngas to be a viable alternative fuel in power generation plants and transportation industry, particularly in ICEs, gasifiers will require greater fuel flexibility and operational availability of more than 0.8, high throughput and fuel conversion of above 64% (Pradhan et al., 2015). They will also need to integrate with gas clean-up and CCS (carbon capture and storage) equipment (Fernando, 2014).

1.3 Problem Statement

The traditional sources of energy such as petroleum oil, nuclear energy and renewable energy are experiencing problems of dwindling supply for petroleum, nuclear accidents coupled with the complexity of waste disposal and large capital cost, land and material resources required in the case of renewable energy (Fallis, 2013; Giraldo et al., 2012; Roberts, 2013). This has given renewed impetus to the use of coal although the stringent environmental regulations now in place make it mandatory that its use is under clean coal technology. Part of this technology is research and development of synthesis gas production and purification in end-use systems (Alam et al., 2013).

Coal remains the second-largest energy source worldwide and its use rises at an average rate of 1.3% per year (Fallis, 2013). When coal is burnt in excess air, carbon will oxidise to carbon dioxide, a gas with greenhouse gas (GHG) which causes global warming (Alam et al., 2013). The other problem being the emission of acid gases such as NO_x, SO_2, particulate matter and contamination that cause air pollution and contamination of water supplies (rivers, lakes and aquifers) (Blesl and Bruchof, 2010).

Application of coal in the solid-state in mobile plants and vehicles, which mainly

use ICEs as their power generators, has proved to be difficult and even impracticable. The main reasons for this include; its handling and storage, excessive wear on surfaces coming into contact with its ash and the problem of emissions' (such as NO_x) control due to the large amount of nitrogen in the coal. This means ICEs operating on alternative gaseous fuels need to be developed (Patton et al., 2010; Pradhan et al., 2015).

Road transport is today strongly dependent on ICEs, which use liquid fossils fuels for their energy supply. Combustion of these fuels contributes 20 - 25% share of the overall CO_2 emissions in industrialized countries. One way of reducing emissions associated with fuel use is to improve their conversion efficiency (Fallis, 2013). Studies have shown that combustible gas mixture can be utilized for power generation with such devices as gas engines with relatively higher conversion efficiency. However, there is a need for modification of the conventional ICEs to improve their energy efficiency and have them fuelled by an alternative, low CO_2 energy carriers (Sansaniwal et al., 2017).

1.4 Objectives

The main objective of this research was to modify and evaluate the performance and emissions characteristics of a compression ignition (CI) engine that utilises syngas produced from an existing small scale coal gasifier as the primary fuel.

The above main objective was achieved via the following specific objectives:

1. To modify the compression ignition engine for it to run sustainably on blend of syngas-diesel.

2. To test the influence of engine parameters on performance, combustion and emissions of a compression ignition engine while running on diesel-syngas blend in comparison to neat diesel.

3. To test the necessary conditions in the engine for the syngas from the gasifier to be sustainably used a dual-fuel CI engine.

1.5 Justification

From the review of earlier studies, it becomes clear that petroleum, natural gas, and coal are the three largest sources of primary energy consumption globally. Renewable energy is important but forms small part (about 6.69%) of the energy flow, although they have the potential to grow (Leahy et al., 2013). However, the two main problems with fossil fuels is pollution, which causes serious environmental degradation and and the danger of depletion in not too not distant future. Therefore, there is need to develop means of utilising these fuels in a way that eliminates or reduces undesirable emissions. Research and technology development on syngas production and purification and fuel processing for fuel cells have great potential in addressing major challenges in the coal energy area. Some gas engines fuelled with syngas have been developed recently. Most of them have a spark-ignition (SI) combustion system. Syngas-diesel blends are now sustainably used in CI engines in dual-fuel mode. This syngas is mostly obtained from an Integrated Gasification Combined Cycle (IGCC), with the centre-piece of the system being the gasifier unit. The unit converts coal or other carbonaceous materials such as biomass into synthetic gas (mainly, a mixture of CO and H_2). There is need to study the composition of syngas produced in small-scale gasifier and the purification necessary to remove unwanted gaseous compounds considering the gasification operating conditions, for it to be supplied to the mixing unit and into combustion chambers of ICEs. Another problem associated with usage of syngas in ICEs is its high auto-ignition temperature. Consequently, it cannot be used in CI engines without a means of initiating combustion, as the temperature attained at the end of the compression stroke is below the flash point for the mixture to be auto-ignited. There is need therefore to perform experiments with syngas to determine engine performance and exhaust emissions in dual-fuel engines and study modifications required to make syngas suitable for use in CI engines under all load conditions.

1.6 Organization of the Thesis

The thesis is divided into five chapters in which the present chapter presents a compressive review of the existing problem related to ever-increasing prices of petroleum-based fuels and the uncertainty of their continued availability. It also discusses the objectionable high levels of emissions from ICE using traditional fuels and the need for alternative fuels for the engines. Chapter 2 examines concepts, theories and inconsistencies of various research studies in the field of alternative fuels for IC engines, specifically the use of syngas as the primary fuel in ICEs. Findings of other researchers and the gaps in their works have been identified and are included in the review.

Chapter 3 outlines the experimental set-up and the procedures involved in the modification of the diesel engine into a dual-fuel engine that uses syngas as the primary fuel and diesel as the pilot fuels. It also presents the parameters measured to establish the performance and emissions characteristics of the modified CI engine. These are torque, load, in-cylinder pressure, engine speed, fuel consumption and emissions. In chapter 4, the empirical results obtained from engine performance tests and emissions analysis from the modified dual-fuel engine are presented and discussed. Chapter 5 presents the conclusions derived from the research study and the necessary recommendations for improving and furthering work in the use of syngas in CI engines.

CHAPTER TWO
LITERATURE REVIEW

2.1 Overview

Review of research woks on coal, reveal coal has readily available energy that is easily harnessed for power generation by burning it in boilers or gasifying to be used gas turbines or engines. Coal in its solid state is widely used to fire boilers but is only applicable in gas turbines and engines after gasification. Gasification is also the means by which coal utilised as a fuel in plants with reduced pollution. The use of coal leads to considerable emissions of greenhouses gases and SO_2 that in turn cause adverse climate changes,air pollution and contamination of water resources. This chapter presents a review of research and development work already carried out by different researchers on coal gasification and utilisation of the product of gasification in power generation for ICEs. The major challenges encountered in the use of syngas in CI engines compared to the conventional liquid, petroleum-based fuels are reviewed and presented. Besides, the gaps left in these works are identified and what was addressed in the present research is discussed.

2.2 Coal Gasification

Coal gasification is the process of reacting coal with oxygen, steam, or air to form a product gas containing hydrogen and carbon monoxide (Eq. 2.1) (Bellman et al., 2007).

$$\begin{aligned} Coal(C_aH_bO_cN_d) \overset{Oxygen/Steam/Air}{\rightarrow} & H_2 + CO + CO_2 + H_2O \\ & + C_xH_yO_z + NH_3 + N_2 \\ & (syngas) \end{aligned} \tag{2.1}$$

Gasification is essentially incomplete combustion as defined by Shadle et al. (2010). Blesl and Bruchof (2010) described the gasification reactor to be the process point where the feedstock (coal or biomass) is transformed into synthesis gas (syngas). Going on to explain syngas being a mixture of H_2, CO and CO_2, and as downstream energy carriers. Further, the researchers observed that the gas may be used as a fuel in integrated gasification combined cycles (IGCC), or as a feedstock for producing H_2 or synthetic natural gas (SNG). The study omitted altogether to discuss the use of syngas as an alternative fuel for ICEs.

Several studies have discussed the use of syngas as an alternative fuel for ICEs. The raw syngas produced in gasifiers cannot be directly used in IC engines. It contains many impurities that are likely to clog syngas supply pipes, filters, air-lines and manifolds; foul and corrode heat exchangers and mixing chamber, cause undesirable deposits in the combustion chamber and choke pistons. The gas conditioning through cooling and filtration is necessary before use in an engine. Studies have shown that syngas has very high auto-ignition temperature (above 500°) beyond the allowable operating temperature range of CI engines. Therefore, syngas is only used in CI engines in dual fuel mode where pilot fuel is injected in the combustion chamber during the compression stroke to initiate combustion. In spark ignition (SI) engines, syngas was shown to work in single fuel mode, albeit with power de-ration of 40 - 50%, mainly due to its low energy density compared to petrol (Pradhan et al., 2015). Many researchers have shown that, overall, CI and SI engines require very modification only of fuel and air inlet systems to run on syngas fuel. Both will require pre-mixing of syngas and air charge before the introduction of the mixture to the combustion chamber. Other modifications pointed out by many studies show that adjustment of compression ratio (CR) and fuel injection timing (IT) is necessary to optimise engine performance and emission characteristics.

Fo et al. (2009) stated that the gasification of coal provides syngas, which is converted to a range of hydrocarbons. Alternatively, the syngas can be converted to liquid speciality or commodity chemicals including methanol or dimethyl ether

(DME), either or both of which also can be used as automotive fuels. While recognising that methanol can be used alone, or preferably as a blend with conventional gasoline, in the SI engine (but not in a diesel engine) because methanol cetane number is too low, the study did not examine the possibilities of direct use of syngas as fuel for ICEs.

Asaro and Smith (2013) investigated emissions from the coal gasification process by focusing on coal used in conventional pulverised combustion plants. The study found that these plants release large amounts of pollutants such as CO_2, acidic gases such as SO_2 and NO_x and dust to atmospheric air. Furthermore, during combustion, carbon oxidises to carbon dioxide, a gas with adverse greenhouse gas (GHG) effects. This study was limited in scope, as it did not point out what should be done in these plants to arrest the objectionable emissions.

Fallis (2013) when discussing future transport fuels, pointed out that coal in solid-state is not used in ICEs due to the problem of handling the fuel as well as in disposing-off the solid residue or ash (after combustion). Further, there are storage and feeding problems associated with solid fuels as compared to gaseous and liquid fuels. In conclusion, the study observed that solid fuels find little practical application today. The present study has not made attempt to study the use of solid coal in ICEs, however, it is observed that coal continue to be applied in solid state, particularly in pulverised coal combustion (PCC) plants for electrical power generation in the developed world and are still causing climatic degradation.

Hagos et al. (2013) studied factors that affect gasification. An investigation was done on particle size, gas and feedstock flow rate, chemical reactor configuration, operating conditions for the gasification process, gasifying agent and catalyst, and gas residence time. First, by using a typical air blown gasification of a solid fuel process. The syngas obtained had a composition of H_2, CO, CH_4 and an insignificant amount of heavy hydrocarbon all amounting to around 50% of the total volume. The rest comprised 50% non-combustible gases, namely N_2 and

CO_2. This gas had a Lower Heating Value (LHV) in the range of 4 - 6 MJ/m^3, identifying it to be a low calorific value gas. When oxygen or steam was used instead of air, the amount of inert gases in the syngas was insignificant and the gas had LHV of 10 - 13 MJ/m^3 and was classified as a Medium Calorific Value (MCV) gas. The study however did not explore ways of conditioning the gas to make it applicable in different conditions and systems.

2.3 Syngas Application in IC Engines

Syngas is used in ICEs either by burning it directly, to produce methanol and hydrogen fuels or by converting it through the Fischer-Tropsch process, into synthetic fuel (Laurence and Ashenafi, 2012). A number of researchers (Baratieri et al., 2009; Laurence and Ashenafi, 2012; Mahgoub et al., 2017) have identified three main requirements or challenges in the use of syngas as an alternative fuel for ICEs. These are: syngas method of supply into the engine, reduced engine power output and the relatively increased end-gas temperature and pressure.The present designed a syngas supplied that cleaned and cooled to improve its energy density.

2.3.1 Syngas Application Requirements

Laurence and Ashenafi (2012) studied the methods of cleaning the raw syngas for use in ICEs. In the study, syngas was cleaned through the removal of the tarry product, ash and corrosive gaseous compounds through a filter, as the main requirement for its use in the internal combustion engine. The effect of particulate matters such as tar and ash on engine performance, emissions, components operation and reliability were examined. In the study, it was observed that the condensible phase of tar caused fouling in the piping system and heat exchangers, leading to the conclusion that it had the potential to cause problems if the synthesis gas was to be compressed. In addition, the gas clean up varied with the composition of the syngas and the gas flowrate. In turn, flowrate depended on gasifier size, the gas requirement for use in IC engine and economic considerations. Further, observing that the effect of impurities lowered the thermal efficiency of

the engine and increased particulate matters (PM) in the engine emissions. The research was limited to the study of producer gas from biomass, which tends to have high contents of tar and fly ash than medium calorific value syngas from high-grade coal. The present study used medium-grade coal that allowed for me MCV coal with lesser impurities.

2.3.2 Reduced Engine Power Output

Some studies have identified power de-rating, resulting from the substitution of conventional fuels, now used in ICEs, with syngas as one of the disadvantages that have to be overcome, if dual fuel CI and SI engines using syngas fuel are to gain currency.

Monteiro et al. (2012) investigated the of reduced power output and high-temperature end-gas in the problems in engines fuelled with syngas blends. In the study, a diesel engine was converted into SI mode to be used in gaseous fuel operation. Besides, syngas with a high composition of CO and CH_4 was used due to its high anti-knock property. The high temperatures, produced by fast flame propagation rate of H_2 during combustion, was countered by including N_2 and CO_2, which act as diluents in fuels. The findings include an increase in NO_x emissions but with reduced power output. In countering the drawback of power de-rating, it was demonstrated that this could partially be balanced by turbocharging and using syngas with high calorific value (HCV). Here, the study was more concerned with the inherent composition of fuel to balance the disadvantages of high flame propagation. The attempted to solve the problem by using gas with HCV and mixing it well with air to form a leaner air-fuel mixture. Such syngas will compensate for power loss without resorting to the more complicated turbocharging system.

The prospect of syngas as fuel for ICE is believed to be very promising and cost-competitive when compared with natural gas. Synthetic gases have significant potential for the effective utilization of low-energy gases in co-generation units (Chrıbik et al., 2012). ICE is more tolerant of contaminants as compared to gas turbines. Even though they are not significant in number like in the area of

integrated gasification combined cycle (IGCC), there are some research studies in the area of syngas utilization in ICEs.

Hagos et al. (2014b) researched syngas use in ICE and categorized engines into spark-ignition (SI) application specifically in the naturally aspirated carburettor, port injection type and dual-fuel compression ignition (CI) engines. In carburreted and port injection engines, the fuel and air were mixed before entry to the combustion chamber. The observation made was that the SI engine had higher pumping and heat losses as compared to direct ignition spark ignition (DISI) engines, resulting in high fuel consumption. The conclusion was to the effect that, a consequence of dual fuelling with syngas was, lowering of the theoretical power output of dual-fuel compression ignition compared to those of diesel and CNG. An extended literature survey, indicates limited study for DISI engines fuelled with coal syngas. Consequently, the present study is directed towards a DISI engine fuelled by syngas obtained with gasifying coal in a small scale locally made gasifier.

2.3.3 Increased End-gas Temperature and Pressure

Several studies have shown that there is a considerable increase of combustion chamber average temperatures where syngas has been used to substitute a proportion of diesel or replace all together petrol in ICEs. Similar studies have also shown that the engine efficiency is directly proportional to the combustion pressure generated during the power stroke. In addition, cylinder pressure (CP) also influences the formation of NO_x emission in the exhaust of an engine.

Raman and Ram (2013) studied the effect of high cylinder pressure and temperature on engine performance. A down draft type gasifier was used to supply producer gas to an engine designed to run on natural gas. The engine performance was evaluated at full load and part load operating conditions at the compression ratio (CR) of 17. The research reported that if high in-cylinder pressures and temperatures developed, it resulted in high efficiency, high specific fuel consumption and high formation of NO_x. Besides, high-pressure rise per degree of crank angle

produced audible knocking sound, a phenomenon identified as 'diesel knock'. The limitation of this study was that it applied producer gas of lower heating value (LHV) of 5.6 MJ/kg as opposed to the syngas used in the present study which had LHV of 10.462 MJ/kg. This high heating value syngas allowed for better-controlled combustion of syngas-diesel-air mixture and adjustment of CR and fuel injection timing (IT) leading to low in-cylinder pressure and temperature.

2.4 Syngas Influence on the Engine Performance and Emissions

Several researchers have investigated the effect of engine load, CR, injection timing and syngas composition on combustion, performance and emissions characteristics of dual-fuel compression ignition (CI) engine using syngas has. In general, the operation of a CI engine with syngas leads to reduced engine power because syngas has a lower heating value compared to diesel (Azimov et al., 2012). However, dual fuel operation is considered a promising way to control the emissions of nitrogen oxides from CI engines. Whereas studies have also shown that dual fuelling with syngas positively affects emissions of carbon dioxide, results report a substantial increase in emissions of carbon monoxide and total hydrocarbons compared to what is observed in neat diesel combustion.

2.4.1 Compression Ratio

Compression ratio (CR) is defined as the ratio of cylinder volume measured from bottom dead centre (BDC) to top dead centre (TDC) at the deck (top cylinder head gasket mating surface) to the combustion chamber volume measured when the piston is at TDC, taking into account the thickness of the cylinder head gasket.

Lal and Mohapatra (2017) studied the effect of CR on the performance, emission characteristics and noise level on a dual-fuelled CI engine. In the study, a single-cylinder, water-cooled, constant speed, 4-stroke, variable compression ratio diesel engine (VCR) was tested with blends of syngas-diesel and neat diesel, in

turns. Performance and emissions data were obtained at varying CRs of 12, 14, 16, 18. The findings on the maximum diesel saving attained were: 8.7%, 31.82%, 57.14% and 64.3% at a compression ratio of 12, 14, 16 and 18 respectively. The reported average reduction of 63.62% in HC emission (from 1555 to 954 ppm) was achieved by increasing the compression ratio from 12 to 18 and that NO_x emission was reduced (in the range of 35.29–56.09% from about 45 ppm for different conditions) as compared to diesel fuel mode. Further, the SO_x emission levels were upto 45.45%, less (from about 7.8 ppm) in the dual-fuel mode. This study did not investigate the effect of advancing or retarding ignition timing for each CR adjudstment of the engine, which has been identified elsewhere and the present study as one parameter with a profound influence on the performance and emissions characteristics of dual fuel mode engine. Another limitation, which the present study has addressed, is the use of only one fraction of diesel replacement.

2.4.2 Syngas Composition

Syngas consists of about 40% combustible gases, mainly carbon monoxide (CO), hydrogen (H_2) and methane (CH_4). The rest are non-combustible gases and consists mainly of nitrogen (N_2) and carbon dioxide (CO_2). Varying proportions of H_2O, N_2, CH_4 and insignificant proportions of sulphur compounds may be present. H_2, as the main component of syngas has very clean burning characteristics, a high flame propagation speed and wide flammability limits (Bellman et al., 2007; Mahgoub et al., 2015c; Stellamaris N. Nzove, 2021).

Azimov et al. (2011) studied the effect of the presence of H_2, CO_2, O_2 and CO in syngas on the performance and emission of the CI engine. This study used a water-cooled, four-stroke, single-cylinder engine using premixed mixture ignition in the end-gas region (PREMIER) combustion, with two intake valves and two exhaust valves. The combustion was initiated via auto-ignition of a small quantity of diesel pilot fuel, injected into the combustion chamber before top dead centre (bTDC). Eight types of syngas, each with different compositions of H_2 and N_2, a few with different composition of CO_2, CO and CH_4 were used. In each

case, engine performance and emissions were measured. The findings obtained indicate that the increase in H_2 content in the combustion of syngas fuel provides a reduction of combustion duration and as a result, an increase in the efficiency of internal combustion (IC) engines. When the level of air in the mixture was varied, it was observed that the lean mixture combustion resulted in low and even extremely low NO_x levels with only a slight increase in unburned hydrocarbons. The mean combustion temperature, indicated mean effective pressure (IMEP), the indicated thermal efficiency and the NO_x showed an increase when CO_2 content in the gas was increased from 16.8% to 23%. However, as CO_2 concentration reached 34%, the combustion characteristics decreased. Further, results obtained showed that the presence of carbon monoxide in a mixture of syngas fuel is very important as it facilitates the mixture reactivity. The investigation however did not study the effect of blending syngas with different proportions of diesel, on the performance and emissions parameters.

Monteiro et al. (2011) investigated the performance of a diesel engine fuelled with producer gas and diesel while changing the H_2 content and keeping the CO content constant. The experiments were conducted in a rapid compression machine (RCM) to visualise combustion characteristics inside the combustion chamber. Five experiments for each syngas-diesel mixture and ignition timing were performed. Data for cylinder pressure was measured using a piezoelectric sensor coupled with an amplifier. The study noted that when the producer gas contained 20% H_2, a greater thermal efficiency, of up to 38% was achieved with a wider range of fuel-air equivalence ratio in the range of 0.42 to 0.79. However, for engine operation with lower H_2 content of 13.7% content in syngas, a similar grade of thermal efficiency was achieved with a narrower range of equivalence ratio from 0.52 to 0.68. The investigation did not study the behaviour of an engine fuelled by blends of diesel with varying volumes of syngas.

2.4.3 Engine Load

Engine load is the resistance torque subjected to an engine by the driven member and works to reduce the engine speed. For the present study, the load was from an eddy current dynamometer which has facilities to vary it. However, in practice, for instance in power generation plants, load is provided by an alternator. In the case of a mobile transport equipment, drive parts, the cabin plus the load carried in it and total resistance provide the load.

Sahoo et al. (2012) investigated the engine performance, combustion and emission characteristics of a diesel engine using syngas under dual fuel mode without varying any of the existing engine design and operating parameters. A constant-speed, water-cooled, four-stroke, single-cylinder, direct injection, compression-ignition engine was operated at varying engine loads of 0%, 20%, 40%, 60%, 80% and 100%. For each load, syngas of varying H_2/CO ratio was supplied to the engine, at the same time manually controlling diesel flowrate by adjusting diesel fuel cut-off valve. Thermal efficiency, specific fuel consumption, emissions of NO_x, HC and exhaust gas temperature (EGT) were measured for each experiment. The research reported that at part-loads, there was a slight improvement in thermal efficiency. However, the thermal efficiency at the dual-fuel operation was enhanced over half-load. At the minimal load situations, the temperature of the cylinder and its force declined because of delayed combustion and ineffective oxidation of the syngas fuel. The volumetric efficiency decreased for dual fuel mode at all loads. An increase in NO_x concentration was noticed when the engine was loaded to a higher level due to the increase in-cylinder temperature and pressure. At low loads, more incomplete combustion was noticed when using syngas with air, which resulted in the emissions of HC at a higher level. The HC emissions started to increase significantly again when over 80% load was applied because the mixture of air and syngas became rich leading to incomplete combustion, thereby diminishing the availability of air. This study, though comprehensively investigated performance and emission parameters, it only considered the effect

of load adjustments, disregarding the effects of advancing of injection timing and varying of CR on the same parameters. The study should also have considered the effect of varying blends of syngas and diesel fuel on different loads. For instance, investigate what would be the effect on NO_x emissions of varying CR and engine speed. The present study seek to fill these gaps.

2.4.4 Injection Timing

Fuel injection timing (IT) is a setting made on an engine to determine the crank angle (CA), measured before top dead centre (bTDC), when fuel is injected into the cylinder and therefore, when the combustion takes place. The time when fuel is injected can be altered by adjusting IT. The timing is fixed by the manufacturer of an engine and is done when the engine is first made. IT adjustment is usually set at the point where power output is a maximum while remaining within legal limits for emissions. Timing can be advanced (increasing CA before TDC) to generate more power or sometimes, adjusted in the opposite direction to reduce smoking or a lag problem.

Hagos et al. (2016) studied the effect of IT on combustion, performance and emissions for a syngas-fuelled (with H_2/CO composition only) engine. The study was conducted using a four-stroke, single-cylinder, DISI research engine with a compression ratio of 14:1. By varying the Crank Angle (CA) measured bTDC, the engine was operated at full throttle, at minimum advance to achieve maximum brake torque with the engine speed ranging from 1500 to 2400 rpm. Two different start of injections (SOI) were selected (120° and 180°) to represent before and after inlet valve closing and the excess air ratio was set at 2.3. Findings recorded indicated that the best engine combustion and performance were at start of injection of 120° bTDC at a speed of 2100 rpm. At engine speeds higher than 2100 rpm, the start of injection of 180° bTDC attained better combustion and performance. The emissions of CO, NO_x and total hydrocarbon (THC) were observed to be lower with the SOI = 180 ° bTDC; the difference being more pronounced with an increase in engine speed. The study assumed that mixing was

complete owing to the large CA after fuel injection. This may not be the case as the present study has shown that retarding the IT had negative effect on the engine performance and emissions. Further, investigation have shown applying different blends of syngas-diesel and varying the CR of the engine could improve its performance and emissions..

2.4.5 Emissions and its Control

Guo et al. (2016) investigated the combustion and emissions performance of syngas-diesel dual-fuel engines at low and medium loads. In the study, a single-cylinder, direct injection diesel engine was modified to operate using a dual fuel strategy. The diesel fuel was directly injected to the cylinder, while syngas was injected into the intake port and mixed with air. The effects of syngas flowrates and composition on energy efficiency, cylinder pressure, exhaust temperature, and combustion stability were recorded. The emissions data, including PM, NO_x, CO, and unburned hydrocarbon were also measured. The study reported that substitution of diesel fuel by syngas caused an increase in CO emissions at a low and medium load conditions with no significant effect on CO emissions when syngas proportion was increased. In addition, the substitution of diesel with syngas generally caused a decrease in NO_x emissions. This study did not look into what happens to the emissions in the exhaust gases when the engine was subjected to higher loads and speeds. Neither did the study address the effect of the higher temperature in the combustion chamber of engine that followed the supply of hot syngas in the cylinder, on its performance and emission.

Wagemakers and Leermakers (2012) reviewed works on emissions of particulate matter (PM), referred to as soot or smoke, from a dual fuel CI engine using different gaseous fuels namely: natural gas, liquefied petroleum gas (LPG), hydrogen and syngas. In noting the very limited research done on the effects of syngas-diesel blend in dual-fuel engine operations on PM emissions, compared to dual-fuel operations with the other gaseous fuels, the study observed that there is marked increase of emissions at high diesel substitution rates and at high loads.

The present research was therefore done to confirm the observation.

2.5 Conditioning of Syngas for Use in ICE

The combustible gases from the gasifier can be used in ICEs, for direct heat applications. However, to use this gas, it should not contain impurities such as tar and dust. In addition, it must be cooled to almost room temperature before its introduction in the cylinder. Cleaning of the gas is very critical and normally three types of filters are available for use in the process. They are classified as dry, moist and wet (Homdoung et al., 2007).

Pradhan et al. (2015) observed that the cooling and cleaning of the gas is one of the most important processes in the whole gasification system. The failure or the success of syngas fuelled units depends completely on their ability to provide a clean and cool gas to the engines or for burners. Noting that, since the temperature of gas coming out of the generator is normally between 200 - 1500 °C, to raise its energy density, the gas had to be cooled first. In the present study, a gas-to-air heat exchanger was used as the cooler. Here, Cooling is effected by passing free convection of air on the outside surface of the heat exchanger. Since the gas also contained moisture and tar, partial scrubbing of gas was provided on the heat exchanger. Ideally, the gas going to an internal combustion engine should be cooled to nearly ambient temperature (Asaro and Smith, 2013).

2.6 Syngas Utilisation in Dual Fuel CI Engines.

Many types research in the use of syngas in IC engines agree that syngas can only be used as fuel in diesel engines in the dual fuel mode where diesel fuel is used as the pilot fuel and syngas as the primary fuel. In such an application, syngas is introduced through the engine air intake system to provide the bulk of the fuel charge.

Bates and Dölle (2017) reviewed the work of a study where Reed and Das (1988) used a slow speed, single-cylinder, direct injection diesel engine to study the performance and emissions of a CI engine in dual fuel mode. The engine was operated

on syngas-diesel blend with the syngas mixed with the intake air stream. A small quantity of diesel fuel was introduced continuously through regular injectors to ignite the gas mixture and provide injection timing. The engine performance was improved by supercharging it. Experiments were conducted to measure performance and exhaust emissions of the engine. The study showed that the engine was able to run on 100% syngas for extended periods when the operating conditions were adjusted to meet self-ignition temperature and pressures of a HCV syngas. Further reporting that dual fuelling CI engines with a compression ratio greater than 17:1 may not be practical and that the amount of diesel necessary as the pilot fuel is variable and largely depended on the quality and energy content of the syngas. it found that syngas could to substitute 60% - 90% of the diesel fuel required at a specific power output. Also the review postulated that emissions from a compression ignition (CI) engines operated on dual fuel mode (syngas-diesel blend), were generally less than when running on neat diesel (ND). That is, greenhouse gases; CO_2, methane CH_4), nitrous oxides (NO_2) and Ozone (O_3) were reduced by a degree proportional to the amount of syngas used. Further, CO and NO_x increased with increase of CR but NO_x decreased when engine ignition timing was retarded. This study dealt with a broad range of ICEs for the investigation. From the study specific information was not provide on the syngas-diesel blend used and the modifications required to make the engine run on 100% syngas, seeing that a number of studies have observed that engine fuelled solely by syngas will not run sustainably and therefore is impractical. Again, many researchers, including the present study, have sustainably operated dual fuel CI engine with CR of 18, contrary to one of the findings of this study.

Bika (2010) studied the effect of varying ratios of H_2/CO in the syngas on the combustion and emission of a four-stroke direct injection (DI) diesel engine with a variable compression ratio (12:1 to 18:1). The experiments were performed on an overhead valve (OHV), air-cooled, single-cylinder engine to establish the engine combustion characteristics and knock limit. The fuel was injected at 4 cms from the intake port. The fuels investigated were pure H_2, 75% H_2/25%

CO, and 50% H_2/50% CO. The study was limited to equivalence ratios (ϕ) of 0.6 to 0.8 and compression ratios of 6:1 to 10:1. The findings of the study showed an increase in the percentage of CO at the knock limit of syngas. Besides, an increase in CO percentage at the advanced ignition timing of maximum brake torque (MBT) was reported. The maximum heat release rate was observed with pure hydrogen. The peak pressure was, however, observed to be more influenced by the compression ratio rather than by the CO percentage. The maximum fuel burn (MFB) was also observed to be broader with an increase in CO percentage. The overall conclusion of the study was that there was an increase in combustion duration with an increase in CO percentage. A maximum indicated thermal efficiency of 32% was reported with 50% H_2/50% CO at ϕ of 0.6 and compression ratio of 10:1. The study was limited to producer gas and a similar study could be conducted using the syngas obtained from coal with higher heating value for comparison. Performance and emission of DISI engines running on the blends of fuels relative to other known fuels were not investigated and a further study aimed at comparing their performance is necessary.

2.7 Modifying Engine for Syngas Fuelling

Many studies have shown that the quality of syngas as fuel is significantly poorer than gasoline and natural gas. Therefore, the engines required certain design modifications to be able to run on syngas. Many studies and experimental investigations have been conducted on both spark ignition and diesel engines, fuelled with syngas, on engine design modifications, including an increase in the compression ratio, and air and fuel systems (Lee, 2010).

Pradhan et al. (2015) carried a study to determine the modification required on the DISI engine for it to run on syngas. In the study, it was reported that the quality of producer gas (syngas) as fuel is significantly poorer than diesel, gasoline and natural gas. Therefore, it is necessary to operate the engine in a dual-fuel mode, in which syngas is used as the primary fuel, and ignited by pilot diesel fuel. The study observed that the engine fuel and air inlet system needed to be

modified for it to run on syngas. For the engine used in the study, the additional components incorporated for dual fuel operation were, gas mixer, non-return valve, pressure regulator and gas carburettor. In the experiment, syngas and air were mixed in the intake collector and then the ensuing mixture introduced into the engine cylinders. Some studies have shown that spark ignition engine overall, requires very little or no modification to run on syngas. Some suggested design modifications include; an increase in the compression ratio and advancing of fuel injection timing. Generally, adjustment made depended upon the CR and speed of the engine, the ignition timing had to be advanced by about 30 - 40 degrees of CA bTDC. This, as explained, was done because of the low flame speed of syngas as compared to gasoline or diesel. This study dealt with modification on engine fuelled with a blend of diesel and syngas. There is a need to expand the study to test the required modifications when using different blends of syngas and diesel-petrol which the present study has pursued.

Hagos et al. (2016) when studying the effect of the start of injection on the combustion, performance and emissions of a direct-injection spark-ignition engine powered by syngas of H_2/CO composition, used a four-stroke, single-cylinder, DISI research engine with a compression ratio of 14:1. The engine set-up needed to be optimised for syngas application by running without any modification except the addition of the syngas supply system. The finding on retrofitting required was; no alteration to the DISI engine fueled by syngas was required when the experiment was carried out, except for the incorporation of a syngas fuelling system through a double fuel line, fitting of injector holder and a piezoelectric pressure transducer to collect the pressure data. The study was limited to identifying the structural modifications necessary. It would have been more technologically revealing to study the effects the variation of CR and fuel IT has on combustion, performance and emissions of the engine.

2.8 Summary of Gaps

1. From the foregoing literature review, As observed from the work that been reviewed, the syngas used was obtained from simulation or commercial grade gasifiers. Other studies have used gas engines fuelled with syngas sourced from integrated gasification combined cycle (IGCC). The present research is therefore an attempt to investigate the practical use of syngas from a bench scale gasifier, to run a dual fuel CI engine.

2. There is a need to perform experiments to test the performance and exhaust emissions in a dual-fuel CI engine that uses syngas-diesel blends and also study the modification and adjustments that will be required on the engine under all load conditions. Some studies have shown that under high load conditions, syngas is unsuitable for use in ICE engines because of the difficulty in achieving stable combustion.

3. There is need to investigate the operations adjustments and modifications requirements in a dual-fuel engine to improve its power output and make the fuel-air mixture self-igniting. Previous studies have reported that syngas is a low-energy-density fuel, the extent of power degrading it produces in an engine is large, and it has high auto-ignition temperature, hence cannot be used in CI engines without a means of initiating combustion.

4. There is a need to investigate the performance and emissions characteristics of direct ignition(DI) CI engine that uses syngas obtained directly from coal gasification in a laboratory-size gasifier. The reason is that, much of the existing work on the use of syngas in ICE engines, shows that the studies have concentrated on the use of producer gas (the product of biomass gasification) than coal syngas. The other source of syngas for research has been, from the simulation of syngas compositions from given gasifier by mixing the main constituent gases as demonstrated by Mahgoub et al. (2015c).

CHAPTER THREE
RESEARCH METHODOLOGY

3.1 Overview

The problem of energy supply for ICEs has emerged because of the uncertainty of sustainability and the cost of petroleum oil due to its dwindling supply and the difficulties of using solid coal due to its greenhouse effect and handling difficulties. The resulting energy crisis has made it necessary to explore non-traditional methods of energy sourcing. One such method is coal gasification.

In this study, examination of the syngas produced from the bench-scale gasifier available at JKUAT thermodynamics laboratories courtesy of Stellamaris N. Nzove (2021), was carried out to obtain a suitable quality of syngas for use in an ICE. This was through conditioning of raw syngas from gasifier through filtering and cooling. Test on the engine performance and emission characteristics were conducted and results compared with those from the conventional diesel engine. Effect of blending syngas of varying quantities with diesel on CI engine performance and emissions were also studied. Further, necessary modifications on the existing engine were done for it to run on syngas. The engine available had a provision to vary compression ratio (CR) and advance or retard ignition as required for different fuel blends. Consequently, experiments were done to evaluate the performance and emission characteristics of the engine for the syngas-diesel fuel blends. The auxiliary systems for direct ignition compression ignition (DICI) engine including the fuel and air supply were retrofitted with necessary components to modify the engine into a dual-fuel engine that uses diesel and syngas fuels; with syngas as the primary fuel. The engine used for this test was directly mounted on a test bench, coupled to a dynamometer with an interface PC that allowed for performance test on the engine and data acquisition.

Table 3.1: Proximate Analysis of Test Coal

S/No.	Coal Property	Average Value
1	Calorific Value	20.47 MJ/kg
2	Fixed Carbon	55.68%
3	Volatile Matter	48.92%
4	Ash Content	23.58%
5	moisture Content	4.3%
6	Torque(Nm)	11.5

3.2 Research Requirements

The performance and emission of the dual-fuelled CI engine was investigated using a modified diesel engine supplied with syngas from a bench-scale gasifier. The gasifier burned solid sub-bituminous coal (Table 3.1), obtained from Kitui, Kenya, to convert it into syngas of varying composition, according to the controlled conditions in the gasifier. Table 3.2 shows the classification of common types of coal and properties attributed to each (P. Breeze, Academic Press). The syngas generated was supplied to a compression ignition engine whose air system was modified for dual engine operation. Modification entailed fitting of mixing device on the engine air intake, where the syngas was mixed with fresh air charge. Its specific purpose was to allow for the homogeneous mixing of syngas and intake air. Afterward, the mixture was allowed to flow normally through the inlet manifold and the opened inlet valve into the combustion chamber (CC), to form the primary fuel. In describing the operation of dual fuel CI engine, Mahgoub et al. (2015c) stated that under the operation of a CI engine in dual-fuel mode, air is mixed with gaseous fuel and the mixture is compressed as in a normal diesel engine. The mixture would not ignite automatically because the air-gas mixture auto-ignition temperature is high (about 500°C). Accordingly, a small amount of diesel fuel is infused and ignited at the end of the compression phase, which boosts the mixture combustion. This is achieved through engine timing where the

Table 3.2: Types of Coal (P. Breeze, Coal-fired Generation. Academic Press)

S/No	Coal Type	Fixed Carbon (%)	Moisture content (%)	volatile content (%)	C.V. (MJ/kg)	Colour/ Texture
1	Peat	<60	75	63-69	15	Dark-brown and soft
2	Lignite	65-70	35-55	53-63	17-18	Brownish and woody
3	Sub-Bituminous	70-76	18-38	42-53	18-23	Dull black/ dark brown
4	Bituminous	76-86	8-18	14-46	23-33	Layered and shiny
5	Anthracite	70-76	7-10	3-14	32-33	Brittle

fuel injection pump is adjusted to supply a metered amount diesel at appropriate piston and crack position according to given fuel injection timing.

Diesel, used as the pilot fuel here, is injected normally in the CC by an injector. The amount of syngas admitted is controlled manually employing a stop valve which was pre-adjusted to allow a fixed and known amount of the gas for a given syngas-diesel blend and syngas volume flowrate (SVF), at the same instant engine governor regulated the amount of diesel injected (Table 3.3). Bates and Dölle (2017) observed that the diesel engine governor in dual fuel mode increases or decreases the amount of diesel fuel injected as necessary to maintain engine output in the face of decreasing or increasing syngas energy content. Therefore, a minimal modification was done on the CI engine with the only unit fitted being the mixing device on the air supply system. Figure 3.1 shows a schematic layout of the experimental setup, illustrating the modification done on the CI engine to allow for the supply of syngas as the primary fuel. The syngas supply system includes the gasifier, heat exchanger, filter and mixing device as shown in the same figure.

Table 3.3: Composition of the syngas-diesel blend at CR 18 and 1500rpm

		Av. Amount of Fuel in the Blend	
S/No.	Syngas Volume Flowrate (%)	Syngas (m^3/s)	Diesel (m^3/s)
1	100	1.67×10^{-3}	6.17×10^{-4}
2	75	1.23×10^{-3}	7.56×10^{-4}
3	50	0.84×10^{-3}	8.83×10^{-4}
4	25	0.43×10^{-3}	1.02×10^{-3}
5	0 (Neat Diesel)	0	1.12×10^{-3}

For all the experiments in this study, a 3.5 kW, four-stroke, single-cylinder, water-cooled engine, with spark ignition (SI) and compression ignition (CI) mode facilities and variable compression ratio (VCR) was used.

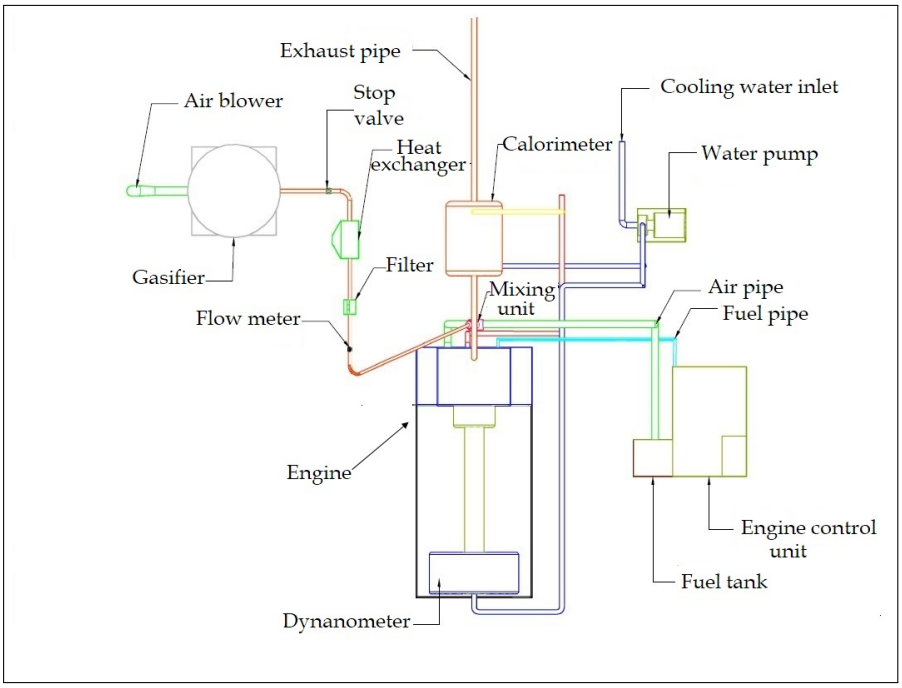

Figure 3.1: Schematic layout of the experimental setup

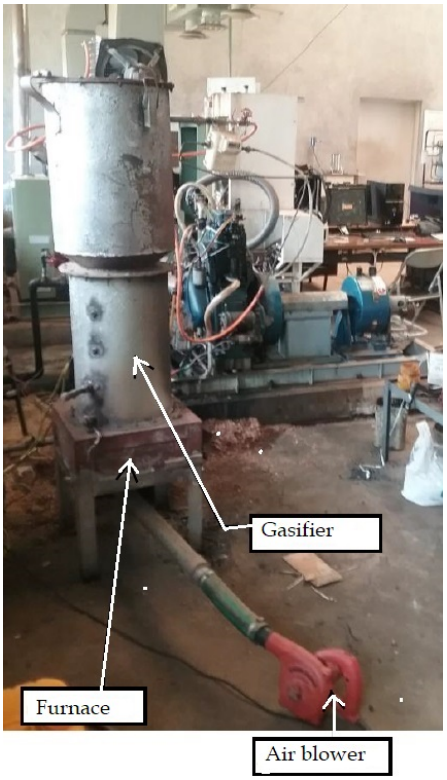

Figure 3.2: A bench-scale fluidised bed-type gasifier

3.2.1 Syngas Production and Conditioning

The gasifier available was a bench-scale fluidised bed-type designed and developed in JKUAT laboratories (Fernando, 2014; Stellamaris N. Nzove, 2021). Figure 3.2 shows a pictorial view of the gasifier coupled to the engine and the air blower for supplying combustion air. The blower had variable speed and air-drying facilities and was used to supply air to the gasifier furnace in order to ensured that the gas produced had minimal moisture and tar, therefore, heat exchangers with partial scrubbing of gas were not necessary. Medium calorific value type of syngas was produced from the small-scale fluidised-bed gasifier whose compositions as obtained in a proximate analysis is given in Table 3.1 and which compares well with results from tests done by Mwiluka (2009)

The operating cleanliness conditions and temperature for the syngas suitable for application in IC engines were obtained by cooling the gas in a air-cooled heat exchanger to almost ambient temperature and filtering to avoid clogging and

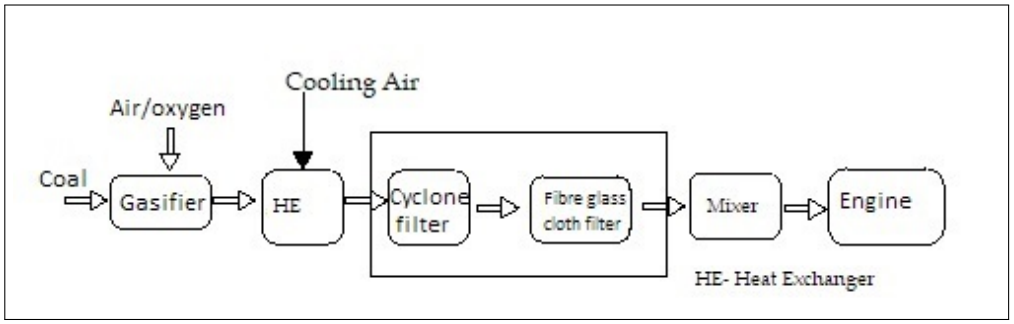

Figure 3.3: Syngas conditioning for use in dual fuel CI engine

fouling of engine lines and components. As observed by Van Paasen and Kiel (2004), fluidised-bed gasifiers are normally operated at substantially lower temperature levels and do produce significant amounts of tar. This was observed in the used gasifier as it produced gas at temperatures that ranged from 250 - 300 °C. To use this gas for ICE applications, firstly it was cleaned of tar and dust - that is hydrogen sulfide (H_2S), sulfur dioxide (SO_2), hydrogen chloride (HCl), nitrogen oxides (NO_x), nitrogen (N_2), and ammonia (NH_3) and then cooled as shown by the flow diagram in Figure 3.3. A gas-to-air heat exchanger was designed to reduce the syngas temperature to near room temperature, which is desirable, as explained by Pradhan et al. (2015). Mostly, heat exchangers are used as coolers and they effect cooling by passing air or water over finned tubes. In this study, as discussed in section 3.3.1 and as shown in Figure 3.4, air cooling, using an air fan was applied. Cleaning of the gas is very critical as observed by Pradhan et al. (2015). Normally there are three types of filters available for this auxiliary gasification process namely: dry, moist and wet. In the present study, dry category cyclone filter was used and was selected based on the volume flow rate of the syngas produced in the gasifier, quantity of impurities (ash, tar, soot and dust) and particle sizes of the impurities as discussed by Coq and Ashenafi (2014). Pradhan et al. (2015) reported that cyclone filters are useful for particle sizes of 5 μm and greater. For this case, the gas was cooled and then passed through a cyclone cork filter for final cleaning, which conforms to recommendations given by Hagos et al. (2014b).

3.2.2 Research Diesel Engine

The engine used in this research was a multi-fuel, single-cylinder, four-stroke engine manufactured by Apex Innovations Pvt. Ltd (Mulay et al., 2014) with the geometrical and operation specifications as shown in Tables 3.4 and 3.5 respectively. The engine was coupled to an eddy current dynamometer for loading as shown in Figure 3.5. The operation mode of the engine could be changed from diesel to engine control unit (ECU) petrol or from ECU petrol to diesel mode.

The research engine used in study had several components and sensors for efficient operation, measurement and data collection:

(A) **Engine**

The test engine is a multifuel VCR engine of Kirloskar-make, with specifications as shown in Tables 3.4 and 3.5. The engine is water-cooled and has a variable ratio (VCR). VCR allows engine CR to be varied in the range

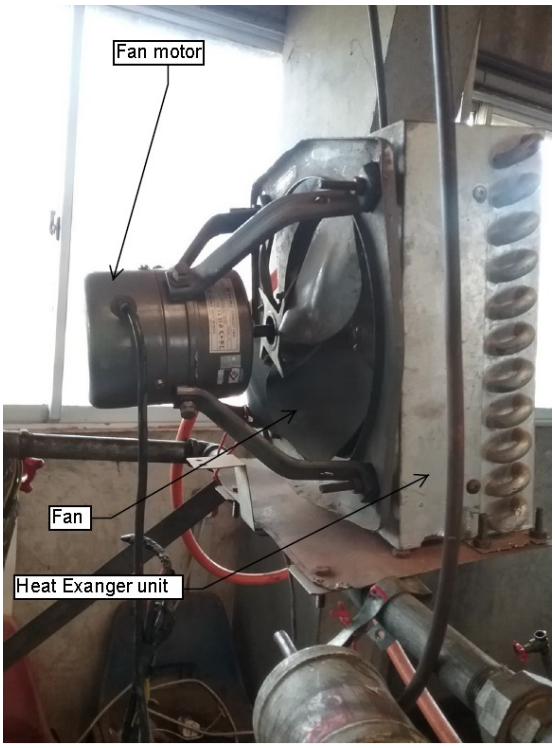

Figure 3.4: Air fan mounted on the air-cooled heat exchanger

of 12 to 18. Different cylinder heads for CI and SI modes are also available for engine operations as either a CI or SI engine.

(B) **Dynamometer**

To engine torque and hence the brake power are obtained using an eddy current (EC) absorption-type constant speed dynamometer of Model AX-155, Make-Apex, which was directly coupled to the engine whilst an in-built tachometer used to measure engine shafts angular speeds (Shital Sharadchandra Mulay et al., 2014). The dynamometer comprises a stator on which are fitted with several electromagnets and a rotor disc coupled to the output shaft of the engine. Figure 3.6 shows a pictorial view of the dynamometer. When the rotor rotates, eddy currents are produced in the stator due to magnetic flux set up by the passage of field current in the electromagnets. These eddy currents oppose the rotor motion, thus loading the engine. A moment arm measures the torque (Mate and Dhande, 2014; Mulay et al., 2014). A strain gauge load cell was attached to the dynamometer and incorporated in the restraining linkage between the casing and the dynamometer bedplate. It was used to measure dynamometer loading due to the rotational torque exerted on the casing. A rotary encoder was fitted on the dynamometer shaft to measure the engine crank angle (Mulay et al., 2014).

(C) **Engine Control Panel**

The research engine consisted of a control panel marked PE3 series ECU, with a piezo powering unit, voltmeter, load indicator, dashboard panel and a fuel level pipe as shown in Figure 3.7.

The piezo sensor of Model SM111A22 manufactured by PCB Piezotronics Inc, USA and the crank angle sensor was connected to a piezo powering unit model AX-409. The signals from the sensors were transferred to the piezo powering unit through coaxial Teflon cables of Model 002C20. The control knobs for regulating speed and the load, as well as the ignition switch for starting the engine were all located in the control panel.

Table 3.4: Research engine geometrical specifications

S/No.	Parameter	Value
1	Cylinder total volume (cm^3)	950
2	Number of cylinders	1
3	Number of strokes	4
4	Stroke (mm)	110
5	Bore (mm)	87.5
6	Connecting rod length (mm)	234
7	Max. rated power (kW)	5.8
8	Compression ratio	18:1

Table 3.5: Engine operation specifications

S/No.	Specification	Value
1	Number of cylinders	1
2	Number of strokes	4
3	Fuel	Diesel/Petrol
4	Power output (kW)	3.5
5	Speed (rpm)	1500
6	Torque(Nm)	11.5
7	Variable compression ratio	12 - 18:1
8	Peak pressure (bar)	76
9	Fuel consumption (g/kWh)	251
10	Injection pressure (bar)	200
11	Injection timing (^{0}btdc)	23
12	Swept volume(cm^3)	661
13	Combustion system	Direct injection

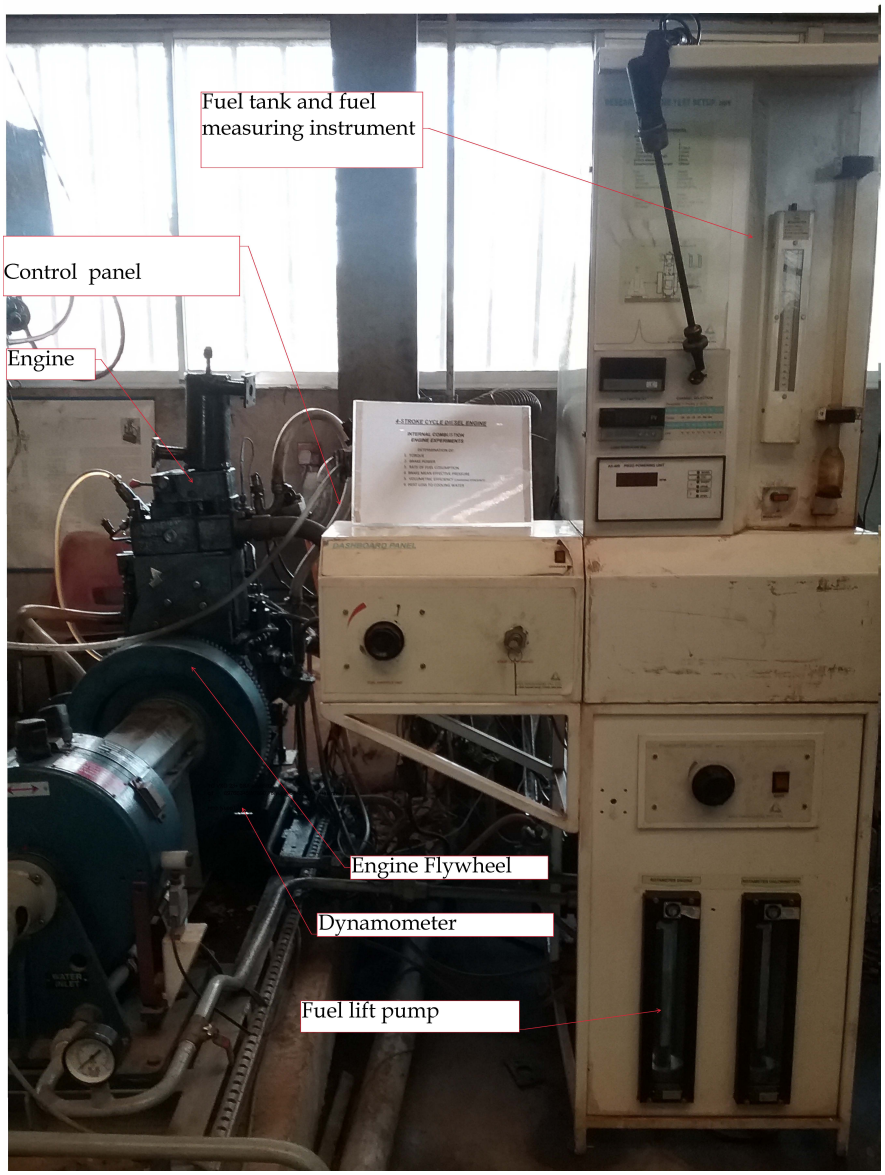

Figure 3.5: The research engine used in the experiment

(D) Fuel Tank

Two fuel tanks are provided on the top portion of the engine panel, one for diesel and the other one for petrol. It is a 15 litre capacity fuel tank partitioned into two sections for diesel and petrol fuel. For diesel fuel, the fuel supply system is equipped with a fuel pump and injectors of Denso make, Maruti 800 model, a glass fuel-measuring unit, Model, FF0.012 and fuel over-flow pipe to regulate fuel overflow.

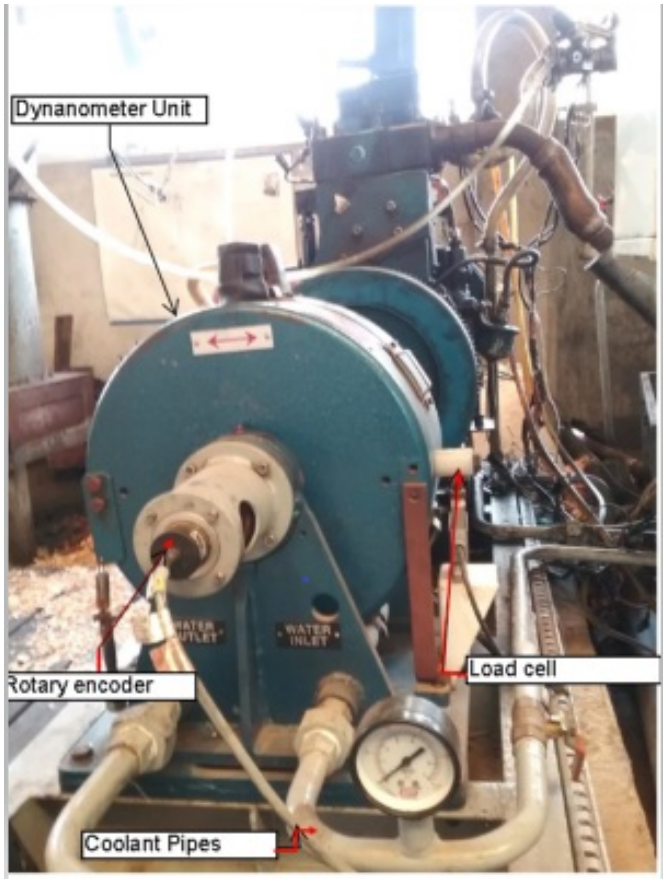

Figure 3.6: Eddy current-type dynamometer

(E) **Air Box**

The engine has one air box fixed just under the fuel tank. Air from the airbox flowed to the engine air-inlet manifold through an air hose pipe. Its purpose was to dampen out the pulsations in the air as it flowed to the engine. It had an orifice for measurement of airflow to the combustion chamber (CC), a manometer- Model MX-104, Range -100 - 0 - 100 mm, and a pressure transmitter to measure the differential pressure across the orifice.

3.3 Design Procedure for the Components

For this experiment, several of design requirements were met. The research engine air system was modified to allow for the supply of syngas. The filter for this experiment was selected to suit the condition and quantity of syngas produced.

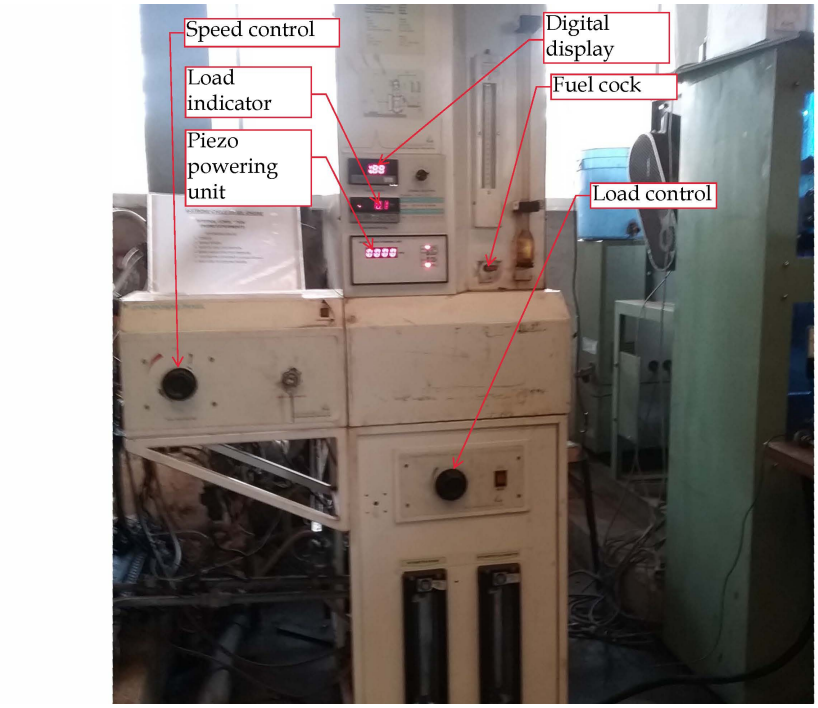

Figure 3.7: Engine control panel

The cooler and mixer were designed and developed using SolidWorks software. Details of designs are outlined in the following section.

3.3.1 Cooler Design

Air cooled heat exchanger (ACHE)was selected as the cooler for this experiment due to its simplicity, its designed makes it easy to miniaturise and match closely to the requirements for the present research study namely; the outlet temperature and the amount of gas to be handled at the lowest cost.

The air-cooled heat exchanger (ACHE) was designed to cool the gas from 250 - 300 $°C$ to 25 - 38 $°C$ (Figure 3.8). Pradhan et al. (2015) discussed the importance of cooling syngas before supplying it to the engine by stating that the temperature of gas coming out of the generator is normally between 300 - 500° C and in order to raise its energy density the gas should first be cooled. Syngas outlet temperature should be equal to or slightly greater than the surrounding ambient air temperature to avoid high temperature before completion of compression stroke a conditions that is conducive to the formation of NO_x species leading to

increased emission of the gas (Baratieri et al., 2009).

(A) **The Air Cooled Heat Exchanger Thermal Design**

An ACHE with a mounted induced draft fan was designed and optimised analytically using standard equations. (Mukherjee, 2017) explained that ACHE design procedure comprises two distinct activities, namely, thermal design and mechanical design. In thermal design the number of tubes and size of tubes of the heat exchanger was established, whereas in mechanical design the thickness and precise dimensions of the various components were determined. As part of thermal design, the present study is guided by the work of Mukherjee (2017); Singh and Pal (2016) who observed that in order to determine the number of tubes and size of tubes in a heat exchanger, the data required is fluid flow rates, pressure drop, allowed number of tubes and their size, face area, lower velocity limit corresponding to limiting fouling factor and upper velocity limit corresponding to limiting rate of erosion. To evaluate the tubes sizes required for designs of components, heart transfer coefficients for both sides of the tubes needed to determine.

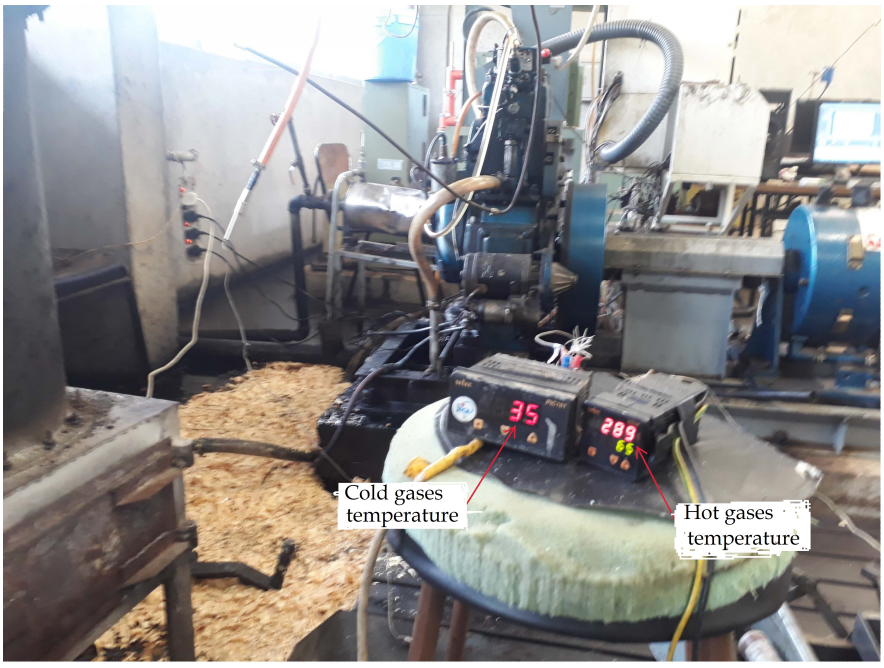

Figure 3.8: Syngas temperatures at heat exchanger inlet and exit

This done using Reynold equation, Eq. 3.1, Prandtl equation, Eq. 3.5 and Nusselt equation, Eq. 3.7 numbers. The general equations that were used to size and select ACHE are as shown in Eqs. 3.1, 3.2 and 3.3

$$\mathrm{A} = \frac{\mathrm{Q}}{\mathrm{U.LMTD}} \tag{3.1}$$

where,

A - heat transfer area in m^2, U - overall heat transfer coefficient in W/m^2K, LMTD - logarithmic mean temperature difference (°) and

$$\mathrm{Q} = \dot{\mathrm{m}}_g c_g(\mathrm{T}_{1,g} - \mathrm{T}_{2,g}) = \dot{\mathrm{m}}_a \mathrm{c}_a(\mathrm{T}_{1,a} - \mathrm{T}_{2,a})$$

with, $\mathrm{T}_{1,g}$ and $\mathrm{T}_{2,g}$ - inlet and outlet temperatures of syngas, $\mathrm{T}_{1,a}$ and $\mathrm{T}_{2,a}$ - inlet and outlet temperatures of air.
also,

$$\frac{1}{\mathrm{U}} = \frac{1}{\mathrm{h}_{air}} + \frac{1}{\mathrm{h}_t} + \mathrm{r}_f(\mathrm{tubeside}) + \mathrm{r}_f(\mathrm{air}) + \mathrm{r}_w \tag{3.2}$$

where, values are as recorded in Table 3.6 ahead.

$$\mathrm{LMTD} = \frac{\theta_1 - \theta_2}{In\frac{\theta_1}{\theta_2}} \tag{3.3}$$

where, $\theta_1 = \mathrm{T}_{1,g} - \mathrm{T}_{1,a}$ and $\theta_2 = \mathrm{T}_{2.g} - \mathrm{T}_{2,a}$

(B) **Tube-side Heat Transfer Coefficient**

The tube-side heat transfer coefficient is a function of the Reynolds number, the Prandtl number, and the tube diameter. The Reynolds number (Re) is given as,

$$\mathrm{Re} = \frac{\mathrm{DG}}{\mu} \tag{3.4}$$

where, D - tube inside diameter (ID) (m), G - mass velocity (mass flowrate of syngas per unit area of tube side) (m/s) and μ - dynamic viscosity as recorded (Ns/m^2) as given in Table 4.3.

The Prandtl number (Pr) is given as,

$$\mathrm{Pr} = \frac{\mathrm{c}\mu}{\kappa} \tag{3.5}$$

where for syngas as in Table 4.3, c - specific heat (J/kgK), μ - viscosity and λ - thermal conductivity (W/M·K)

The fundamental equation for turbulent heat transfer inside tubes is as shown in Eq. 3.6 and Eq. 3.8 and therefore for h_t in this case, is as in Eq. 3.9 (Mukherjee, 2017)

$$\mathrm{Nu} = 0.027(\mathrm{Re})^{0.8}(\mathrm{Pr})^{0.33} \tag{3.6}$$

where, Nusselt number = Nu

$$= \frac{hD}{\kappa} \tag{3.7}$$

$$\frac{hD}{\kappa} = 0.027\left(\frac{\mathrm{DG}}{\mu}\right)^{0.8}\left(\frac{\mu \mathrm{c}}{\kappa}\right)^{0.33} \tag{3.8}$$

and

$$\mathrm{h}_t = 0.027(\mathrm{Re})^{0.8}(\mathrm{Pr})^{0.33}\left(\frac{\kappa}{\mathrm{D}}\right) \tag{3.9}$$

where h_t is tubeside heat transfer coefficient.

(C) **Design of Air Flow System**

The most widely accepted correlations for the airside heat transfer coefficient and airside pressure drop are those resulting from the experimental work of Young *et al.* (Barbee et al., 2007; Mukherjee, 2017) as shown in Eqs. 3.10 and 3.11,

$$\mathrm{Nu} = 0.027(\mathrm{Re})^{0.681}(\mathrm{Pr})^{0.33}\left(\frac{S}{h}\right)^{0.2}\left(\frac{S}{b}\right)^{0.1134} \tag{3.10}$$

where, S - fin spacing = 5 mm, h - fin height = 6.125 mm and b - fin thickness = 2.5 mm., all available from the TEMA standard (Barbee et al.,

2007) for ACHE design. Substituting the values in Eq.3.10 will help solve for Pr number that will used to size the tubes as shown in Eqs. 3.10 to 3.12 that follow. The heat transfer and friction factor correlation for air side of finned tubes was studied by Kim and Bullard (2002) (Mukherjee, 2017) and developed a relationship as shown in Eq. 3.11

$$\mathrm{f} = 18.93(\mathrm{Re})^{-0.316}\left(\frac{\mathrm{R}}{\mathrm{d}}\right)^{-0.927}\left(\frac{\mathrm{P}_t}{\mathrm{P}_l}\right)^{0.515} \tag{3.11}$$

where, f is the friction factor

and, R - LMTD correction factor $(\mathrm{T}_{2,g} - \mathrm{T}_{1,g}/\mathrm{T}_{2,a} - \mathrm{T}_{1,a})$, d - tube outside diameter (OD) = 10 mm, P_t - transverse tube pitch = 25 mm and P_l - longitudinal tube pitch = 5 mm.
Then, Eq. 3.12 will give airside heat transfer coefficient(h_{air}).
i.e.

$$h_{air} = 0.027(Re)^{0.681}(Pr)^{0.33}\left(\frac{S}{h}\right)^{0.2}\left(\frac{S}{b}\right)^{0.1134}\frac{\kappa}{D} \tag{3.12}$$

Considering tube size, mass velocity, syngas post treatment conditions and drop drop; the magnitude of fouling resistance for both tube side (material of tube in contact with syngas) and air side (for the stream of air passing through the heat exchanger coil) were obtained. The values were obtained from the TEMA standard tables (Barbee et al., 2007) as tabulated from experimental data for different flow conditions and material.

Solving the Eqs 3.10 and 3.12 and using values obtained from the standard charts for constants assigned to different heat transfer coefficients and resistance as shown in Table 3.6 the following results were obtained: Tube diameter (D) = 10.4 mm and Cooled syngas temperature (T_2) = 33.7 $^{\circ}C$. The details of the ACHE designed is shown in Figure 3.9

Table 3.6: Values of Heat Transfer Coefficients and Resistances

S/No.	Coefficient/Resistance	Value
1	Airside heat transfer (h_{air})	50 W/m^2
2	Tubeside heat transfer (h_t)	60 W/m^2
3	Fouling resistance(r_f)	0.42 mK/W
4	Finned tube wall resistance (r_w)	0.00704 mK/W

(D) **Fan Selection**

The most important factor considered in the selection of the fan was the outlet temperature of the gas, which therefore informed the fan air power hence, quantity of output air. An induced draft fan was selected because it generally requires less power for an air temperature rise less than 10°C and it has a better air distribution over the exchanger (Srivastava et al., 2014). The fan specifications are as shown in Table 3.7.

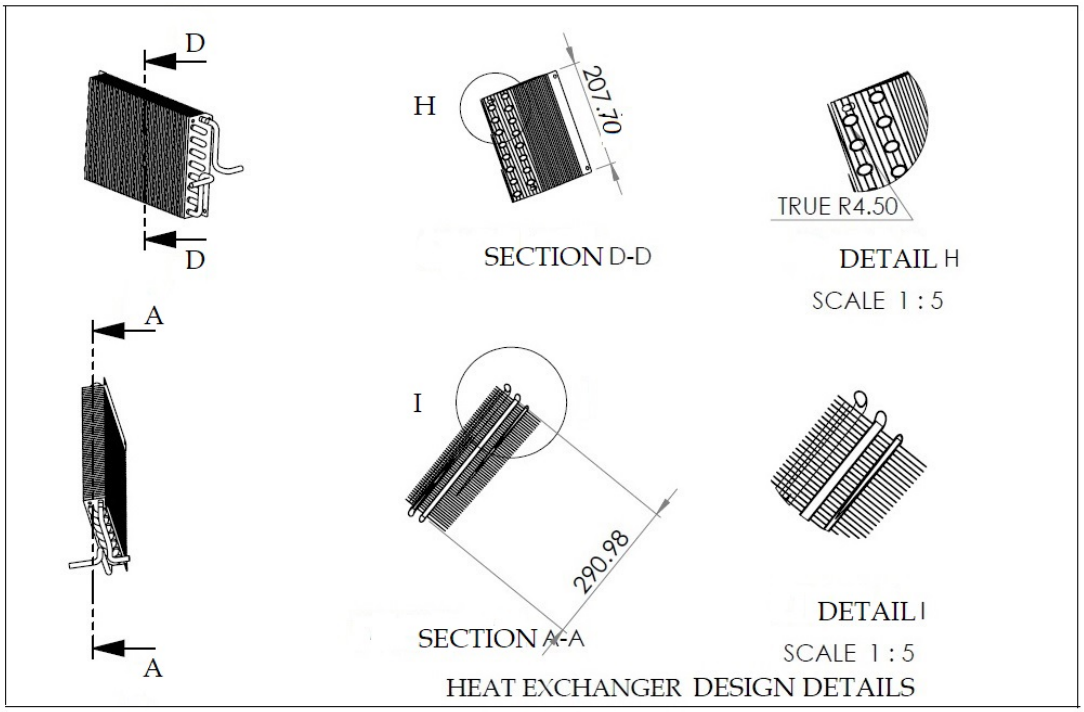

Figure 3.9: 2D view of heat exchanger design

Table 3.7: Cooling Fan Specifications

S/No.	Parameter	Value
1	Air displacement (cm^3/min)	600
2	Power Consumption (W)	42
3	Number of blades	3
4	Speed (rpm)	1400
5	Sweep (mm)	225
6	Material	Mild steel
7	Type	ID

(E) **Material and Size for Air Cooled Heat Exchanger Construction**

Aluminium was selected as the material for the heat exchanger due to its affordability. It has good thermal conductivity and reasonable cost per square meter (the cost of heat transfer surface per square meter), has adequate corrosion resistance for most air cooled heat exchanger (ACHE) applications (though some doubts have been raised on this property). Aluminium fins in helical design fitted on round tubes are widely used in ACHEs. The performance of aluminium fins is much better than that of steel fins, and they are much cheaper than copper helical fins (Kolmetz and Widiawati, 2015).

Tube size for ACHE was selected guided by American Petroleum Institute (API) standards. Tube size here means; tube outside diameter (OD), thickness, and length. As per the API 661 Standards, 25.4 mm is the smallest OD of tubes to be used in air-cooled heat exchangers. This being a small scale gasifier whose flow is comparatively low, the smallest tube diameter of 10 mm was selected as 25 mm result into unnecessarilyy large and dear HE that will remain largely underutilised beside reducing the velocuty of the syngas flow when used with a bench-size gasifier.

(F) **Selection of Suitable Pass for Air Cooled Heat Exchanger (ACHE)**

In selecting the optimum number of passes in a heat exchanger there was need to increase velocity of the produced syngas. This was done by incorporating pass partition plates (and corresponding gaskets) in the headers and passing the syngas eight times through the forced air from left to right and then from right to left. The velocity recorded in this condition was twice that of the velocity of a single pass. It was noted that, were the gas made to flow through all the tubes (single tube pass), it would result in a unacceptably low velocity that would yield a very low heat transfer coefficient (Mukherjee, 2017).

At the design stage, it was found that a very large number of tube passes would have led to much complications in fabrication of ACHE. To keep the number of passes required low a small diameter pipe was selected, as stated earlier, 10 mm considering the relatively low tubeside mass flow rate applicable here. This situation applies here for a higher mass velocity is required to obtain a satisfactory Reynolds number (Eq. 3.11). The present study used 8 passes based on simulated results.

3.3.2 The Mixing Device

A simple mixing device (chamber) of T-junction was designed in SolidWorks suite. An enlarged T-junction of a tube with two inlets; one for air and the other for syngas and an outlet for the mixture was fabricated of steel material (mild steel) for this experiment, because of its low cost and ease of fabrication. The outlet was connected to the intake manifold of the engine as shown in Figure 3.10. For the control of the engine power a gate valve was used to control3e the fuel gas supply. The valve was hand-operated with the quantity of diesel injected being regulated by the normal engine governor.

(A) **Design Considerations**

One objective of this design was to provide, in the mixing chamber, a means for more effective mixing of syngas fuel and inlet air before diesel injection and combustion. This was meant to achieve a more complete combustion in the engine. Details of the structure of mixing chamber are shown in Figure 3.11, where the mixing chamber is shown alongside air and syngas delivery tube. The Mixing chamber had a hollow tubular T-shaped housing, the T-sections being connected to two inlets for syngas and air, each at an angle of 90 degrees. Syngas delivery pipe was welded to one side of the the outer surface of the housing member and the air delivery on the opposite end.

(B) **Design of the Mixing Chamber**

Performance of a dual fuel engine largely depends on the proper mixing of air and fuel gas; hence design of the mixing chamber plays a big role in this process.

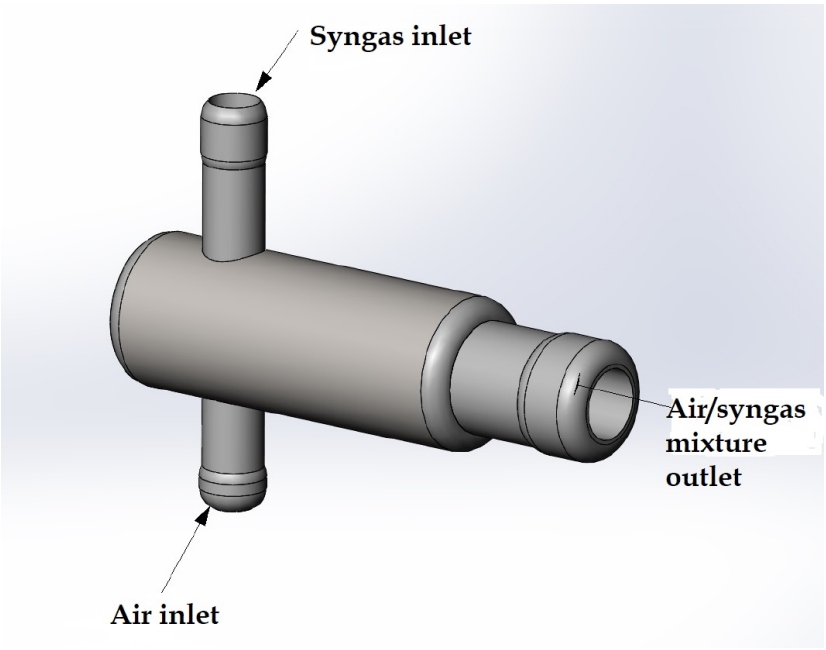

Figure 3.10: Air/Syngas mixing unit

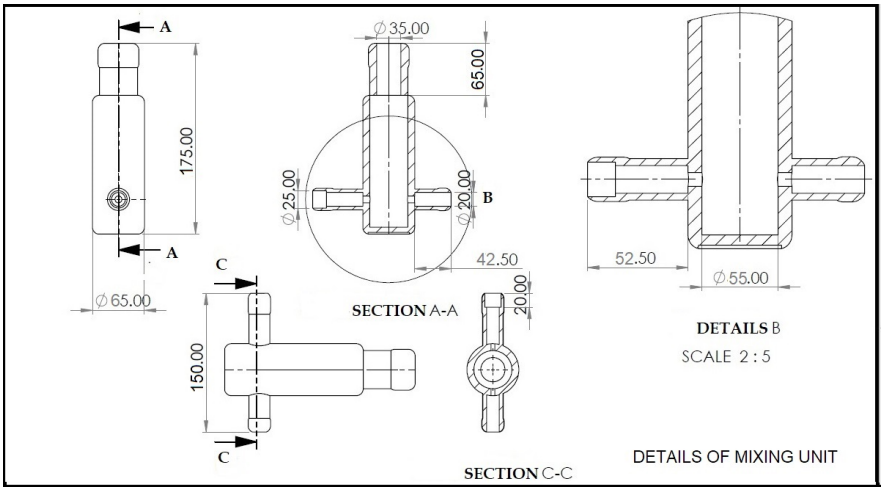

Figure 3.11: Design details of the mixing unit

The mixing chamber was designed with the volume large enough to provide sufficient time for syngas and air to form a homogeneous mixture. The volume of the mixing chamber should be equal or bigger than the engine volumetric capacity so that sufficient air is supplied to the engine (Hagos et al., 2014a; Reed and Das, 1988). The volumetric capacity (swept volume) of the engine used in this research was 661 cm^3, so the volume of the mixing chamber was designed to be slightly more than 661 cm^3. Using a cylindrical carbon steel pipe of an internal diameter of 86 mm and using Eq. 3.13, the length that would give the volume of 661 cm^3 for the mixing chamber would be 113.8 mm. The closest reasonable length is 120 mm, which gives a volume of 697 cm^3, and therefore could suitably be used. However, considering sufficient resident time for homogeneous mixing to be achieved and installation conditions to the modified engine, a length of 175 mm was selected for the design.

$$V = \frac{\pi D^2 L}{4} \tag{3.13}$$

(C) **Design of Inlet Pipes**

In design of inlet pipes for the mixer, Reed and Das (1988) observed that the syngas mixer must mix a proper ratio of air with the syngas, approximately a 1:1 ratio of fuel to air by volume. In the present study, it was concluded that variations in the syngas mixture cause sharper changes in engine power compared to similar variations in gasoline mixture. In a research study, Raman and Ram (2013) explained that in mixing gaseous fuel with air, dimensioning of the syngas inlet pipe plays a very important role in the performance of a dual fuel engine. The study reported that performance depends mainly on the fuel energy required by the engine operating at its maximum power and maximum speed, and the calorific value of syngas used in the dual fuel operation.

The engine used in this research had maximum power of 3.5 kW at operating speed 1500 rpm. The syngas inlet pipe was designed using Eqs 3.14 to 3.17 . The volumetric flow rate of air into the engine (Q_a) for a 4-stroke engine was calculated as in Eq. 3.14,

$$\dot{Q}_a = \frac{60 V_c N}{200} \rho_A \eta_{vol} \tag{3.14}$$

where, V_c, η_{vol} and N are engine volumetric capacity (cm^3), volumetric efficiency (%) and maximum speed respectively (rpm), ρ_A is the air density at the engine operating conditions (kg/m^3.

At the top speed of 1500 rpm, the engine average volumetric efficiencies recorded were 57% with 0% flowrates of syngas and 42% with full flow of syngas. With the engine having a volumetric capacity of 661 cm^3 and maximum speed, N = 1500 rpm and operating on 4-stroke cycle, the calculated volumetric flow rate was, $\dot{Q}_a = 4.7 \times 10^{-3}$ m^3/s. The recorded airflow into the engine is the product of air intake velocity V_{in} and inlet area normal to the flow direction of air and was calculated using Eq 3.15. From Eq 3.15, A

is the cross-sectional area of the engine inlet manifold (Hagos et al., 2014a).

$$\dot{\mathrm{Q}}_{\mathrm{a}} = \mathrm{V}_{in}\mathrm{A} \tag{3.15}$$

The engine designs had the manufacturer set the inlet-manifold diameter set at 20 mm. Then from continuity equation, Eq. 3.15, the calculated value of the inlet air velocity at outlet of the mixing chamber hence engine inlet manifold V_{in}, was 14.96 m/s. The velocity applies for both air and syngas and is after the mixing chamber, thus the difference with the value of velocity 16.5 m/s (Table 4.4) obtained from engine ICEngineSoft system.

$$\mathrm{Q}_s = \mathrm{A}_{si}\nu_{in} \tag{3.16}$$

$$\mathrm{d}_{si} = \sqrt{\frac{4\mathrm{Q}_s}{\pi\nu_{in}}} \tag{3.17}$$

The evaluated diameter for the syngas inlet pipe was 21 mm. However, considering the standard pipe available and that diameter of the syngas inlet should not be less than 0.5 times the diameter of the engine air inlet manifold, 20 mm was taken to be the diameter designed for this experimental study. The air inlet pipe size was calculated in similar manner considering its 17.5 kg/hr (4.15×10^{-3} m^3/s) flow rate into the mixing chamber. The value obtained was 18.9 mm, but standardised to a diameter of 20 mm. The outlet diameter was fixed at 20 mm, to correspond with engine manifold.

3.3.3 Filter Design

The filter is a cylindrical chamber with an inlet tube and fitted with baffles to generate a cyclone and an outlet oppositely positioned and separated from the inlet by a dry cloth. The filter was sized based on maximum gas flow rate and

particle sizes of impurities in the syngas generated. To determine the particle size of the impurities, standard tables were used that provide information on nature of particles produced by different types of gasifiers when factors such as oxidation methods, types of feed stock and gas velocity are considered and methods of measurement (Dirgo and Leith, 1985; Reed and Das, 1988).

Figure 3.12 shows the cyclone filter design features stipulating the major dimensions.

In the design, Leith-Licht method (Dirgo and Leith, 1985), Eq. 3.18, was used to determine the filter diameter, D_c

$$n = 1 - \left[(1 - 0.67 D_c^{0.14})(T/283)^{0.3}\right] \tag{3.18}$$

where, T is syngas temperature = $(289° + 273) = 562$ K and experimental studies of cyclone flow patterns have measured n in the range of 0.5 to 0.9. For this small-scale gasification process and considering the relatively low mass flowrate that was passed through the filter the least value of 0.5 was adopted. For the inlet and outlet diameters and filter height, the Dietz (1981) model (Kumar and Shukla, 2016) in Eq. 3.19 was applied.

i.e. efficiency, referring to Figure 3.12:

$$\eta = 1 - exp\left[- 2\left(\left[\frac{G\tau\ V_o}{D_c^3}(n+1)\right]\frac{0.5}{n+1}\right)\right] \tag{3.19}$$

where, V_o = syngas volume flow rate in $m^3/s = 1.67\times\ 10^{-3}$, G and V represent the following:

$$G = \frac{16 D_c (2V_s + V)}{\pi D_i^2}$$

and

$$V = I + II + III$$

where,

$$I = \pi D_c^2 (H_b - L)$$

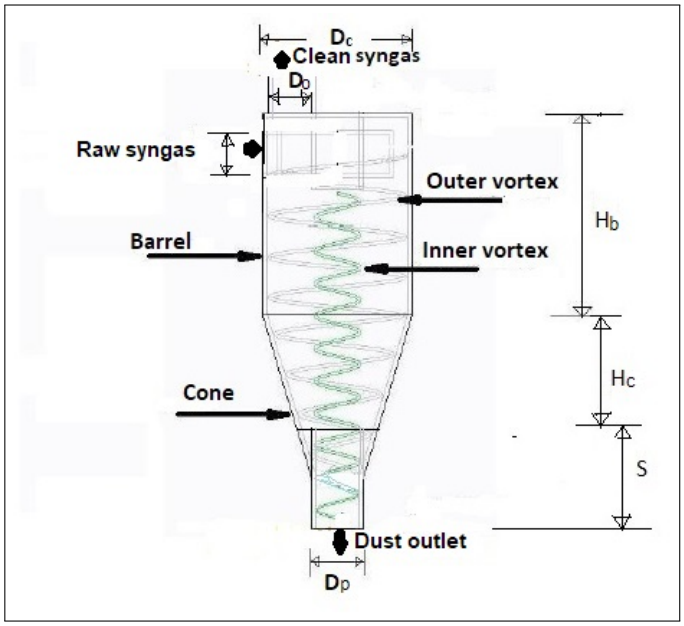

Figure 3.12: Design features of syngas cyclone filter (Kumar and Shukla, 2016)

H_b is the height of cyclone barrel and Alexander (1949) (Dirgo and Leith, 1985) defined L, the natural length of the cyclone, as the furthest distance the spinning gas extends below the gas outlet duct;

$$L = 2.3D_o\left(\frac{4D_c}{\pi D_o}\right)^{1/3}$$

where, D_o is diameter of cyclone syngas outlet.

$$II = \frac{\pi}{4}D_c^2\left(\frac{Z_c + L - H_b}{3}\right)\left(1 + \frac{d_c}{D_c}\right) + \left(\frac{d_c}{D_c}\right)^2$$

where d_c is the cone diameter at the natural length, L.

$$d_c = D_c - \frac{D_c(S + L - H_b)}{H_c})$$

where S is the cyclone dust outlet height,

$$III = \pi\left(L - \frac{D_o}{2}\right)(D_c^2 - D_o^2)$$

Table 3.8: Syngas Filter Design Specifications

S/No.	Quantity	Value (mm)
1	Filter barrel diameter (D_c)	90
2	Cyclone cone height (H_c)	120
3	Cyclone gas outlet duct length(S)	30
4	Cyclone barrel height (H_b)	40
5	Inlet diameter (D_i)	12.5
6	Outlet diameter (D_o)	15

$$V_s = \frac{\pi}{4} D_o^2 Z_c$$

$$Z_c = 2.3 D_o \left(\frac{4 D_c^2}{\pi D_i^2} \right)^{1/3}$$

and,τ is the relaxation term.

$$\tau = \frac{\rho_p d_p^2}{18\mu}$$

Data for syngas and particles used to evaluate filter dimensions are as follows: Hasler and Nussbaumer (1999) (Kumar and Shukla, 2016) have shown that particle size - Particle diameter (m) - for IC engine should be less than 10 micron and for gas turbines it is less than 5 microns. Hence, impurities particles diameter (d_p) for syngas from low rank coal ranges from 8 - 10 micron. Selecting 8 micron gave an efficiency (η) of about 30%, average density of impurities (tar, soot and dust) particles (ρ_p) = 2200 kg/m^3. Evaluated values for sizing of filter according to the standard specifications are outlined in Table 3.8:

3.3.4 Engine Design Modification

Structurally, the CI engine required no alteration for it to run in dual fuel mode. The modification needed were only in the auxiliary systems and included fuel

and air supply systems. The changes done were minor adjustments to allow for supply of the gaseous fuel into the engine, which the research engine had in-built provision for. For these modifications, listed are the considerations:

The energy density of syngas as a fuel is significantly lower than diesel or natural gas. Therefore, the engine required design modifications to be able to run on syngas-diesel blend (Homdoung et al., 2015; Mahgoub et al., 2015c). Figure 3.13 shows the modification, made on CI engine to allow for its operation in dual fuel mode.

The engine was operated in a dual-fuel mode, where syngas was used as the primary fuel, and ignited by the pilot diesel fuel. Pilot fuel is necessary because syngas cannot be used in CI engines without a means of initiating combustion, since the temperature at the end of the compression stroke is lower than the auto ignition temperature of syngas. Discussing the application of syngas in CI engines, Pradhan et al. (2015) have explained that a compression ignition (CI) engine would operate more efficiently with syngas because of its inherent high CR (12 - 24).

The dual fuel CI engine was operated at high Compression Ratios (CR) to increase power output. Researchers have observed that syngas is a low energy density and low calorific value fuel compared to diesel. Therefore, the power degradation in CI was extensive compared to when fuelled with high energy density fuels such as diesel or natural gas (Homdoung et al., 2015). Other studies have shown that syngas with higher heating value and those with high proportion of H_2, could be used to improve the power generated (Mahgoub et al., 2017). However, according to Bates and Dölle (2017), dual fuelling of diesel engines with a compression ratio greater than 17:1 may not be practical. The gas entering the combustion chamber of an ICE was cooled to near ambient temperature and cleaned of dust and tar, by fitting a heat exchanger that was designed and matched with the gasifier output (syngas) quantity and condition by incorporating in the design, a filter for cleaning the hot syngas.

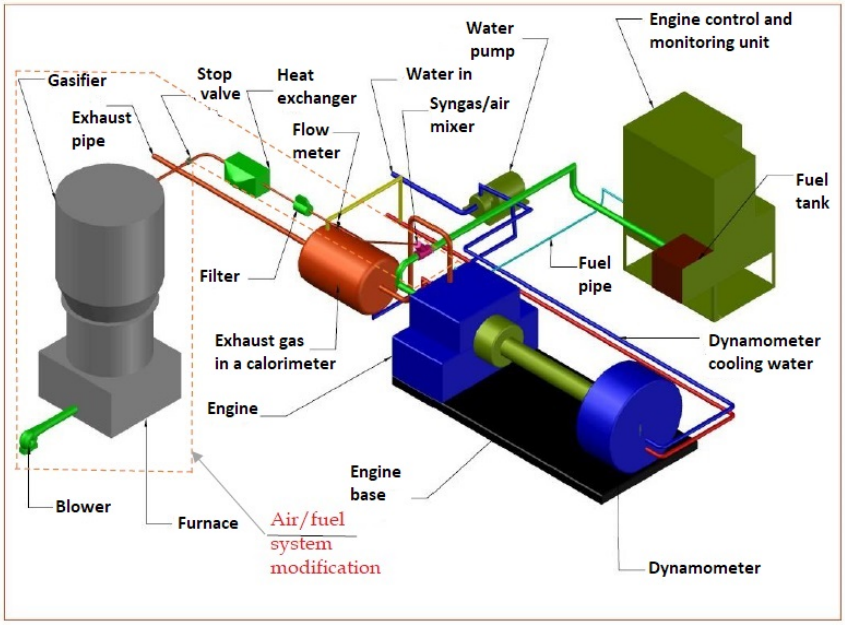

Figure 3.13: Schematic diagram of the experimental setup showing the modified air-fuel system of the CI engine

Higher temperatures in the inlet gases caused higher combustion temperatures resulting in improved engine performance but there was a notable increase of NO_x emission (Mahgoub et al., 2015c; Pradhan et al., 2015).

For this design, only hot gases were passed through the cloth filter from the cooler. This was done since the filter used as shown in Figure 3.14 was a fine one, and any condensation of water in it could stop the gas flow because of the increased pressure drop across it.

The exhaust system was modified by fitting a stop valve to provide means of measurements and analysis of exhaust emissions.

3.3.5 Modification and Adjustment Required on the Engine

Generally, depending upon the compression ratio and speed of the engine, the ignition timing is advanced to about 30 - 40 degrees before top dead centre (bTDC). This is done because of low flame speed of syngas compared to diesel.

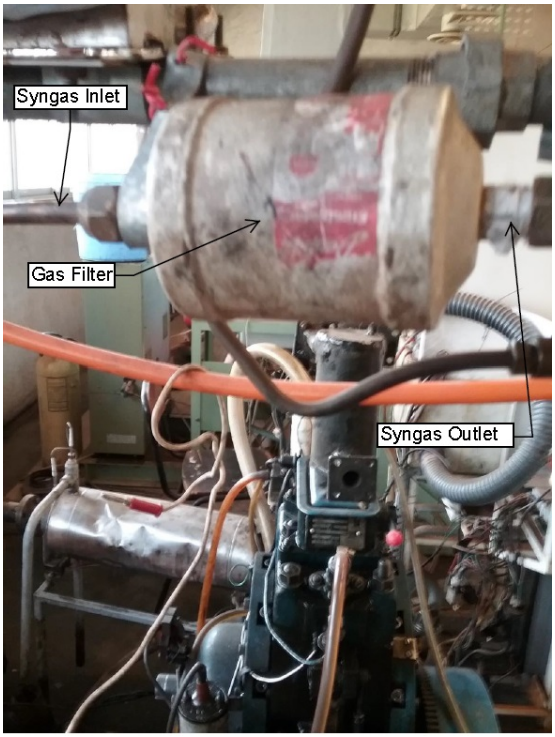

Figure 3.14: Syngas filter

The low flame speed of syngas is more efficiently used in low speed engine (Homdoung et al., 2007). Thus, an engine, which operates at 1500 to 2500 rpm is ideal for syngas application.

3.4 Instrumentation

The engine performance was determined by running the engine using neat diesel in the single fuel mode and then operating it with varying quantities of syngas as the primary fuel and diesel as the pilot fuel in the dual fuel mode. For single mode conditions, the values of cylinder pressure, heat release rate, brake specific fuel consumption, brake thermal efficiency and other performance parameters were directly obtained from the PC interface. In the dual fuel mode, brake specific fuel consumption and brake thermal efficiency were re-evaluated taking into account the effect of energy from the syngas fuel. For this to be done, the quantities of fuels (syngas and diesel) consumed by the engine and the resulting brake power at each condition needed to be measured. In this section, the instruments used

to

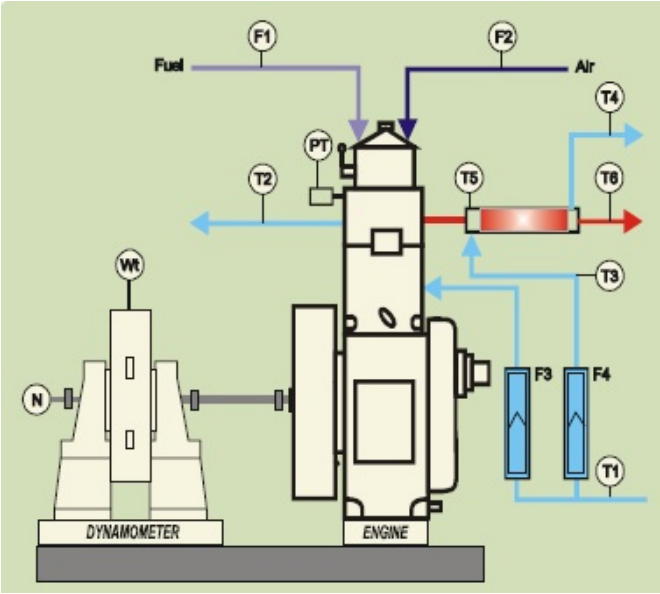

Figure 3.15: Schematic diagram of part of the engine test bench used to record temperatures and flowrates (Mulay et al., 2014)

determine the rate of fuel consumption, engine brake power and exhaust emissions are presented.

The test engine allowed for variation of compression ratio and injection timing to accommodate ignition of different fuels. It also incorporates a pressure sensor and transducer for combustion chamber pressure monitoring. The engine torque under different operating conditions (different injection timing, syngas volume flowrates, varying compression ratios, different engine loads and speeds) were measured using the dynamometer. The direct readings obtained were load (w_t) and speed (N).

A pressure transducer (piezo sensor) measured the in-cylinder pressure variation and the signal sent to the computer data-acquisition system. The rate of heat release for each cycle was calculated in the ICEnginesoft data using Eq. 3.20, where Q, θ, p, V and γ are the heat release rate, crank angle, cylinder pressure, cylinder volume at that point and specific heat ratio respectively (Mulay et al.,

Table 3.9: Research engine temperature

S/No.	Thermocouple No.	Engine Point of Measured Temperature in ^{o}C
1	T_1	Jacket water inlet
2	T_2	Jacket water outlet
3	T_3	Calorimeter water inlet
4	T_4	Calorimeter water outlet
5	T_5	Exhaust gas to calorimeter inlet
6	T_6	Exhaust gas from calorimeter outlet

Table 3.10: Research engine flow measurement.

S/No.	Flowmeter No.	Engine Point of Measured Flowrate in kg/h
7	F_1	Fuel supply to engine
8	F_2	Air supply to engine
9	F_3	Jacket water inlet
10	F_4	Calorimeter water inlet

2014).

$$\frac{\mathrm{d}Q_n}{\mathrm{d}\theta} = \frac{\gamma}{\gamma - 1}\mathrm{p}\frac{\mathrm{dV}}{\mathrm{d}\theta} + \frac{1}{\gamma - 1}\mathrm{V}\frac{\mathrm{dp}}{\mathrm{d}\theta} \tag{3.20}$$

Exhaust emissions and syngas composition were tested, analysed and recorded for different operating conditions using an gas analyser of ecom-J2KNpro model shown in Figure 3.17.

3.5 Measurement of Parameters

The parameters measured are those that indicate the combustion characteristics, engine performance and emissions from engine. The combustion data includes in-cylinder pressure and heat release rate burning rates whilst performance data include power developed in the engine,

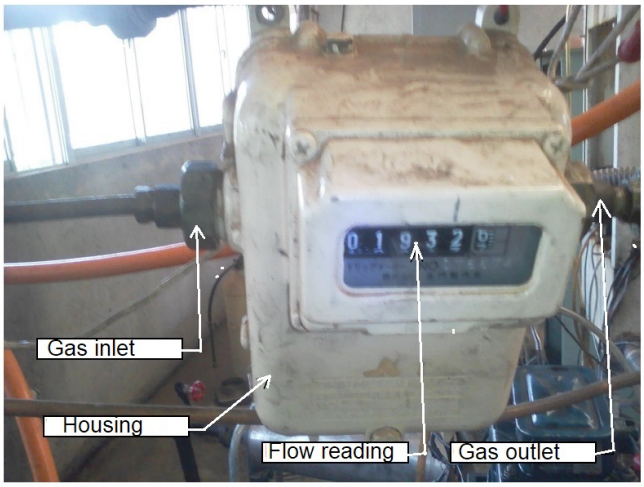

Figure 3.16: Syngas flow meter

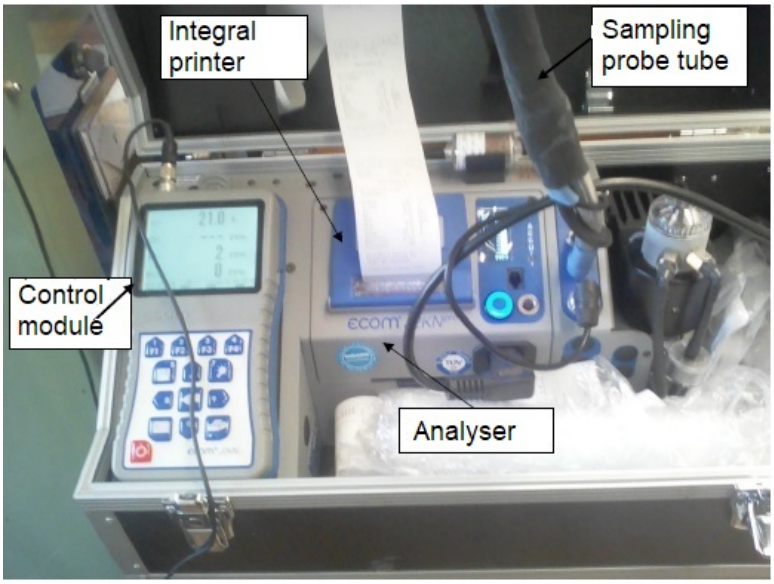

Figure 3.17: Exhaust emissions and gas analyser

the quantity of fuel (syngas and diesel in varying volumes) consumed in developing this power and engine efficiency in converting the energy from fuel into useful energy is also analysed. Emissions characteristics invovles analyses of different gases comprising the exhaust gas. These emissions may include CO, NO_x, CO_2, HC, PM (smoke and soot). Analyses of exhaust temperature was also carried out.

3.5.1 Combustion Measurement

Combustion characteristics are analysed by measurement of cylinder pressure, net heat release rate and mass fraction burned.

3.5.1.1 Measurement of Cylinder Pressure

Cylinder pressure is obtained over crank rotational angle for the compression and expansion strokes of the engine operating cycle and provides quantitative information on combustion progress. Both heat release and fuel mass burned are important factors that indicate completeness of combustion (Heywood, 1988). The cylinder pressure measurement has two system states; the instantaneous angular velocity of the crankshaft and the pressure of the firing cylinder. The crank angle is measured using a crank angle sensor of Kubler make, model 8.3700.1321.0360 and an incremental shaft encoder used to determine the position of the engine crankshaft rotation at 360 pulses per revolution. The cylinder pressure was measured with miniature piezo sensor Models

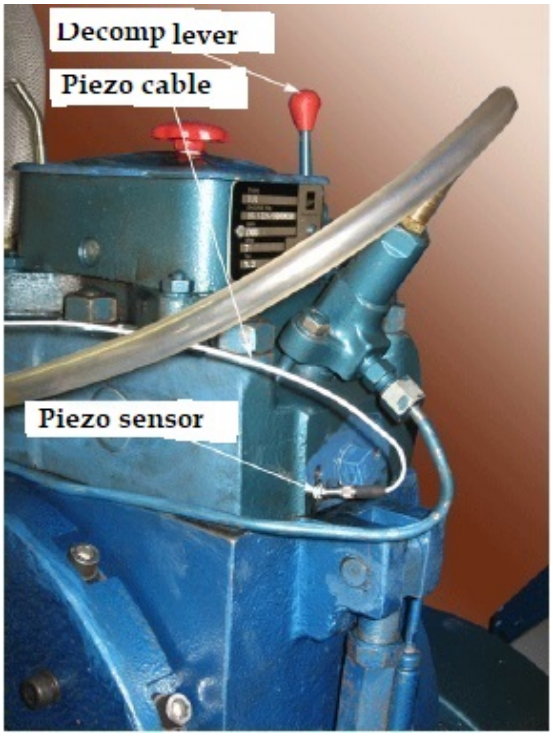

Figure 3.18: Cylinder pressure sensor

SM111A22 and M108A02 alongside a versatile transducer purposely designed for dynamic measurement of compression and combustion pressures (Figure 3.18). All signals were sent to a data acquisition system (ICEngineSoft ver.9.0) to analyse the data (Shital Sharadchandra Mulay et al., 2014).

3.5.1.2 Heat Release Rates

Heat release patterns were analysed based on cylinder pressure data corresponding to the crankshaft position. The values of in-cylinder pressure (p) corresponding to crankshaft angle (θ) position were used to obtain the heat release rate ($\frac{dQ_n}{d\theta}$) of the engine. The heat release rate can be calculated by fuel chemical energy suppressed by the heat loss into the coolant system. The cylinder pressure traces are also used to calculate the mass fraction burnt by the assumption that the mass of the charge burned for the crank angle interval is proportional to the pressure rise due to the combustion (Vipavanich et al., 2018).

$$\frac{\mathrm{dQ}}{\mathrm{d}\theta} - \mathrm{p}\frac{\mathrm{dV}}{\mathrm{d}\theta} + \dot{\mathrm{m}}_f \mathrm{h}_f = \frac{\mathrm{dU}}{\mathrm{d}\theta} \tag{3.21}$$

where,
$\frac{\mathrm{dQ}}{\mathrm{d}\theta}$ - the difference between heat released by combustion of the fuel and heat transfer from the engine, $\frac{\mathrm{dV}}{\mathrm{d}\theta}$ - the rate of work transfer done by the system across the system boundary at a given location, $\dot{\mathrm{m}}_f$ - is the mass flow rate into the combustion chamber h_f - the enthalpy of injected fuel and U - the sensible internal energy of the charge inside the cylinder

Two methods were used to evaluate combustion parameters from the measured pressure data using Eq. 3.21. In both approaches, the cylinder contents were assumed to be at a uniform temperature in each instant during the combustion process. One method yielded fuel energy or heat release rate; the other method yielded a fuel mass burning rate. Where cylinder content is assumed an ideal gas as was done here, the net heat release, $\frac{\mathrm{dQ}_n}{\mathrm{d}\theta}$ is given by Eq. 3.20 (Heywood, 1988).

Eq. 3.22 developed by Krieger and Borman (Vipavanich et al., 2018) for non

flow heat transfer process is used to generate the apparent fuel mass burning rate (MBR) from cylinder pressure. The data obtained so is then used to draw MBR versus crank angle diagram. The equation is also used by the engine data analysis system to obtain these heat release and the fuel burning rate curves.

$$\frac{\mathrm{d}}{\mathrm{d}\theta}(\mathrm{mu}) = -\mathrm{p}\frac{\mathrm{dV}}{\mathrm{d}\theta} + \frac{\mathrm{dQ}}{\mathrm{d}\theta} + \mathrm{h}_f\frac{\mathrm{dm}}{\mathrm{d}\theta} \tag{3.22}$$

where, Mu (= U) is the internal energy of burning fuel and $\frac{\mathrm{dm}}{\mathrm{d}\theta}$ is rate fuel mass burned w.r.t. to crank angle.

3.5.2 Performance Measurement

The parameter measure are the torque, speed. indicated and brake power, quantity of fuel consumed, fuel and air flow to combustion chamber.

(A) **Measurement of Torque**

Brake power is the actual engine power output obtained at the engine crankshaft. The engine brake power was determined through the measurement of torque and angular speed of the engine crankshaft. Subsequently, the engine torque and the corresponding angular speed were used to determine brake power as shown in Eq. 3.23 (Heywood, 1988). On the other hand, Indicated Power (IP) is power developed in the cylinder by combustion of fuel. There are two methods of finding the IP of an engine i.e. by use of indicator diagram and morse test. The first method was applied in this research to determine the IP.

The output torque from the engine was measured using the EC dynamometer described in referenceB. The measured values were then recorded in the PC for various operating conditions. The data obtained was analysed to obtain the engine performance characteristics under the given operating conditions.

From the torque(τ) measured and the given engine specifications, it was possible to determine the brake power using Eq. 3.23 and brake mean effective

pressure (bmep), (Eq. 3.24) (Heywood, 1988; Mulay et al., 2014). Other performance parameters obtainable from torque measurement are brake thermal efficiency and brake specific fuel consumption (Eqs. 3.26 and 3.27) (Heywood, 1988).

To evaluate P_b from torque (τ_b) which was measured in the dynanometer, Eq. 3.23 is applied:
i.e.

$$\tau_b = \frac{P_b}{2\pi N} \tag{3.23}$$

where,

$$P_b = 0.5 \cdot \text{bmep} \cdot NV_d, \tag{3.24}$$

and bmep is the brake mean effective pressure, N is the number of revs the engine runs per second and referring to Figure 3.19, V_d - the swept (displacement) volume, V_d:

$$V_d = N_c(\pi/4)B^2S \tag{3.25}$$

where, N_c - number of engine cylinders , S - Stroke, and B is cylinder bore (m).

To determine brake thermal efficiency (η_{th}) and brake specific fuel consumption (bsfc) when ran in dual-fuel mode Eqs. 3.26 and 3.27 are applied:
i.e.

$$\eta_{th} = \frac{P_b}{m_s LHV_s + m_D LHV_D} \tag{3.26}$$

and

$$\text{bsfc} = \frac{m_s + m_D}{P_b} \tag{3.27}$$

where, m_s and m_D are mass flows of syngas and diesel consumed in kg per hour respectively. However, values were converted from values (m^3/min) read from the flow meters whose accuracy has been quoted at $\pm$ 5% of m^3/s

(Table 3.12 in ref. 3.8.2). For this engine, and when running on neat diesel, Eq. 3.28 and Eq. 3.29 apply (Mulay et al., 2014),
i.e.

$$\eta_{Bth} = \frac{360\mathrm{P}_b \times 10^3}{\mathrm{m}_D \mathrm{LHV}_D} \tag{3.28}$$

$$\mathrm{bsfc(kg/kwh)} = \frac{\mathrm{m}_D}{\mathrm{P}_b} \tag{3.29}$$

(B) **Measurement of Indicated Power**

A dynamic pressure sensor (piezo sensor) was fitted in the cylinder head to sense combustion pressure. A rotary encoder was fitted on the engine shaft for crank angle signal. Both signals were simultaneously scanned by an engine indicator (electronic unit) and communicated to the computer. The computer software draws in-pressure-crank angle, pressure-volume plots, computes indicated power of the engine and converts pressure-crank angle plot to pressure-volume plot (Mulay et al., 2014);

Work per cycle and thus the Indicated Power (IP) were determined analytically using the geometry of IC engine in Figure 3.19 and Eqs. 3.30 to 3.34 (Heywood, 1988). The stroke,S and crank radius, 'a' are related as shown in Eq. 3.30;
i.e.

$$\mathrm{S} = 2\mathrm{a} \tag{3.30}$$

and, Average Piston Speed, U_p :

$$\mathrm{U}_p = 2\mathrm{SN} \tag{3.31}$$

also,
Compression Ratio (CR) of the engine is as defined by Eq. 3.32:

$$\mathrm{CR} = (\mathrm{V}_c + \mathrm{V}_d)/\mathrm{V}_c \tag{3.32}$$

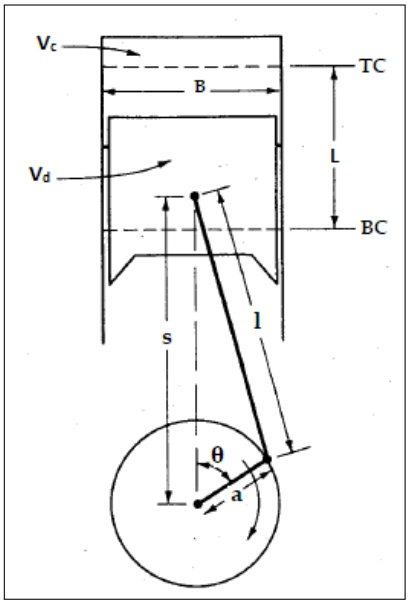

Figure 3.19: Geometry of cylinder, piston, connecting rod, and crankshaf (Heywood, 1988)

where, V_c - engine clearance volume. The surface area of a flat-topped piston, A_p is as given Eq. 3.32,

i.e.

$$A_p = (\pi/4)B^2 \tag{3.33}$$

and, work per cycle,W is a given in Eq. 3.34,

i.e.

$$W = \int pA_p dx \tag{3.34}$$

where, p - pressure in combustion chamber and x - the distance the piston moves. and Indicated Power (IP) is evaluated as shown in Eq. 3.35,

i.e.

$$\text{indicated Power (IP)} = \frac{W_d\left(\frac{N}{n}\right)}{6N_c \times 10^4} \tag{3.35}$$

where, W_d - workdone in a cycle/number of cylinders.(Nm), N - engine speed in rpm and n - Number of strokes per revolution (for this engine = 2).

The value of W_d in Eq. 3.35, for this research engine, was obtained from Eq. 3.36.

$$W_d = A_d X_f Y_f \times 10^5 \tag{3.36}$$

where, X_f represent the volume of cylinder in m^3, Y_f represent in-cylinder pressure in bar and A_d is the area of diagram in m^2, all obtained in the engine PV diagram.

(C) **Measurement of Fuel Consumption and Thermal Efficiencies**

The measurements of fuels and airflow rates were done to determine fuel consumption, thermal and volumetric efficiencies. In the dual-fuel mode, measurement of fuel consumption for the two fuels (syngas and neat diesel) was done separately. Further, flow rates were measured under different engine operating conditions. The values obtained from the ICEngine softdata were adjusted for each measurement to take into account the contribution or the effect of syngas in the final fuel consumption, thermal and volumetric efficiencies used in engine performance analysis.

The flow of syngas into the combustion chamber was measured using a gas flow meter. The syngas from the gasifier had sufficient pressure to flow through the gas filter, the heat exchanger coil and onward through the flow meter, mixing chamber (where it mixes with suction air) and into the engine chamber. The pressure drop observed all through the system was less than 1 bar except in the mixing unit where due to gas expansion pressure fell to 2 bar. The flow meter was mounted on the engine and its inlet connected to the outlet of syngas filter (Figure 3.16) and by use of a flexible hosepipe was connected to the engine via the syngas-air mixer.

(D) **Diesel Fuel Consumption**

In dual-fuel mode, engine power is obtained from the combustion of the two fuels. Each fuel contributes a percentage to the total fuel energy. The contribution of diesel in this experiment was computed by measuring the diesel fuel flowing into engine for different flowrates of syngas. The ICEnginesoft data recorded the diesel flow to the engine at every instance during engine operation.

To test the recorded flowrate values, random measurements were done. The volumetric flow was measured using a glass burette having graduations in millilitres (ml). During each test, the volume flow was measured after every six minutes for each speed or load and then using the diesel density (873 kg/m^3), fuel consumption in (kg/hour) was calculated. This was compared with the data recorded by ICEngines soft data. No major variation were observed, thus the system values were adopted throughout for both diesel and airflow.

Indicated thermal efficiency η_{Ith} was determined using Eq. 3.37.
i.e.

$$\eta_{Ith} = \frac{360000\mathrm{P}_d}{\mathrm{m}_D \mathrm{LHV}_D} \tag{3.37}$$

and, Mechanical efficiency (η_{mech}) defined as the ratio of brake power (BP) (delivered power) to the indicated power (IP) (power provided to the piston) (Eq. 3.38) (Heywood, 1988),
i.e.

$$\eta_{mech} = \frac{\mathrm{BP}}{\mathrm{IP}} \tag{3.38}$$

Also, Volumetric efficiency, η_{vol} is defined as the ratio of the air actually induced at ambient conditions to the swept volume of the engine. In practice, the engine does not induce a complete cylinder full of air on each stroke, and it is convenient to define volumetric efficiency as in Eq. 3.39 (Heywood, 1988).

$$\eta_{vol} = 60\rho_{air}\frac{\dot{\mathrm{m}}_a}{\frac{\pi}{4}\mathrm{B}^2\mathrm{S}\frac{\mathrm{N}}{\mathrm{n}}\mathrm{N}_c.} \tag{3.39}$$

where, η_{vol} - Mass of air consumed/mass of flow of air to fill swept volume at atmospheric conditions, N - Rotational speed of engine rpm, n - number of revolutions required to complete one engine cycle, N_c - number of cylinders, B - bore and S - stroke.

The airflow to the engine was measured and evaluated based on Eq. 3.40 (Mulay et al., 2014).

$$\dot{\mathrm{m}}_a = 3600\mathrm{C}_d\frac{\pi}{4}\mathrm{B}^2\sqrt{2\mathrm{g}\ \mathrm{h}_w\rho_w/\rho_{air}} \tag{3.40}$$

where, $\dot{\mathrm{m}}_a$ - air flow (kg/hr), ρ_w - water density, ρ_{air} - air density at working condition and h_w - water height in the fitted piezometer (Mulay et al., 2014).

3.6 Emissions Test

For this test, emissions contained in the exhaust gases were analysed using an ecom-J2KNpro model gas analyser. It comprised a control module, different gas sensors and filters, sampling probe, gas cooler, condensate evacuation unit and an integral printer as shown in Figure 3.20.

The parameters analysed in the particular unit are shown in Table 3.11

The sample of the exhaust gas collected was allowed to flow through a gas hose that directed it to the emissions analyser where parameters outlined in Table 3.11 were measured and recorded under the various operating conditions. Measurements were performed in the core stream of the exhaust gas channel (probe was placed in the highest gas temperature area). A trend indication for $\mathrm{T}_{exhaust\,Gas}$ helped in the search for the right temperature level. As long as the display showed a plus (+) symbol,

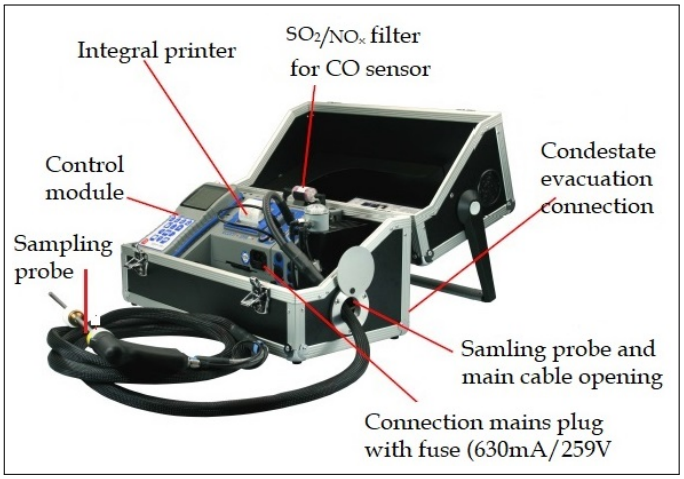

Figure 3.20: Gas analyser of model ecom-J2KNpro (Binz and Binz, 2015)

the measured temperature was increasing, meaning the probe tip moved towards the core stream. When a minus (-) symbol was displayed, the probe was pulled out of the core stream and the temperature sunk and then readings were obtained.

CO_2, efficiency, losses, excess air and dew point values were determined only when realistic values for the basic parameters of O_2 and temperatures were obtained. Ferguson and Kirkpatrick (2016) presented Eqs. 3.41 and 3.42 for calculations of other parameters that could not be measured directly. For these values to be determined, the manufacturer of the analyser (Binz and Binz, 2015) indicated that it was necessary to ascertain that:

$O_2 <$ 20.5 % and $T_{exhaust\,gas}$ - T_{air} > + 5^{o}C. Correct measured values were displayed first after a short delay, which was necessary for the gas transport and the build-up of a stable electrochemical reaction at the sensors. This period lasted between 1 and 1.5 minutes. For recording, printout and evaluation it was necessary to wait until steady readings were displayed. In some instances, unstable pressure conditions in the exhaust channel caused deviations of more than 2 ppm in the readings. When the measured values stabilised the results were printed out (Binz and Binz, 2015).

3.6.1 Emission Measuring Procedure

The sampling probe was positioned in the exhaust pipe so that the in-built thermocouples were fully surrounded with the gas (Figure 3.21). The content of the exhaust gas was displayed on the gas analyser control unit display. The readings of HC, NO, NO_2, NO_x, SO_x, CO_2, O_2, C_xH_y and soot and oil traces (particulate matter) for each test were allowed to stabilize and then the results were printed out. Sensors for gases indicated in the Table 3.11 (marked "optional") needed to be fitted in the provided slot for analyses of those gases to be possible

3.6.2 NO_x and HC Emissions

(I) The rate of NO_x formation is given by Eq. 3.41:

$$\frac{\mathrm{d}[NO_x]}{\mathrm{dt}} = \frac{6 \times 10^{16}}{\mathrm{T}} exp\left(\frac{-69,090}{\mathrm{T}}\right)[O_2]_e^{1/2}[N_2]_e \tag{3.41}$$

where [ ] denote species concentrations in moles per cubic cm and are determined from the gas analyser, $[\,]_e$ species concentration at equilibrium and T is the maximum absolute temperature in combustion chamber as read from the pyrometers.

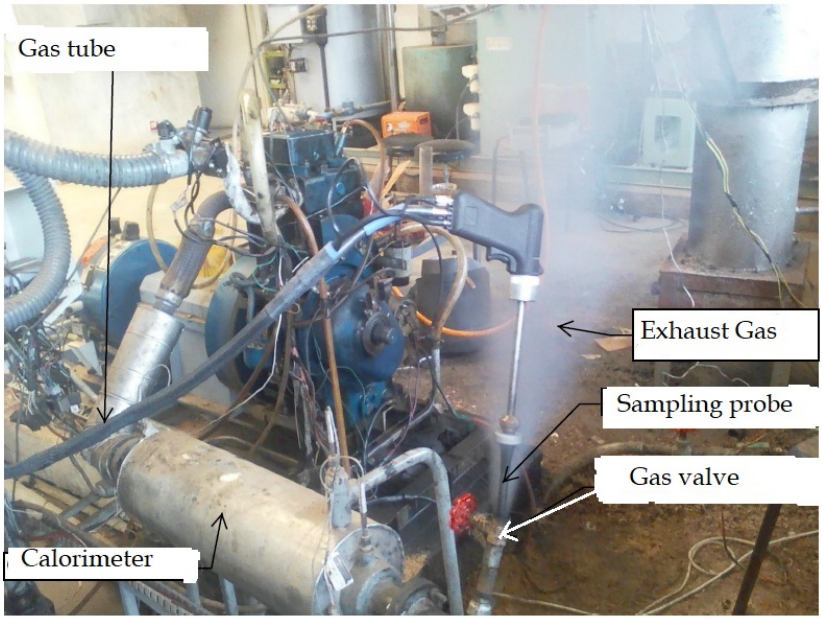

Figure 3.21: Engine exhaust gas sampling

(II) The rate of HC formation is given by Eq. 3.42:

$$\frac{\mathrm{d[HC]}}{\mathrm{dt}} = -6.7 \times 10^{15} exp\left(\frac{-18,735}{\mathrm{T}}\right) \tilde{\mathrm{x}}_{HC} \tilde{\mathrm{x}}_{O_2} \left(\frac{\mathrm{p}}{\mathrm{RT}}\right)^2 \tag{3.42}$$

where, $\tilde{\mathrm{x}}_{HC}$ and $\tilde{\mathrm{x}}_{O_2}$ are the mole fractions of HC and O_2 respectively also obtained from exhaust gas analyser and t in seconds (Ferguson and Kirkpatrick, 2016).

3.7 Experiment Procedure

In this section, the procedures followed to determine the optimal engine condition for the raw syngas from gasifier to become usable in fuelling ICEs are discussed. Steps followed to carry out the experiments including varying of syngas-diesel composition; compression ratios (CR) and injection timing (IT) are presented below. The experimental set conditions provided and fixed by the engine manufacturer were three set constant speed; 1000, 1250 and 1500 rpm, four constant loads; no-load, half, three-quarter and full loads, and four injection timing positions; 20.8° CA bTDC, 23° CA bTDC, 25.175° CA bTDC and 27.4° CA bTDC. These adjustment could only be done in respect of those set positions hence their adoption for the present research.

3.7.1 Experimental Apparatus

The experimental setup is as shown in Figure 3.22. A PC was used as an interface and displayed the engine parameters. A single cylinder 4-stroke engine coupled to a dynanometer and control panel also formed part of the unit.

3.7.2 Control of Fuel-air Mixture

This subsection describes methods of fuel selection, fuel preparation and fuel regulator and stop valves calibration. The engine governor controlled the pilot diesel. The governor regulated fuel based on the engine speed. In dual fuel mode, it increased or decreased the amount of diesel fuel injected as necessary, to maintain engine output in the face of decreasing or increasing syngas energy content (Wagemakers and Leermakers, 2012).

Table 3.11: Parameters and Range Analysed by the Gas Analyser (Binz and Binz, 2015)

Parameters	Range	Principle of measurement
O_2	0 ... 21 vol-%	Electrochemistry
CO	0 ... 4000 ppm	Electrochemistry
CO % (Option)	4000 ... 63000 ppm	Electrochemistry
NO	0 ... 5000 ppm	Electrochemistry
NO_x	0 ... 1000 ppm	Electrochemistry
SO_2	0 ... 5000 ppm	Electrochemistry
H_2S	0 ... 500 ppm	Electrochemistry
H_2	0 ... 2000 ppm	Electrochemistry
HCL	0 ... 100 ppm	Electrochemistry
C_xH_y	0 ... 4 vol-% (CH_4) ppm	Catalytic
C_xH_y	0 ... 2000 ppm (C_3H_8)	Infrared
C_xH_y	0 ... 30000 ppm (CH_4)	Infrared
CO % (Option)	0 ... 63000 ppm	Infrared
CO_2	0 ... 20 vol-%	Infrared
Air Pressure	300 ... 1100 hPa	DMS bridge
CO_2	0 ... CO_{2max}	Calculation
$T_{Ex.Gas}$	0 ... 500^oC	NiCr/Ni
T_{Air}	0 ... 99^oC	Semi-conductor
Difference Pressure	300 ... +/- 100 hPa	DMS bridge
Efficiency	0 ... 100%	Calculation
Losses	0 ... 99.9%	Calculation
Excess air	0 ... ∞	Calculation
Soot and oil trace (Particulate Matter)	0 ... 9.9%	Calculation

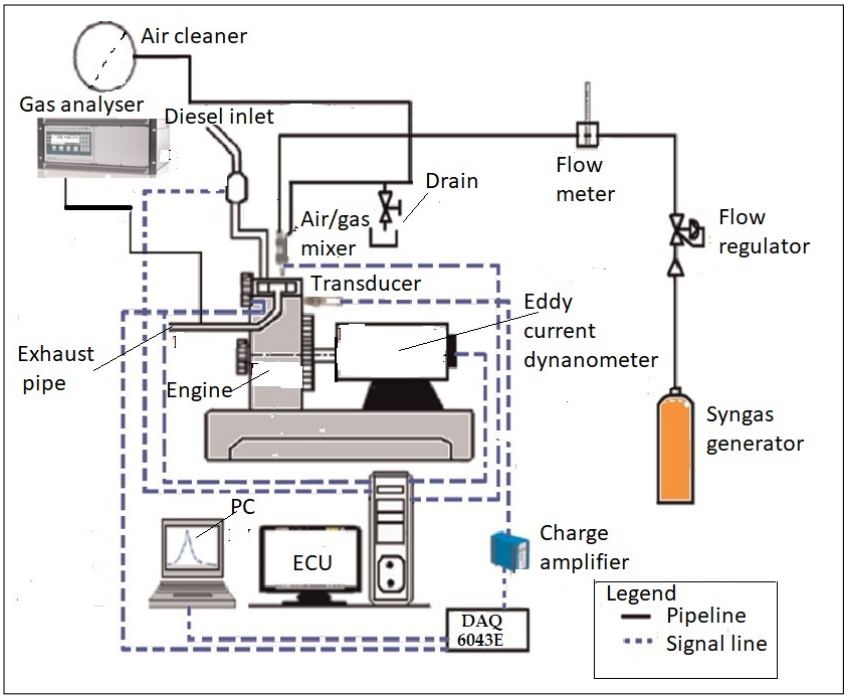

Figure 3.22: Research engine pipes and control circuit (Hagos et al., 2016)

The engine air system comprised air box with an orifice meter and manometer, airflow and pressure transmitter. The transmitter had a range of 0 - 250 mm water column (WC) and was connected to engine performance analysis software (ICEngineSoft), where air volume flowrate and pressure were processed and recorded. The volume flow rate of engine air supply was controlled by removing the air tank and pipes connected to it to reduce the air pressure losses and increase volumetric efficiency. The disconnected hosepipe was then connected to the syngas-air mixing unit (Mahgoub et al., 2017).

To deliver a homogeneous syngas-air mixture into the combustion chamber a mixing device was designed and developed as described in subsection 3.3.2. Other components added to control the supply of syngas were; a non-return valve, pressure regulator, and flow meter (Figure 3.22). Before the measurement of syngas volume flowrates, the stop valve and the flowmeter used were calibrated as follows: syngas was passed through the flowmeter and the stop valve, with the same volume then passed through a factory calibrated LPG mechanical flowmeter.

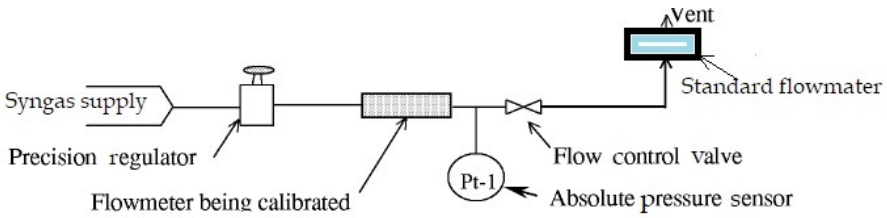

Figure 3.23: Flowmeter and stop valve calibration

By measuring the rate of flow through the standard flowmeter, the volume flow rate of the syngas was accurately determined. Values for the two flowmeters were correlated and the flowmeter in use was adjusted until its readings were the same with those of the standard flowmeter (Figure 3.23). Five positions on the stop valve that corresponded to 0°, 180°, 360°, 540°, and 720° were marked and the flowrates associated with each mark obtained from the standard flowmeter. During the calibration, the precision flow regulator controlled flowrate. The syngas volume flowrates (SVF) calibrated on the manually operated stop valve as indicated by the five marked positions were: complete valve shut off (0°), 0% SVM; 180°, 25% SVM; 360°, 50% SVM; 540°,75% SVM and 720°, 100% SVM. The flowmeter readings were taken after every 6 minutes for each valve settings. Two fuels were used in the experiment, petroleum diesel and syngas. Their compositions are given in Table 4.1.

In fuel preparation, petroleum diesel fuel was used for basic engine testing under a normal diesel operation without any modification being made to the engine. For the engine operation under dual fuel mode, a blend of diesel and syngas, in varying SVM and diesel, used as the pilot fuel, were prepared. The quantity of syngas provided for the dual fuelling process was controlled to vary the equivalence ratio. Mixing of syngas with air and diesel was achieved in the combustion chamber. Performance, combustion and emissions measurements were done for diverse blends of diesel and syngas volume flowrate of 100%, 75%, 50%, and 25%. Numerous studies have shown that syngas-diesel blend operated in dual fuel mode engines leads to reduced pollutant emissions in exhaust gases. To achieve this

state, some degree of modification needed to be done on the engine. Some are structural as seen in Figure 3.22 and others are effected by carrying out engine adjustments as described earlier in subsection 3.3.4.

3.7.3 Varying of Compression Ratio

The research engine used in this experiment had a feature for varying the compression ratio (CR). A fitted tilting block mechanism is used to vary the CR without changing the geometry of the combustion chamber. The mechanism works by varying the TDC position of the piston (Ferguson and Kirkpatrick, 2016; Tomar et al., 2013).

To study the effect of varying CR on performance and emission characteristics of the dual fuel engine, the engine was operated in the CR range of 12 - 18. Performance and emission experimental data was collected for CRs of 18 (17.5), 16, 14 and 12. Figure 3.24 illustrates the mechanism for adjusting compression ratio of the engine. By opening provided Allen bolts and moving the adjuster, compression ratios of 18, 17, 16, 15,14 and 12 can be set as per the mark.

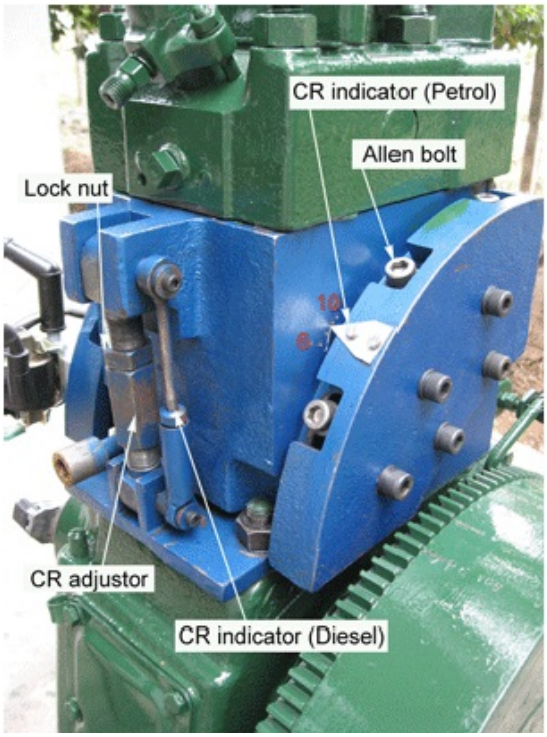

Figure 3.24: Compression ratio adjustment mechanism

3.7.4 Varying the Injection Timing (IT)

Fuel injection system is designed to deliver fuel into the combustion chamber, in the atomised form and most appropriate piston position during the compression stroke. These two factors (fuel form and position of piston) greatly influences the engine performance and emissions characteristics. The fuel form is dictated by the design and the maintenance state of the injectors, whilst the fuel IT is determine by the piston/crank position when diesel injection occurs. Thus, an optimum point where the engine performance and emission characteristics are maximum can be achieved through injection timing.

Figure 3.25 shows the engine mechanism for adjusting the fuel injection timing (IT). Adjustment is effected by manually rotating the flywheel and monitoring when the fuel spills from the high-pressure fuel pipe connector in the injection pump. Timing, for the engine injection point was set at 23° bTDC and was marked point "F" on the flywheel which was eight teeth from TDC mark as shown in the the figure. To adjust the injection timing, the high-pressure fuel pipe from the fuel pump was removed and the decompression lever raised to a vertical position to free the flywheel for hand operation (Mulay et al., 2014). In adjusting the engine was set for diesel operation and also diesel fuel made available at the fuel pump, then the procedure adapted was as follows:

Each two teeth from the "F" mark on the flywheel represent crank angle of 2.2°. Therefore, from the standard set injection timing of 23°, addition of two teeth advanced injection timing to 25.2° bTDC. Investigation was done for the injection timings of 20.8°, 23.0°, 25.2°, 27.4° and 29.6° bTDC. Performance for the engine in dual duel mode and with advancement of 29.6° was observed to be erratic, thus was unreliable.

For this analysis, engine performance, combustion and emissions were studied to optimising the fuel blend and engine specifications for dual fuel engine that uses syngas and diesel as the fuels. These characteristics were investigated under the following conditions:

(a) Varying engine load: loads of 0 kg, 6 kg, 10 kg and 12 kg were applied at varying speeds and varying syngas volume flowrate,

(b) Varying speeds when the engine was operated with syngas-diesel blend of different syngas proportions,

(c) Varying composition of syngas-diesel blend and operated under varying conditions of load, speed compression ratios, fuel injection timing,

(d) Varying compression ratios at different speeds and with varying proportions of syngas-diesel blend,

(e) Varying injection timing by advancing the timing to 25.2° and 27.4° bTDC, and retarding it to 20.8° from the standard of 23.0°.

Figure 3.25: Injection timing adjustment system

3.8 Uncertainty in Experiment Analysis

The accuracy of an experiment, as Bevington and Robinson (2003) observed, is generally dependent on how well systematic errors that made results different from the "true" values with reproducible discrepancies, could be controlled or compensated. They identified faulty calibration of equipment, in-dexterity or bias on the part of the observer as the main source of these errors. Errors lead to uncertainties in the obtained results. Uncertainties in experimental results can be separated into two categories: those that results from fluctuations in measurements and those associated with the theoretical description of the results. The preoccupation with the error analysis was for the purpose of extracting from the data the best estimates of theoretical parameters and help in understanding the effect of the errors on the results. This helped to determine the confidence placed on the presented results.

For this research, the performance and emission of the modified research engine was determined by measurement using a number of equipment. The resultant uncertainties obtained by considering independent and dependent variables for several measurements such as torque and brake power are presented. In this research, two sources of uncertainties were identified: instruments and statistics. The equations used to combine uncertainties in separate measurements to find the error in a calculated result are presented.

3.8.1 Instrumental Uncertainties

Instrumental uncertainties are generally determined by examining the instruments and considering the measuring procedure to estimate the reliability of the measurements. In this experiment, several instruments were used to measure the required parameters. These equipment had inherent inaccuracies as indicated by the manufacturers that influenced the overall measurements. Manufacturers regularly specify equipment accuracy in tolerance form in the operating manuals was the case here.

Bevington and Robinson (2003) showed that it was possible to make repeated measurements, then an estimate of the standard deviation is calculated from the spread of these measurements. Further, it was explained that the resulting estimate of the standard deviation corresponded to the expected uncertainty in a single measurement. In principle, this internal method of determining the uncertainty should agree with that obtained by the external method of considering the equipment and the experiment itself. This is the technique that was adopted for calculating the uncertainties in this experiment.

The investigation of the engine performance involved measurement of torque, fuel consumption (diesel and syngas), airflow in a given time and the engine speed at a given load. The measured quantities were used to calculate the brake power, brake specific fuel consumption, brake thermal efficiency and volumetric efficiency among other performance parameters as seen in the example below regarding brake thermal efficiency (BTE).

For instance, the BTE is evaluated from the brake power, fuel consumed, heating value of fuels and time taken for the fuel consumption as related by Eq. 3.26 in Section 3.4. The total uncertainty analysis values and measurement accuracies of equipment are calculated using Kline and McClintock method, Eq. 3.43 (John R. Taylor, 1997).

$$\sigma = \sqrt{\left(\frac{\partial BTE}{\partial p}\right)^2 \sigma_p^2 + \left(\frac{\partial BTE}{\partial v}\right)^2 \sigma_v^2 + \left(\frac{\partial BTE}{\partial t}\right)^2 \sigma_t^2 + \left(\frac{\partial BTE}{\partial s}\right)^2 \sigma_s^2} \quad (3.43)$$

Using the 'fractional error add' rule Eq. 3.43 is reduced to Eq. 3.44,

$$\frac{\sigma}{BTE} = \sqrt{\left(\frac{\sigma_p}{p}\right)^2 + \left(\frac{\sigma_v}{v}\right)^2 + \left(\frac{\sigma_t}{t}\right)^2 + \left(\frac{\sigma_s}{s}\right)^2} \quad (3.44)$$

where σ_p^2, σ_v^2, σ_t^2 and σ_s^2 are the uncertainties in the measuring instruments: dynamometer (p), fuel flowmeters(v), stopwatch (t) and fuel burette (s) respectively.

Applying Eq. 3.44 to evaluate uncertainties in BTE using the instruments errors shown in Table 3.12 and the ICEngineSoft errors for sensors ($\pm$ 2.5%) and trans-

ducers (± 2.5%) in the dynamometer when measuring torque and speed, a value of 9.78% was obtained.

3.8.2 Experimental Uncertainty

If the measured quantity, such as fuel consumption, torque and air flow rate represents the quantity recorded per unit time interval, then the uncertainties are called statistical because they arise not from a lack of precision in the measuring instruments but from overall statistical fluctuations in the collections of data. For these statistical fluctuations, the standard deviation for each observation was estimated analytically, without necessarily having to determine it experimentally. Bevington and Robinson (2003) have shown that, if the same measurement were made repeatedly, values were distributed about their mean in a Poisson distribution instead of a Gaussian distribution. The data collected repeatedly under a specified condition showed a spread about the mean. The deviations of these data from the mean was evaluated for a sample result to determine the experimental uncertainty (Eq. 3.45). The coefficient of variation (COV) was used to measure the variability of the obtained data relative to its mean as given by Eq. 3.46.

$$\sigma = \sqrt{\frac{1}{\mathrm{N}-1}\sum_{i=1}^{\mathrm{N}}(\tau_i - \bar{\tau})^2} \tag{3.45}$$

$$\mathrm{COV} = \frac{\sigma}{\bar{\tau}} \tag{3.46}$$

where σ is the standard deviation, N is the number of the repeated measurements, τ_i the instantaneous average torque and $\bar{\tau}_i$ is the mean torque as given by Eq. 3.47.

The standard deviation was expressed as a percentage to give Eq. 3.48.

$$\bar{\tau} = \frac{1}{\mathrm{N}}\sum \tau_i \tag{3.47}$$

$$\sigma = 100 \times \frac{\sqrt{\frac{1}{\mathrm{N}-1}\sum(\tau_i - \overline{\tau})^2}}{\overline{\tau}} \tag{3.48}$$

Here the measured torque was used as the sample parameters for purpose of evaluating experimental uncertainties. The importance of evaluating experimental uncertainties was to establish the suitability of the modified engine to produce reliable results for each engine operating condition. The connected PC and the standard accuracies of measurement as given by the manufacturers of different equipment aided in carrying out measurements. The calculated uncertainties are given in Table 3.12. The uncertainties in each case was below 10%. To determine the uncertainty, five readings were taken at each data point for engine operation at maximum speed of 1500 rpm for no load to full load when fuelled with neat diesel. The results in Table 3.13 indicate the reproducibility of the data at 1500 rpm. The deviation corresponded with the range of accuracy of instrumental uncertainties (John R. Taylor, 1997).

The obtained instrumental and experimental uncertainties show that the data obtained over a repeated set of experiments accurately represented performance of the engine under test.

The details of the collected data and its analysis for engine performance, emissions and exhaust gas temperature are presented and discussed in the subsequent chapter.

Table 3.12: Standard Deviation of Torque

S/No	Engine Loading (kg)	Average Torque (Nm)	Standard deviation (%)
1	0	0.94	2.72
2	4	6.52	2.65
3	6	10.77	2.38
4	8	16.14	2.64
5	12	20.55	2.76

Table 3.13: Accuracies of the Measurements and Uncertainties in the Results

S/No.	Parameter	Accuracy
1	Load	± 2.5% Nm
2	Speed	±3% rpm
3	liquid Flowrates	±1% m^3/s
4	Gas Flowrates	±2.5% m^3/s
5	Time	± 2.5%
6	Temperature	±2.5% °C
7	NO_x	±2.5%
8	HC	±2.5%
9	CO	±2.5% ppm
10	PM	±2.5%
11	CO_2	±2.5%
12	Heat Values	±4.5%
S No.	Parameters	Uncertainty Analysis
1	Speed	±3%
2	BSFC	± 6%
3	BTE	±9.78%
4	Load	±2.5%
5	Combustion pressure	±4.5%

CHAPTER FOUR
RESULTS AND DISCUSSION

4.1 Overview

In this chapter the experimental results on ICE performance and emissions under the conditions of varying ratios of syngas-diesel fuel blends, are presented and discussed. Also included in this chapter is the effect of compression ratio, injection timing, engine load and varying syngas substitution on the combustion, performance, emissions and exhaust gas temperature of the engine running in dual fuel mode. The analysis examines steps that were taken to test a 3.5 kW, four-stroke, single-cylinder, water-cooled research engine, with SI and CI mode facilities and variable compression ratio operated on dual fuel mode where syngas is used as the primary fuel and diesel as the pilot fuel. The chapter is into four sections arranged to explain the effect of varying compression ratio, load, injection timing and syngas-diesel blend on the engine performance and emission characteristics.

The results for the combustion, performance and emissions characteristics are presented and discussed in subsequent sections. To provide concise results, all the data obtained was analysed, but it is only the best results for combustions, performance and emissions that are presented in this chapter.

4.2 Measured Properties of the Working Fluids

The syngas and air properties and their flow conditions as used in components designs are outlined in the tables that follow. Table 4.1 shows the syngas conditions at the outlet of the small-scale gasifier which were obtained through measurement in a procedure outlined in section 3.5, Moreover, the table shows the diesel fuel properties and flow conditions as obtain in engine information system.

Table 4.1: Syngas Conditions at Gasifier Outlet

S/No.	Quantity	Value
1	Syngas flowrate (m^3/s)	1.67×10^{-3}
2	Temperature of syngas at gasifier outlet ($^\circ C$)	289
3	Syngas pressure at the gasifier outlet (bar)	9
4	Syngas velocity before cooling (m/s)	21.3
5	Syngas temp. after cooling ($^\circ C$)	35
6	Diesel density(kg/m^3)	850
7	Diesel flowrate(m^3/s)	4.71×10^{-7}

Table 4.2: Composition of Syngas

Syngas Composition (%)				
H_2	CO	CH_4	CO_2	Others: COS, N_2, H_2S, SO_2, NH_3
40.6	18.5	3.8	2.4	34.7

The composition of syngas obtained through measurement, as explained in section 3.5, in the gas analyser and evaluation is shown in Table 4.2.

The standard properties and constants applicable to syngas are shown in Table 4.3.

1. The density of syngas was estimated by assuming syngas to be an ideal gas and given equations. By using the molar mass, $\tilde{m}$ and molar gas constant, $\tilde{R}$ = 8314.5 N m/kmol K., specific gas constant, R (Armstrong and Jobe, 1982).

$$\text{i.e.} \qquad R = \frac{\tilde{R}}{\tilde{m}}$$

$$\text{or} \qquad \dot{m} = \frac{\tilde{m}p}{RT} \cdot \dot{V}$$

and,

$$\text{density, } \rho = \frac{\dot{\text{m}}}{\dot{\text{V}}}$$

2. Specific heat cap was determined using rule of mixture calculator:

$$\text{i.e.} \qquad \text{c}_{p(syngas)} = \left(\frac{\text{m}_{H_2}}{\text{m}_{syngas}}\right)\text{c}_{pH_2} + \left(\frac{\text{m}_{CO}}{m_{syngas}}\right)\text{c}_{p_{CO}} + \left(\frac{\text{m}_{CH_4}}{\text{m}_{syngas}}\right)\text{c}_{pCH_4} + \cdots \qquad \text{where, m - atomic mass mass} \tag{4.1}$$

and the standard table of heat capacities for gases (Udoetok, 2013).

3. HHV (Higher Calorific Value or Gross Calorific Value) and LHV (Lower heating value or net heating value) were determined experimentally using an auto adiabatic bomb calorimeter, GallenKamp type. The results from the calorimeter were then used to estimate the values as follows:

$$\underline{\text{HHV} = (\text{K}_1\Delta T) - \text{K}_2}$$
$$\text{m}_{gs}$$

where, ΔT - is the temperature difference of final and starting temperature, K_1 and K_2 are apparatus constant = 10.35 and 0.126 respectively.and,

$$\text{LHV} = \text{HHV(1-W)} - 2.447\text{W}$$

where, W is the weight of moisture content and 2.4447 MJ/kg is the enthalpy of vapourisation for water at 25°C (Acar and Ayanoglu, 2012).

4. Similarly, the thermal conductivity and viscosity for syngas was evaluated using standard tables for thermal constants of gases, Wassiljewa equation for thermal conductivity and Chapman-Enskog model for viscosities (Poling et al., 2001).

$$i.e. \qquad \lambda_m = \sum_{i=1}^{n} \frac{y_i\lambda_i}{\sum_{j=1}^{n} y_j A_{ij}}$$

Table 4.3: Properties of Syngas [Engineering ToolBox, (2003)]

Syngas properties				
Density (kg/m^3)	Specific heat (C_p) (J/kg-K)	Thermal conductivity. (W/m-K)	Viscosity kg/m-s	LHV (MJ/kg)
1.32	2349	0.0185	3.89×10^{-5}	10.462

Table 4.4: Air Conditions at Engine Inlet Manifold

S/No.	Quantity	Value
1	Engine air supply mass flowrate (m^3/s)	4.52×10^{-3}
2	Air temperature at mixer inlet (°C)	26.5
3	Air density (kg/m^3)	1.17
4	Air velocity at mixer inlet (m/s)	16.5
5	Air/syngas temp. after mixing ($°C$)	30

where,

λ_m = thermal conductivity of the syngas,

λ_i = thermal conductivity of the constituents gases,

y_i, y_j = mole fraction of components, and

$$A_{ij} = \frac{\epsilon[1 + (\lambda_{tr_i}/\lambda_{tr_j})^{1/2}(M_i/M_j)^{1/4}]^2}{[8(1 + M_i/M_j)]^{1/2}}$$

where, M = molecular weight, g/mol

ϵ = numerical constant = 1

λ_{tr} = monatomic value of the thermal conductivity and,

$$\frac{\lambda_{tr_i}}{\lambda_{tr_j}} = \frac{\mu_i M_i}{\mu_j M_j}$$

where, μ_i, μ_j = the viscosity of components.

The relation for estimating mixture thermal conductivities is also applicable to viscosities by simply substituting μ for λ (Poling et al., 2001). The air conditions that were measured before mixing with syngas are as outlined in section 3.5 and recorded after mixing (at the entrance to the combustion chamber) are indicated in Table 4.4

4.3 Combustion Characteristics

The three parameters that indicate the nature and quality of fuel combustion in the engine are: in-cylinder pressure (CP), net heat release (NHR) and mass fraction burned (MFB). The combustion process is normally shown on a pressure crank angle diagram with a heat release rate curve sometimes superimposed. This section examines the effect of dual-fuelling on the combustion process of the CI engine when CR and IT are adjusted. Investigation was done for the speeds of 1000, 1250 and 1500 rpm but only results for 1500 rpm and CR 18 (where applicable) since at this speed and CR the In-cylinder pressure, NHR and MFB results were the best.

4.3.1 In-cylinder Pressure

In-cylinder pressure in IC engines is directly related to the power output. Raman and Ram (2013) observed that engine efficiency is directly proportional to the combustion pressure generated during the power stroke. Besides, in-cylinder pressure also influences the formation of NO_x emission in the exhaust of an engine. Another problem associated with in-pressure comes when its rise rate is high. A high-pressure rise per degree of crank angle produces an audible knocking sound in a phenomenon is called 'diesel knock'.

Figure 4.1 shows the variation of in-cylinder pressure as a function of crank angle for varying composition of syngas volume flowrate in an engine operating in dual-fuel mode. Noted was a sharp increase of pressure as the piston approached TDC during the compression stroke, which was followed by a drastic fall in

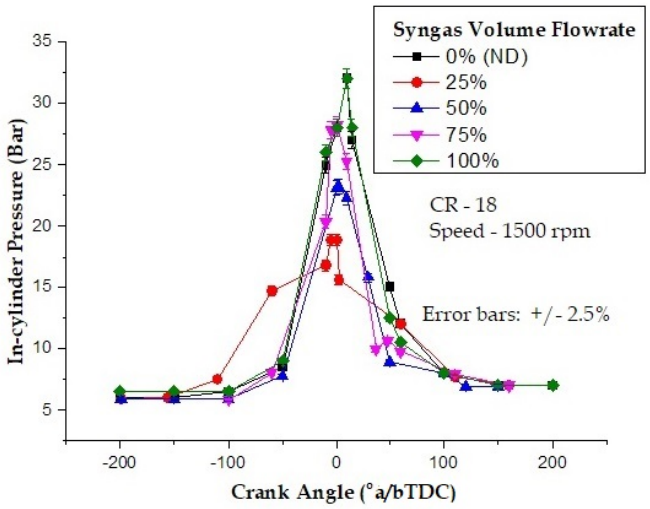

Figure 4.1: Variation of in-cylinder pressure with syngas-diesel blends

pressure after the peak value. Low peak values for the cylinder pressure were noted under dual-fuel operation for all syngas-diesel blends except when neat diesel was substituted with syngas volume flowrate (SVF) of 100%. Neat diesel (ND) and SVF of 100% each had a peak CP value of 32 and 31.8 bar respectively, which was 27.4% higher than the third highest value of 23.22 bar recorded with SVF of 50%. The low values obtained could be attributed to the higher specific heat capacity of the syngas-air mixture, whilst the high mean values recorded for SVF of 100%, probably were due to the prolonged burning duration of charge caused by more fuel in the cylinder, due to there being more syngas and almost a constant amount diesel as in other blends. Brusca et al. (2014) in simulating a variation of in-cylinder mean temperature in a small-size engine reported identical results for diesel and dual-fuel engines. Dhavale et al. (2015) observed similar trends when working with a dual-fuel engine using other gaseous fuel similar to syngas as the primary fuel. Both researches attributed the effect to there being more energy in the syngas-diesel blend with SVF of 100% than in the other blends.

Figure 4.2(a) shows the effects of varying the fuel injection timing (IT) on in-cylinder pressure for the syngas-diesel blend that had a syngas volume flowrate

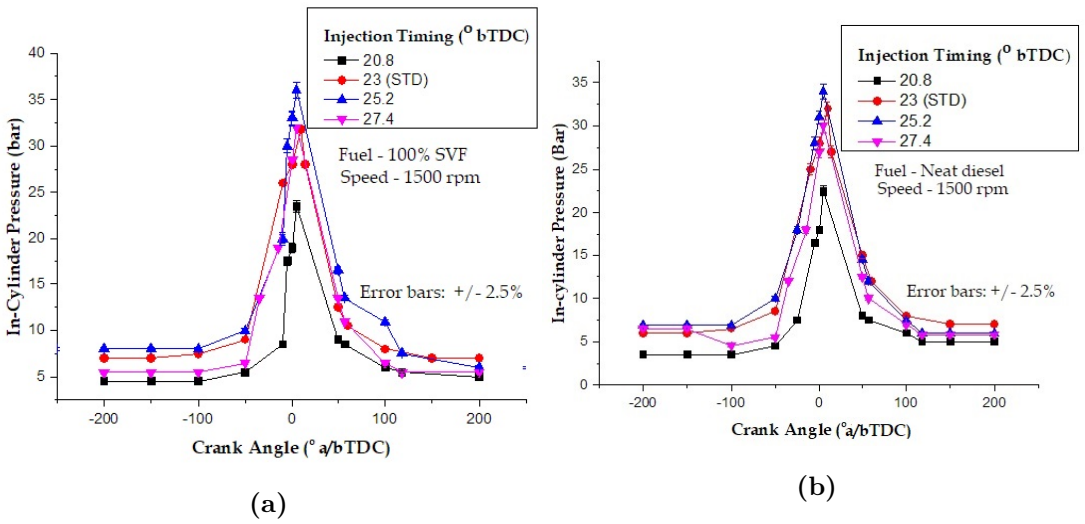

Figure 4.2: Variation of cylinder pressure with injection timing for (a)syngas volume flowrate of 100% (b) neat diesel

(SVF) of 100% . It was observed that the magnitude of the peak pressure (CP_{max}) was higher for advanced IT compared to retarded or standard IT. On the figure it is observed that the pick CP values for an advanced timing of 25.2° CA bTDC in the 100% SVF were 36.0 bar compared to 31.8 bar for standard IT, which is 12.5% higher. Similarly, Figure 4.2(b) shows the effects of varying the fuel injection timing (IT) for neat Diesel (ND). In this case, it was observed that the magnitude of the peak pressure (CP_{max}) was highest for advanced IT of 25.2° CA bTDC reaching a value of 34 bar at 5° CA aTDC. These increases could be attributed to the presence of syngas which has lower flame propagation property compared to neat diesel but due to longer delay periods in early fuel injection, the slow burning fuel will ample time to reach complete combustion that resulted in higher temperatures and pressures in CC. The same engine response was not replicated when the advanced was increased to CA 27.4° bTDC, as the pressure recorded was 32 bar. That would mean the optimum in-cylinder pressure for dual fuel engine are realised with a given fuel IT, the same way the highest pressure of 34 bar a engine fuel with neat diesel reached the peak pressure of 34 bar in standard (CA 20.8° bTDC) fuel IT. Retarding the fuel IT to CA 20.8° bTDC decreased the peak cylinder pressure during first-stage combustion by 29.7% for

ND and by 26.6% for SVF of 100%. This was attributed to more of the fuel being burned after TDC in the expansion stroke. Azimov et al. (2012) have explained the effect on CP of advancing IT to be as a result of better diesel fuel evaporation and mixing with the in-cylinder gas, causing early auto-ignition. Soni and Gupta (2016) observed that a shorter delay period is obtained when injection timing is advanced from 6° to 10° CA bTDC. Adding that shorter delay period results in higher pressure and temperature of diesel and diesel blend at 10° CA bTDC

4.3.2 Net Heat Release

Quantitative information on the heat release rate is obtained by using data from cylinder pressure versus crank angle for the compression and expansion strokes of the engine operating cycles (Heywood, 1988).

Figure 4.3 shows variation of the net heat release (NHR) characteristics with the crank movement under conditions of varying syngas-diesel fuel. Rapidly increasing values were observed in all cases, with dual-fuel mode of syngas volume flowrate (SVF) of 100%, NHR curve exhibiting higher values than even for neat diesel (ND). The largest heat release occur at the CA range of 20 - 40 ° aTDC during the period when burst into spontaneous flame. Values for 50% increased from 0.15 to and 12.5 J/deg. and those for 75%; 3.4 to 16.5 J/deg. for crank angle (CA) interval of 25°. Which indicate heat release takes place within a very short interval hence uncontrolled flame propagation.

This, compared with an increase of about 101% (3 - 7 J) for ND and 90.7% (4.7 - 9 J) in SVF of 100% for the same CA interval. The results indicated a slow followed by rapid flame propagation in all SVFs in dual fuel mode which could be explained as having been caused by the delayed combustion of the syngas fuel. Similar results trends were reported by Mahgoub et al. (2017, 2015c) when studying a four-stroke single-cylinder, water-cooled, direct injection (CI) engine under a dual fuelling mode using simulated syngas with hydrogen content produced from biomass gasification. The study attributed the obtained results to the progress of hydrogen combustion being better controlled at leaner modes of the fuel mixture

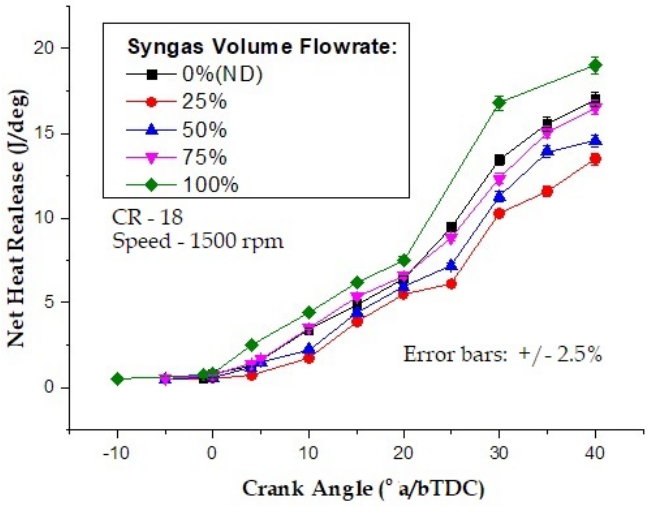

Figure 4.3: Variation of net heat release with syngas-diesel blends at CR 18

which the cases blends with more syngas which has a larger content of diluent. Figure 4.4(a) shows the effect of varying the compression ratio (CR) on the Heat Release Rate (HRR) for ND mode. Low values of HRR, 4.7 - 6.8 J/deg and 0.5 - 5 J/deg., are noted for lower CRs, 12 and 14 respectively, an increase of 50% for the entire period of ignition for CR of 12. Rapid increases were observed for higher CRs,5 J/deg for the CA interval of 25° at CR 18. Similarly, Figure 4.4(b) shows the effect of varying CR on HRR under 100% SVF fuel conditions. The same behaviour was observed, an increase of(4.5 - 8 J/deg) about 56% was recorded for CR 16 and 4.8 - 9 J/deg increase for CA interval of 25° at CR 18. An apparent negative heat release value is seen in the diagrams which occurred before the main start of combustion. The cause was the cooling of the mixture as a result of the interaction between it and the engine surfaces and also due to the expansion it experienced. In the present study, it was shown that HRR values under dual-fuel operation were marginally higher than those for the neat diesel operation which can be attributed to the presence of more fuel (syngas and diesel) in the combustion chamber than is the when fuelled by only diesel. At CR of 18, values recorded for blend with 100% SVF in dual fuel mode was 28.6% higher than for diesel mode. This was caused by the longer crank interval for the combustion of

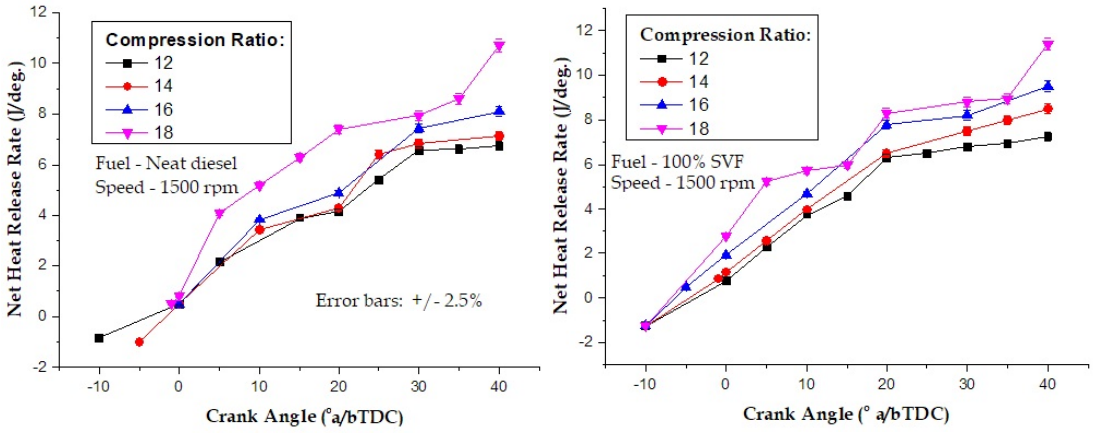

Figure 4.4: Variation of heat release rate with varying CR for (a) neat diesel (b) syngas volume flowrate of 100%

the syngas fuel. The lower but steady values at lower CRs could be attributed to longer ignition delay which in turn increased mass fraction burned (MFB) during the pre-mix phase. On the other hand, increasing CR led to higher combustion temperatures due to higher pressures and subsequent more complete combustion. Mahgoub et al. (2017) obtained similar results were using imitated syngas. Dhavale et al. (2015) in a similar study obtained negative heat release and attributed it to the cooling effect of injected liquid fuel. Figure 4.5 shows the effect of advancing or retarding IT on the HRR of the CI engine operated on diesel fuel mode. A rapid rise of HRR after top dead centre (aTDC), with almost five times increase noted at 25.2° CA bTDC for a CA interval of only 25° was noted. When curves for the two advances 25.2 and 27.4° CA bTDC were compared it seen the curve 27.4° beginning to fall rapidly before CA 40°. This is attributed to the early completion of combustion with fuel the having been supplied earlier than for other IT adjustments.

Figure 4.6(a) shows the same effect when the engine was operated in a dual-fuel mode of SVF 50%. In this case, for a CA interval of 25° at the same IT advance, HRR increased by more than 5 times. Values of HRR recorded with SVF of 100% shown in Figure 4.6(b) indicated lower values by 5.1% compared to those of SVF

50% which is contrary to prediction.

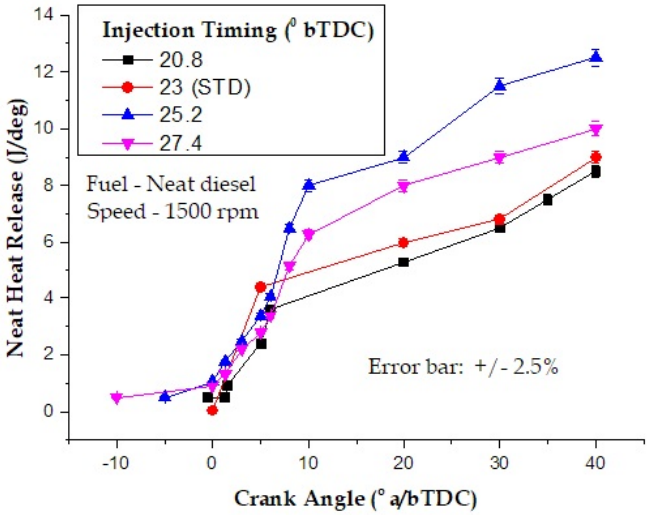

Figure 4.5: Effect of injection timing on heat release rate for neat diesel (CR18)

This behaviour could to there a more homogenous mixture theat provided conducive conditions for a better controlled and complete combustion. Generally, the research observed that advancing the injection timing resulted in early combustion during the cycle. The cause of the rapid rise was due to the heat released from the first-stage combustion. It induced local temperature increase which caused the pilot diesel fuel to self-ignite rather quickly. This resulted in a more complete diesel fuel combustion and more rapid gaseous fuel flame propagation during the first stage. Azimov et al. (2012); Liu et al. (2015) observed a similar trend of heat release in a CI engine and attributed it to the first stage ignition that induced rapid combustion and an increased high heat release rate during the second stage due to the rapid heating of the end-gas region.

4.4 Performance Characteristics

Brake thermal efficiency (BTE) and brake specific fuel consumption (BSFC), are the two parameters that are key indicators of engine performance.

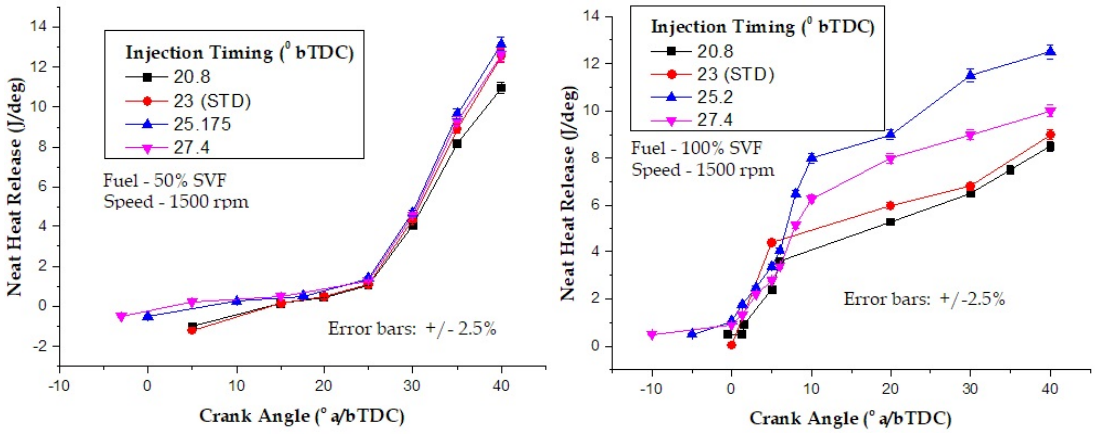

(a) **(b)**

Figure 4.6: Variation of heat release rate with injection timing at CR18 for syngas volume flowrate of (a) 50% (b) 100%

Other performance parameters are volumetric and mechanical efficiency, which are also used for analysis of engine performance.

4.4.1 Brake Specific Fuel Consumption

For the present study, tests were conducted at CRs of 18, 16, 14 and 12 for neat diesel and the syngas-diesel blend of 25%, 50%, 75% and 100% syngas volume flowrate (SVF), as the load was varied at constant speeds of 1000rpm, 1250 and 1500 rpm. Results obtained showed that the lowest values of BSFC were obtained when the engine ran at a full speed of 1500 rpm and CR of 18.

Figure 4.7(a) shows the effect of load on BSFC for various syngas-diesel blends for a dual-fuelled CI engine at the speed of 1500 rpm and CR 18. It was noted that BSFC value reduced by 90% as the load was increased from no-load to three-quarter load. Figure 4.7(b) also shows the same effect on BSFC for the same fuel and speed but with CR adjusted to 16.

The investigation observed that BSFC decreased to a third when the load was increased from no-load to full in diesel mode. Comparing the results obtained with CRs of 16 and 18 at 1500 rpm and full load: for neat diesel, the value decreased by 12% (0.93 - 0.82 kgkWh) and by 118% (1.7 - 0.78 kgkWh) for 100%

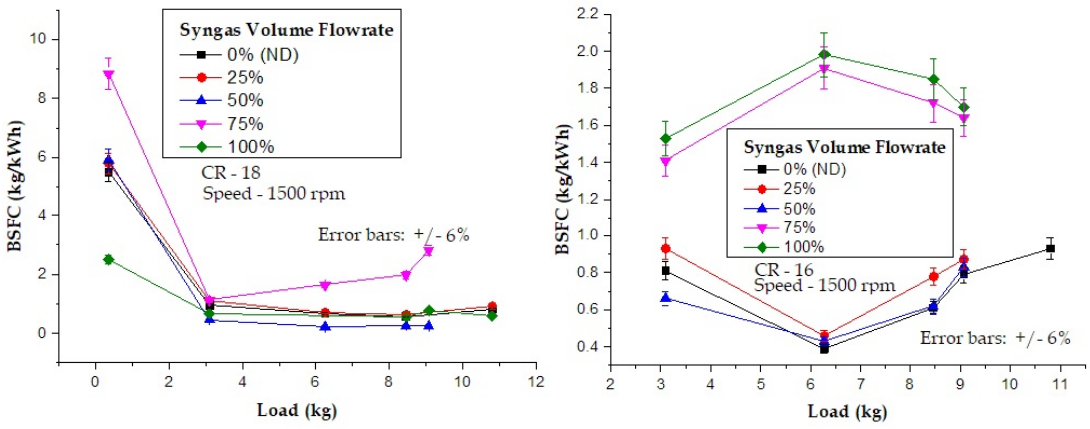

Figure 4.7: Variation of BSFC with load for compression ratios of (a) 18 (b) 16

syngas volume flowrate (SVF) blend, when CR was adjusted from 18 to 16. This confirmed that BSFC reduced with an increase of CR. This was attributed to better combustion and less heat losses at higher CR. Similar CR effects on BSFC have been reported by Hariram and Vagesh Shangar (2015) and by Murthy et al. (2012). Dhavale et al. (2015) reported similar results in the case where load and syngas volume flowrates were varied. The study observed that BSFC increased with an increased percentage of syngas substitution at part loads, while at higher loads BSFC improved with the increase of syngas substitution and attributed it to incomplete combustion of the gaseous fuel at lower loads.

Figure 4.8 shows the effect of diesel substitution with syngas on BSFC of a dual fuel CI operated at 1500 rpm for varying compression ratios and in a full load.

In CRs of 12 and 14 the diagram shows BSFC value being high but lower than those obtained in high CRs of 16 and 18. This is attributed to blends having a high proportion of diesel which studies have to burn better than syngas in low temperature and pressures. The converse is true at CRs of 16 and 18, with blends rich in syngas(75% and100% SVFs). In high temperature and pressures combustion of syngas is more complete, thus supplying engine with the required energy with less contribution from diesel for set speed.

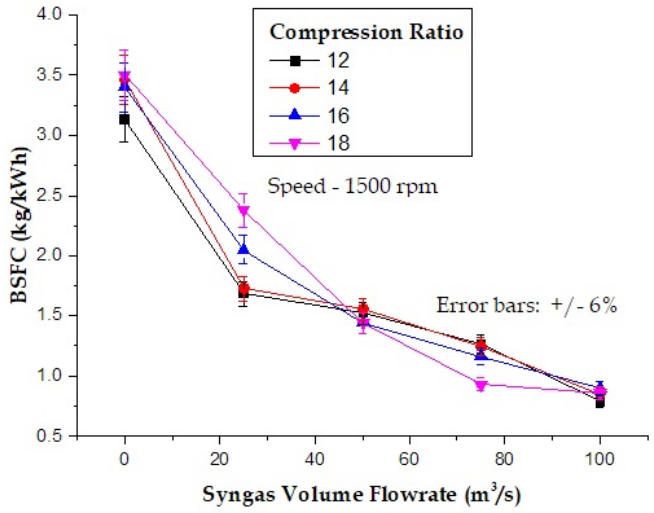

Figure 4.8: Variation of BSFC with syngas volume flowrate

The result is less diesel drawn to the engine. These same results were obtained by Dhavale et al. (2015) who proferred the same explanation.

At full load, engine speed of 1500 rpm and for CR 16, BSFC values decreased by about two and half times for the substitution of neat diesel (0%) with SVF of 100%. The effect was attributed to incomplete combustion caused by oxygen deficiency in the combustion chamber and the lower heating value of syngas compared with diesel. Similar results were reported by Ahmed et al. (2018). Karagoz et al. (2016) obtained similar results and attributed it to the low LHV of the syngas fuel, which is considerably lower than that of diesel fuel.

In an attempt to improve the BSFC in dual-fuel operation, fuel injection timing was advanced to CA 25.2° and CA 27.4°. Tests were also performed for the retarded injection timing of 20.8°. Figure 4.9(a) shows the effect of advancing or retarding fuel injection timing (IT) on the BSFC of a CI engine operating in dual-fuel mode with a blend of 100% SVF. It was observed that BSFC values decreased (improved) by 7% and 13% when the engine was advanced to CA 25.2° and CA 27.4° respectively. The syngas being of fuel burn slowly requires, longer period, high temperatures and pressures to achieve complete combustion. Therefore, when the engine was advanced and CRs adjusted to 18 and 16, the

complete combustion was realised thus the high power output and less fuel consumption per brake power. Figure 4.9(b) shows the same trend under similar advance/retardation conditions but with the engine operated in diesel-fuel mode. Compared to performance values obtain with dual fuel mode, the values in lower CRs (12 and 14) were high for retardation and standard IT in dual-fuel mode of 100% SVF, a trend reported by all studies reviewed earlier (Hagos et al., 2014b; Monteiro et al., 2012), but lower than for high CRs (16 and 18). Since the engine is optimised to run at standard (CA 23°) IT when fueled by neat diesel as depicted in Figure 4.9(b), there is less consumption for brake power output from under the stated conditions.

The study noted that the values of BSFC increased slightly by 4% and 6% for similar advanced conditions. Poor results, which showed an increase of BSFC by 8% for SVF of 100% and 7% for neat diesel were obtained for the retarded IT conditions. The improved results in an advance mode for dual fuel mode were attributed to the increased residence time for the fuel in the combustion chamber of the engine, thus allowing it more time

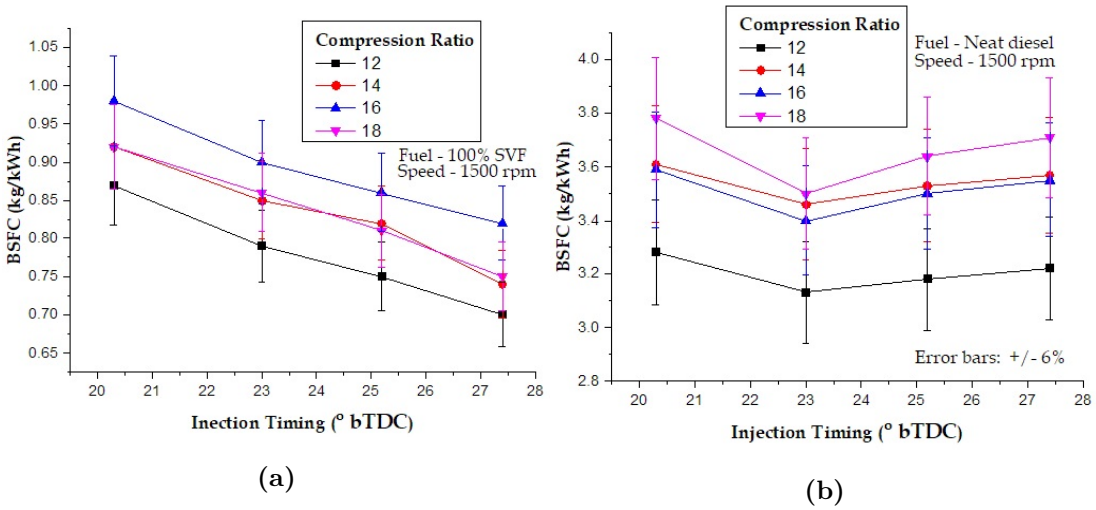

Figure 4.9: Variation of BSFC with injection timing and CRs for (a) dual-fuel mode (b) diesel mode

for combustion. Hassan et al. (2011) obtained similar results with a supercharged

dual-fuel engine operated on syngas-diesel blend, also attributing the effect to improved combustion. It may be concluded that it is possible save on fuel an engine consumes by running a CI engine on dual-fuel mode when the CR and fuel IT are adjusted appropriately.

4.4.2 Brake Thermal Efficiency

In the present study, investigations were carried out on the effects of varying load on Brake Thermal Efficiency (BTE) of a CI engine operated. First, in diesel mode and then on varying syngas volume flowrate (SVF) at set compression ratios (CRs). Among the different test performed for particular variables, only the best results are presented for each case.

Figure 4.10 shows the variation of BTE against engine load at a speed of 1500 rpm and CR.18.

Values of BTE obtained for diesel mode were observed to have risen from 0.4% to maximum BTE of 28.18% when the load was increased from no-load to half-load of 6.3 kg . BTE values for similar conditions, but with diesel substituted with 100% syngas volume flowrate (SVF)

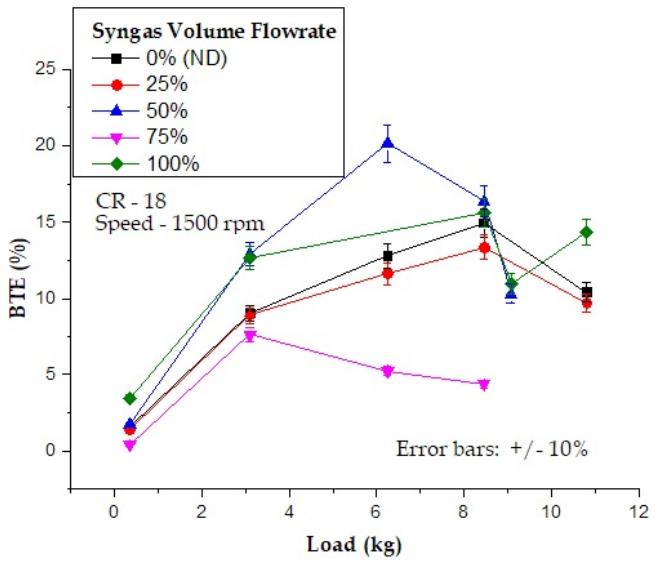

Figure 4.10: Variation of load and syngas volume flowrate with BTE (CR 18)

increased from 1.73% to 20.15 %. This demonstrated a decrease in efficiency as diesel was substituted with increased volume flowrate of syngas; by 27.9% at no-load and by 28.5% at full load. Moreover, very high load causes the engine to stall slightly causing a decrease in air intake with subsequent poor combustion even as the engine tend to draw more diesel fuel. As shown in Figure 4.10, the maximum thermal efficiency of 20.15% in dual-fuel mode was obtained with the CR 18 at a speed of 1500 rpm for syngas volume flowrate of 100% at half load. The phenomenon of power degradation at low and intermediate load conditions, was attributed to poor utilization of syngas leading to incomplete combustion of syngas. This is so, since with a high quantity of pilot diesel in the mixture of the syngas-air-diesel, and diesel fuel having higher heating and better combustions characteristics than syngas, but with presence of more fuel in the combustion chamber, the mixture burned better resulting in more complete combustion. In turn higher brake thermal efficiency in dual fuel mode was realised. Some previous studies have reported similar trends; (Dhavale et al., 2015; Hagos et al., 2014b; Raman and Ram, 2013). Hagos et al. (2014b) observed that the syngas engine delivers about two-third of the power at its maximum load as compared to the performance of engines using liquid fuel. Mohammed et al. (2011) reported that reduction in energy density and a reduction in compression ratio result in 20% de-rating of the engine as compared to when operating on diesel. Dhavale et al. (2015); Raman and Ram (2013) noted that higher brake thermal efficiency is due to better mixing of syngas with air, which results in better combustion and also due to wider ignition limit and high flame propagation.

Figure 4.11 shows the effect on BTE of running the engine at lowered CR of 16 and varying load in the same fuel conditions and constant speed of 1500 rpm.

It was noted that maximum efficiencies of 21.73% and 19.43% respectively were achieved at CR 16 and half load with neat diesel and for the blend with 100% SVF respectively. These results were attributed to factors like energy content of fuel mixture, volumetric efficiency and balanced air-fuel mixture, all interacting better to produce improved efficiency.

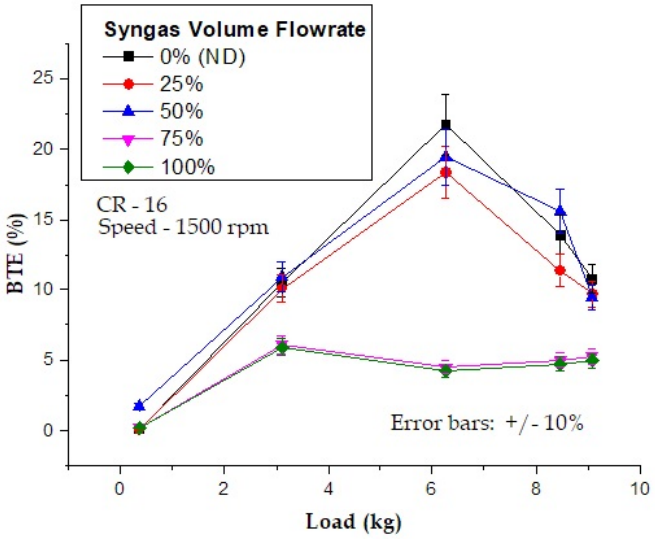

Figure 4.11: Variation of BTE with load and syngas volume flowrate (CR 16)

BTE recorded with the blend with 25% SVF were relatively high (18.37% at half-load) compared to those of 50% and 75% SVF. The most probable reason being the large quantity of diesel fuel in the 25% SVF blend. Atiqh (Ahmed, 2016) in studying a CI engine fuelled with gaseous fuel of similar properties made alike observations which he attributed to the same factors combining to produce the same effect. To improve the BTE of the engine in dual fuel mode, studies have identified the following methods: use of syngas with high calorific value without adding much complications and cost or optimizing adjustment of ignition timing (IT) and compression ratio (CR). The present study investigated the effect of adjusting IT and CR on BTE.

Figure 4.12(a) shows the effect of varying CR on BTE with diesel substituted with a syngas volume flowrate (SVF) of 100% for different injection timings at a constant speed of 1500 rpm. Rapid fall of BTE values when engine is adjusted to CR 16 from 14 for all fuel IT in dual fuel mode of 100% was observed. This trend could be attributed to a given fuel burning better under specific conditions than in others. Apparently, pressure and temperature conditions at CR of 16 were not conducive for the blends of syngas-diesel investigated.

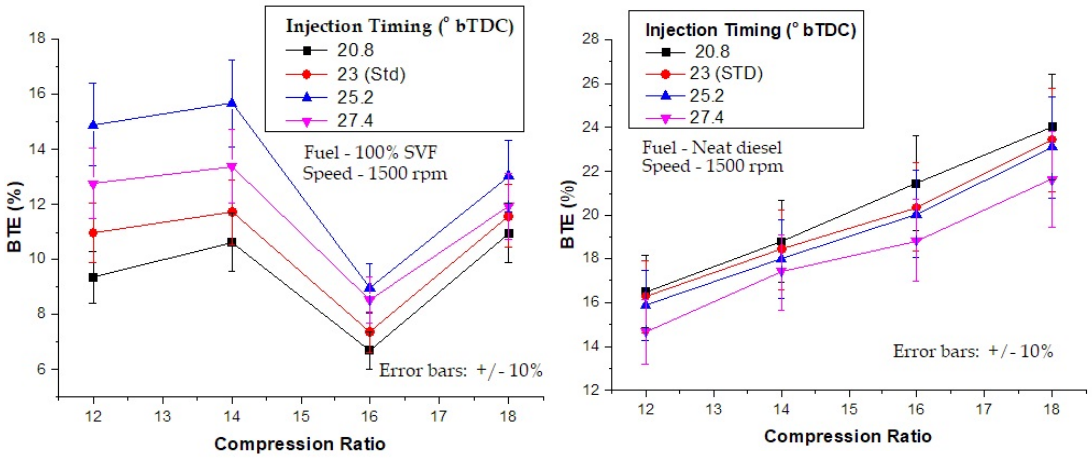

Figure 4.12: Variation of BTE with injection timing and CR on BTE for (a) dual-fuel mode (b) diesel mode

There was a decrease of 2.6% in BTE when CR was adjusted from 14 to 18 for the IT of CA 25.2°. This was reversed for the retard of CA 20.8°, where a marginal increase of 0.56% was noted for the same CR adjustment. The cause for this insignificant change in engine efficiency when both CR and IT are adjusted could be attributed to the fact that retarding IT shortened the ignition duration which could have caused a certain degree of incompleteness of combustion, thus lowered power output however effect of increased temperature and pressure due to high CR of 18 condition compensated for the loss occasioned by the IT retardation. Rahman et al. (2014) recorded similar results pattern and attributed the result to better energy conversion under increased pressure and temperature.

Similarly, Figure 4.12(b) shows the effect of varying compression ratios on BTE at similar fuel injection timing and speed conditions, but with engine operated in diesel mode.

The highest BTE results of 24.03% were obtained at standard injection timing (CA 23°) for neat diesel (ND) at CR 18. Adjusting CR to 16 lowered the BTE by 3%. At the advance of CA 25.2°, BTE values fell by 3% for the same CR adjustment. The fall in BTE values at lower CRs was caused by poor combustion

due to low pressures and temperatures, which compromised fuel-air mixing and combustion temperatures. Dhavale et al. (2015) made a similar observation and attributed the results to incomplete combustion.

To optimize for CR at advanced IT conditions, CRs of 18 and 16 at 1500 rpm were selected as they exhibited the highest BTEs, compared to CRs of 12 and 14. Figure 4.13(a) shows the effect of varying fuel IT on BTE while keeping the speed constant at 1500 rpm and CR at 18, for diesel substitution with different quantities of syngas. The BTE increased by the highest value of 7.3% for syngas mass flowrate (SVF) of 50% by advancing IT to 27.4°. The results are attributed to the likelyhood that at SVF of 50% the homogenuity of syngas-diesel-air mixture is achieved more readily for these particular fractions. This coupled with longer residence time for the charge in the combustion chamber (CC), could have allowed for more complete combustion. Sayin and Canakci (2009) reported the same observation and attributed it to better fuel combustion. Similarly, Figure 4.13(b) illustrates the effect of varying fuel IT on BTE while keeping the speed constant at 1500 rpm and CR at 16, for different levels of diesel substitution with syngas.

Identical trends for neat diesel fuel were observed in the two test of varying CR of 16 and 18; lower BTE values for the three fuel IT adjustments compared to those of standard IT. The possible cause for this behaviour is the fact that engine are optimised during manufacture, apparently for this particular engine was optimisation was done around its standard IT of 23° CA bTDC. At the CR of 16 , the BTE increased by 6.9% for SVF of 50% by advancing IT to 27.4°. An increase of about 2% was observed at IT of CA 25.2° when CR was adjusted from 16 to 18. Examining closely the results, improved for fuel IT of 27.4° CA bTDC were noted compared to those realised with 25.2° CA bTDC. The possible cause is for this behaviour was the engine responding better to increased ignition delay and the conditions arising out of the more advance adjustment. Generally, the possible cause for the improved result in the advance mode was the longer residence time for the charge in the combustion chamber, which allowed for more complete combustion. Hariram and Vagesh Shangar (2015) reported that BTE

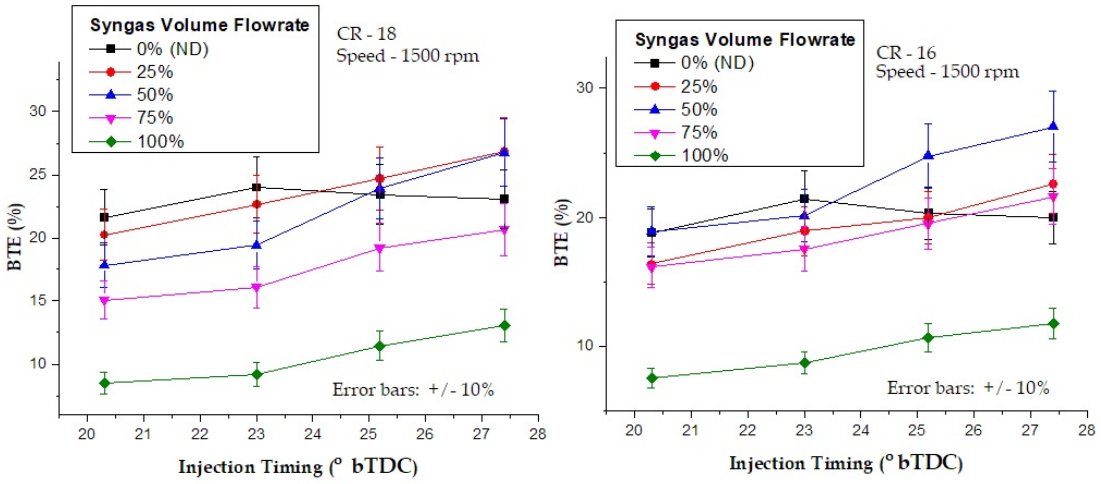

Figure 4.13: Variation of BTE with injection timing for compression ratios of (a) 18 (b) 16

was higher by almost 13% at full load when CR was increased from 16 to 18 due to better combustion at higher compression ratios.

4.4.3 Volumetric Efficiency

Volumetric efficiency (VE) of an engine is the amount of air drawn into the engine cylinder, or as per definition, the actual ratio of air mass flow to the ideal flow in the engine. Shown in Figure 4.14 is the variation of VE for different values of syngas volume flowrate (SVF) at set CRs.

VE value for neat diesel (ND) at CR 18 increased by 6.7% when the CR was adjusted to 12 and by 3.4% were varied from CR 14 to 16 for same conditions. VE values also decreased from a peak of 54.66% to 45.5% when neat diesel was substituted with a blend made of diesel and 100% SVF at CR 12. In dual fuel mode, there was a rise of 22.8% in VE values when CR was adjusted from 18 to 12 for blend with 100% SVF fuel also icreasing from 37.06 to 46.75% with SVF reduced to 25% at CR 18. The effects were attributed to the fact that a part of the cylinder space is taken by the syngas when diesel was substituted with syngas, thus leaving reduced space available for the fresh air charge.

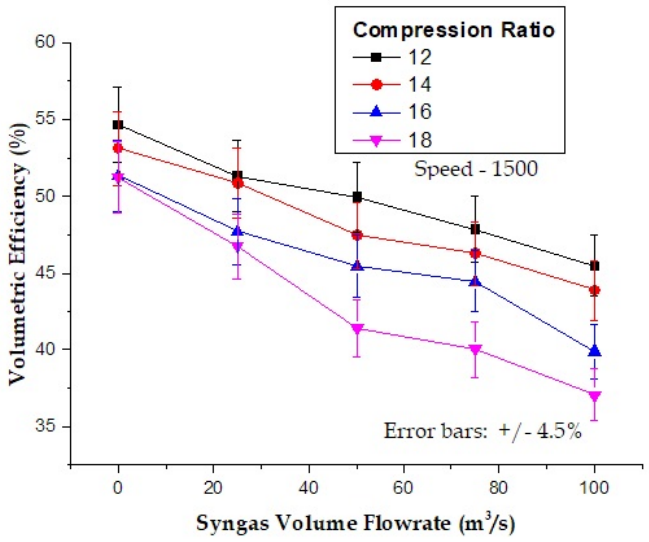

Figure 4.14: Variation of volumetric efficiency with syngas volume flowrate

Hagos et al. (2014b) made a similar observation and attributed the results to the displacement of induced air by syngas with lower LHV.

Figure 4.15 shows the variation of volumetric efficiency with various engine speeds. Compared to the syngas volume flowrate (SVF) of 100% in dual-fuel operation, the neat diesel operation showed 11.2% higher volumetric efficiency, at 1000 rpm compared to its value of 61.4%, a value 17.5% higher than for SVF 100%, at a speed of 1500 rpm. When comparisons were made based on speed, a reduction of 11% was recorded with speed increase from 1000 to 1500 rpm for diesel mode while it also reduced by 17.4% for SVF of 100% for same increase. This occur because at high speeds duration for charging engine with fresh air is shortened for the same crank angle in suction stroke though this maybe compensated by an improved vacuum at air inlet valves or ports. Further, the volumetric efficiency decreased by 25.8% when the syngas volume flowrate was increased from SVF of 25% to SVF 100%. The cause of the decrease is attributed to the substitution of the fresh-air charge by syngas. Here it was observed that syngas being less dense than air, it displaced some air already sucked into the cylinder in dual-fuel mode. This resulted in volumetric efficiency reduction at all engine speeds.

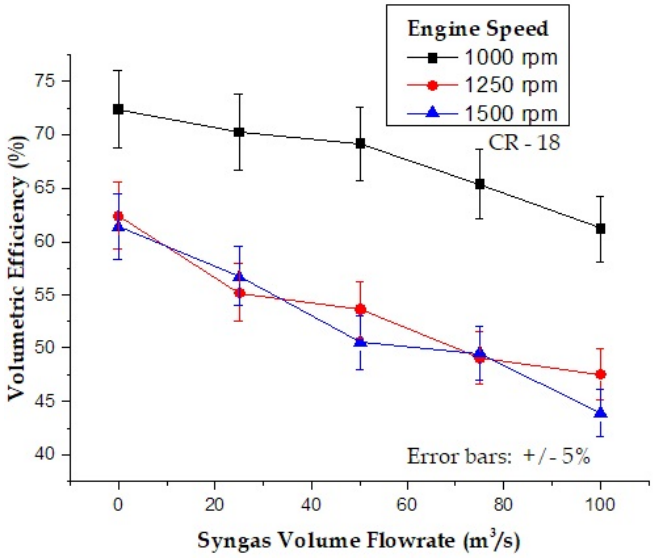

Figure 4.15: Variation of volumetric efficiency with speed

Cheenkachorn et al. (2013); Hagos et al. (2014b) in explaining the cause of engine de-rating in dual fuel mode when diesel substitution with syngas was increased, reported that besides other combustion parameters, the main contributing factor to power reduction was the volumetric efficiency penalty caused by an appreciable amount of air getting displaced by the lower calorific value syngas. Mahgoub et al. (2015b) reported different observations from those described in the present study and by many other studies, when they investigated the characteristics of simulated syngas in a dual-fuel CI diesel engine running at speeds of 3000 and 2000 rpm. In this study, volumetric efficiency was shown to be higher at these high engine speeds than for the speed of 1200 rpm. The effect was observed to be caused by the high vacuum at the air intake port generated by high speeds which consequently drew a higher airflow rate inside the engine cylinder.However, the study obtained similar results with increased substitutions of diesel with syngas.

4.5 Emission Characteristics

This section presents the analysis of emission results for carbon monoxide, nitrogen oxides, hydrocarbons, soot and smoke (particulate matter) and carbon dioxide emissions, in addition to exhaust gas temperatures.Explanation has also

been given, where applicable, for the cause of emissions characteristics observed.

Comparison was made through analysing results and to maintain brevity it is those results that are most definitive that are presented here.

4.5.1 Carbon Monoxide

Carbon monoxide (CO) is an intermediate product in the combustion of a hydrocarbon fuel, so its emission results from incomplete combustion (Sayin and Canakci, 2009). Due to deficiency of oxygen, the carbon present is not fully oxidised during combustion process and appears in the engine exhaust in the form of CO.

Figure 4.16(a) shows the effects of varying compression ratio (CR) on CO emission under different loads for a CI fuelled with neat diesel (ND). With an increase in load from no-load to three-quarter load, CO emission decreased by 92% at CR of 16. A similar trend was observed with the full-load; CO emission reduce by 83% at same CR of 16. At CR of 18 under same load conditions of 10 kg and 12 kg , emission reduced from 0.1% at 0 kg to levels that were untraceble for both cases. This could be attributed to starving engine of diesel due to demand occasion by need to burn more in order restore and maintain set speed and torque requirement for load. Similarly, Figure 4.16(b) illustrates the effect of variation of CR on CO emission under similar load conditions but with the engine operated in dual fuel mode of 100% syngas volume flowrate (SVF). The present research noted that at the part load of three-quarter, and full- load CO emission was eliminated for CR of 18. This could have resulted from the engine governor responding to reduced speed through load increase, by allowing for the injection of more diesel fuel but which does not increase in proportion to load/speed demands led to leaner air-fuel mixture. The resultant leaner mixture in the condition of high pressures and temperature leads to improved and more complete combustion which probably is has ratio below stoichiometric ratio. Pradhan et al. (2015) in reviewing works on emissions from ICEs, noted that several studies had reported CO emissions to

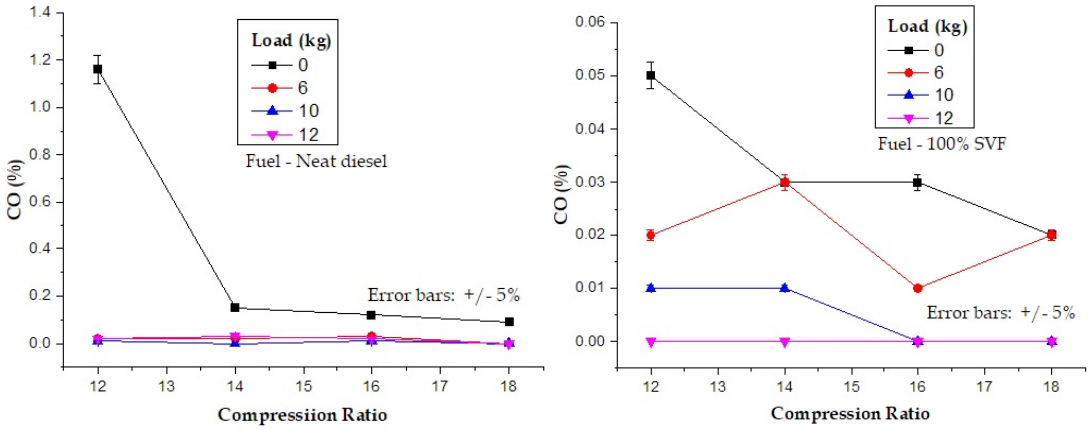

(a) (b)

Figure 4.16: Variation of CO emission with compression ratio for (a) neat diesel (b) syngas volume flowrate of 100%

have been higher for dual fuel mode at low and moderate loads but decreased with the increase of engine load attributing it to the improvement in fuel conversion efficiency.

Figure 4.17(a and b), shows the effect of varying compression ratio (CR) on the CO emission when speed is maintained at 1500 rpm and 1000 rpm for different fuel conditions.

CO emission was observed to decrease as the compression ratio increased, even at low speeds. It is seen in Figure 4.17(a) that at the speed of 1500 rpm CO emission reduced by about 45% when CR was adjusted from 12 to 18. Similar behaviour was observed at lower speeds with CO emission falling by 54.5% for the same CR adjustment at 1000 rpm (Figure 4.17(b)). Emission obtained from the engine fuelled with diesel blend of 50% SVF was 37% higher than from the engine when operated in diesel mode at CR of 18 and constant speed of 1000 rpm. The results indicates higher CO emission in dual fuel mode than in neat diesel fuelled engine are attributed to low oxygen present in the air-syngas mixture which caused an incomplete combustion. Shrivastava et al. (2014) obtained similar results and reported that the maximum concentration of CO was 10 ppm in diesel mode and

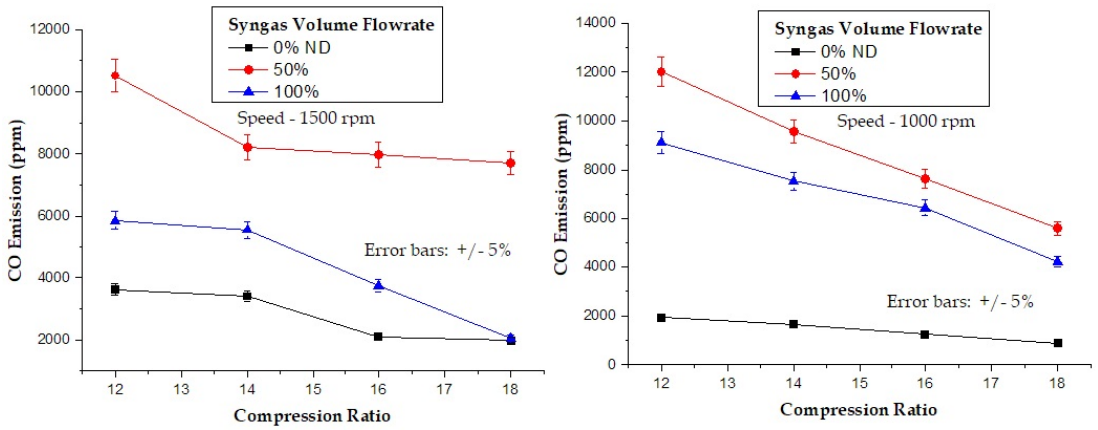

Figure 4.17: CO emission for varying CR and syngas flowrate at (a) 1500 rpm (b) 1000 rpm

250 ppm in dual fuel mode. Lal and Mohapatra (2017) reported the maximum concentration of CO of 700 ppm in diesel mode and 1300 ppm in dual fuel mode. Both studies also attributed the effect to poor combustion due to inadequate air charge in the engine cylinder.

Figure 4.18(a and b) shows CO emission results for different syngas volume flowrate (SVF) fuels and injection timing (IT) at CR 18 and speeds of 1500 rpm and 1000 rpm respectively. When the injection timing was advanced to CA 27.4°, the level of CO emission decreased for SVFs of 100% by 7.5% but increased for neat diesel (ND) by 5.3% at 1500 rpm. At 1000 rpm, the reduction was by 8% for the same dual-fuel mode and an increase of 5.5% for ND. This is attributed to the increased duration for combustion made possible by the adjusting of fuel IT to start early. The extra CA degree allowed for complete burning of diesel and syngas in the blend. The same will not be the case for neat diesel, instead the injection of fuel will be under altered optimised fuel IT and air compression conditions which could have led to improper mixing of fuel with the supplied air, subsequently causing unburned fuel to escape with exhaust. Similarly, Figure 4.19(a and b) shows CO emission results for different syngas volume flowrate (SVF) fuels and injection timing (IT) at CR 12 and speeds of 1500 rpm and

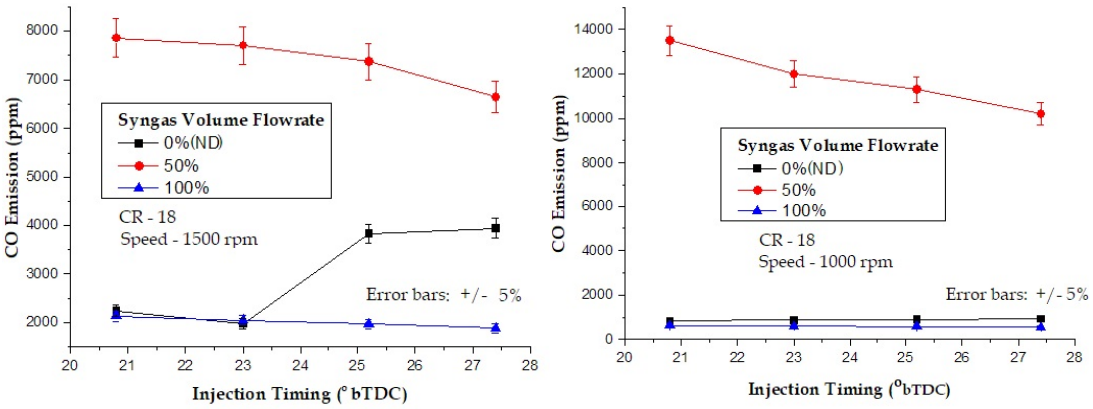

(a) **(b)**

Figure 4.18: CO emission with varying injection timings and speeds for compression ratio of 18

1000 rpm.

When the engine was operated at 1000 rpm and CR of 12 for different blends of syngas and diesel; CO emission reduced by 8.3% for SVF of 100% at advance of CA 27.4° . Retardation of IT caused higher levels of CO emission in CR of 18 than in CR 12. As is inferred from the obtained data, retarding of IT to CA 20.8°, increased emissions by 13.9% for ND and 4% for 100% SVF. These results are attributed to higher cylinder temperature which increased the oxidation process between carbon and oxygen molecules on advancing IT. O.M.I. Nwafor (2012); Sayin and Canakci (2009) obtained similar results using an engine with the same injection timings and primary gaseous fuels of same properties and also attributed the effects to higher cylinder temperatures.

4.5.2 Nitrogen Oxides

The main factors that promote NO_x formation are high temperature, enough oxygen and sufficient reaction time (Liu et al., 2015). Figure 4.20(a) shows the variation of NO_x emission with engine loading for each set of compression ratio (CR) in dual-fuelled engine ran on diesel mode.

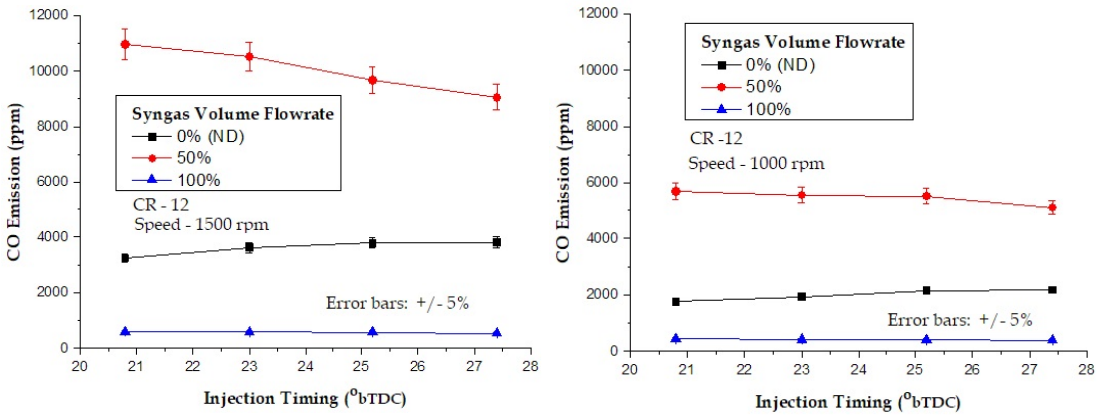

Figure 4.19: CO emission with varying injection timings and speeds for compression ratio of 12

NO_x emission was observed to increase proportionately with the load and in the case of dual-fuel mode, with CR. When engine is run on diesel single mode, at full-load the of NO_x decreased from 46.00% to 42.00% when CR was adjusted from 16 to 18. The main cause of increased NO_x emission in CI engine is the high temperatures and pressures that are generated especially under high CR condition as as shown in both the figures in Figure 4.20 except for the aforementioned case of CRs 16 and 18. The reason for the special occurrence is found in the fact that the supply of diesel fuel, air and timing (both for fuel IT and valve) are optimised at CR 17.5 which is closer to 18 than 16. For the diesel mode at CR 18, NO_x emission increased by 8.1% for load adjustment from no-load to full. At CR 12, emission values increased by 7.9% for the same load adjustment. High NO_x emission are generated under high load condition due to high temperature resulting from drawing of more fuel in the combustion chamber, which when burnt to completion caused more heat generation. Similarly, Figure 4.20(b) illustrates the variation of the NO_x emission under similar loading and compression conditions as those described in the immediate case but with engine operated in syngas volume flowrate (SVF)

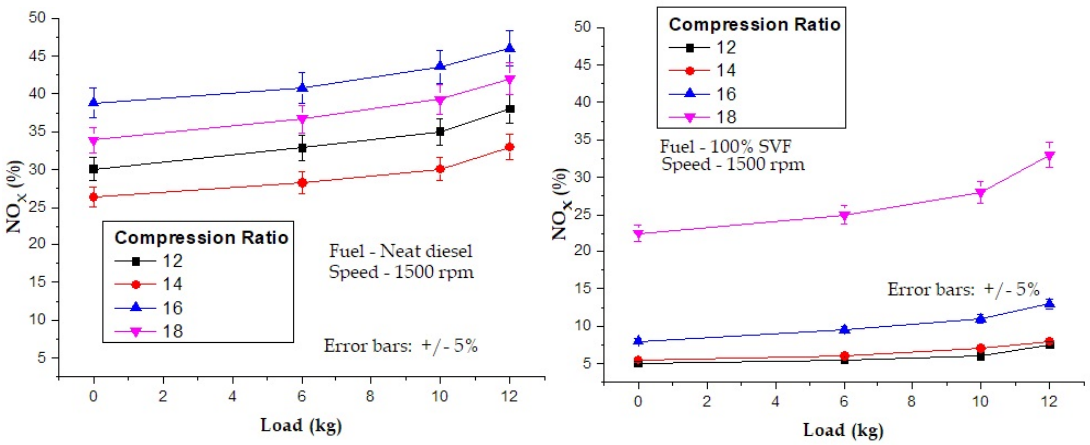

(a) **(b)**

Figure 4.20: NO_x emission for varying loads and compression ratio for (a) neat diesel (b) syngas volume flowrate of 100%

of 100%. The same effect was noted in the dual-fuel mode of 100% SVF. At CR 18, emission increased by 10.5% for the adjustment from no-load to full load and 2.5% for CR of 12 for the same load increase.

The results observed in the present study were attributed to more fuel injected at higher load conditions and also higher temperatures and pressure in the engine cylinder at higher compression ratios, leading to conducive conditions for NO_x species formation. In a previous study, Dhole et al. (2014) reported a maximum NO_x concentration of 904 ppm in dual fuel mode at 80% load condition and attributed it to higher temperatures caused by the injection of more fuel at higher loads. Also Figures 4.20(a and b) reveal that the NO_x emission in diesel mode was higher by about 22% to 33% than in dual fuel mode. The lower NO_x emission obtained in dual-fuel mode is caused by the low flame propagation in the fuel-air mixture due to the presence of a high amount of syngas and a lower concentration of oxygen in the cylinder that led to lower temperatures. Shrivastava et al. (2014) reported similar results and observed that maximum NO_x concentration of 325 ppm in diesel mode and 180 ppm in dual-fuel mode at three-quarter load conditions are generated by higher temperatures and pressures obtained in the cylinder at higher load conditions.

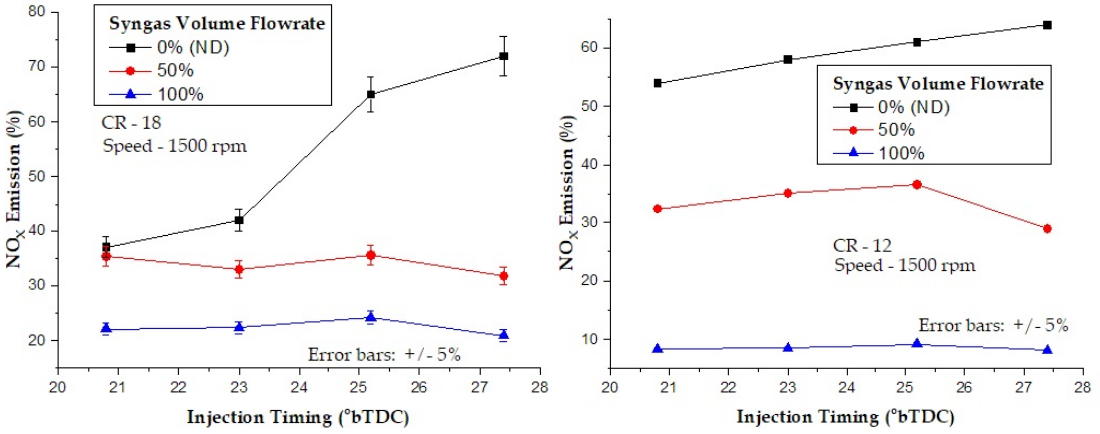

Figure 4.21: NO_x emission with varying injection timing for compression ratios of (a) 18 (b) 12

Figure 4.21(a) shows the effect of varying fuel injection timing on NO_x emission from a dual-fuel CI engine operated at CR of 18. A higher concentration of NO_x in exhaust gases was recorded in neat diesel mode, with an increase of 30% for an advance to CA 27.4°. Also noted was that a decrease of 51% in emission when ND was substituted with a syngas-diesel blend containing 50% SVF. When IT was retarded to CA 20.8°, a decrease of 1.3% in NO_x emission was observed with the same syngas-diesel blend. Figure 4.21(b) illustrates the same emission results under the same fuel conditions but with CR set at 12. The values obtained, indicated the emission to have decreased by 3.8% for IT advance of CA 27.4° for a dual-fuel mode of SVF of 50% but increased by 6% for ND. NO_x emission decreased by 24.3% when neat diesel was substituted with a diesel-syngas blend of SVF 50% with IT retarded. In overall, NO_x emission was observed to increase sharply with the advance of fuel injection timing that caused peak pressure and therefore temperature to with both fuel IT advance as demonstrated in section 4.3.1. This conformed with the earlier explanation that when fuel injection timing is advanced, the combustion time is extended as the ignition delay period is prolonged allowing for more complete combustion thus attaining of higher temperature. Similar results trend were reported by

Sayin and Canakci (2009)to the effect that, when injection timing was retarded by 6° CA bTDC, NO_x emissions decreased by 37.3% under half-load condition. Hassan et al. (2011); Mahgoub et al. (2015a); Núñez (2008) reported similar results pattern and also observed that retarding of the injection timing decreased the peak cylinder pressure because more of the fuel is burned after TDC.

4.5.3 Unburned Hydrocarbon Emission

The two main causes of hydrocarbon (HC) emission in diesel engines are: (a) during the delay period, the fuel mixture is leaner than that of the lean combustion limit and (b) under-mixing of fuel (Rahman et al., 2014). Therefore, an inference could be made that HC emission arises when a part of the fuel inducted into the engine escapes combustion..

Figure 4.22(a) shows the variation of HC emission as the compression ratio (CR) is changed from a minimum of 12 to a maximum of 18 for different engine loads when the CI engine was operated at neat diesel mode. At ND mode and CR 18, HC emission decreased by 78% (from 9 - 2 ppm) for change from no-load to full load. When CR was set at 12, emission readings obtained indicated a decrease of 98.2% (from 114 - 12 ppm) for the same loading adjustment. Similarly, Figure 4.22(b) shows the effect of engine load and CR on HC emission when the engine is operated in dual fuel mode for syngas volume flowrate (SVF) of 100%.

Emission values decreased by 93% (from 1068 to 74 ppm) for CR of 18 and by 99% (from 1857 - 24 ppm) at CR of 12 when the load was changed from no-load to full. These effects on emission are attributed to the fact that at light loads the fuel was less apt to impinge on surfaces; but because of poor fuel distribution, large amounts of excess air and low exhaust temperature, lean fuel–air mixture regions may hold out to escape into the exhaust.

Mahgoub et al. (2015a); Sayin and Canakci (2009) reported similar results, also attributing the effect to lack of homogeneity of the fuel-air mixture and non-uniform temperature distribution within the cylinder. Figure 4.23(a) shows the variation of HC emission as fuel injection is either advanced or retarded when the

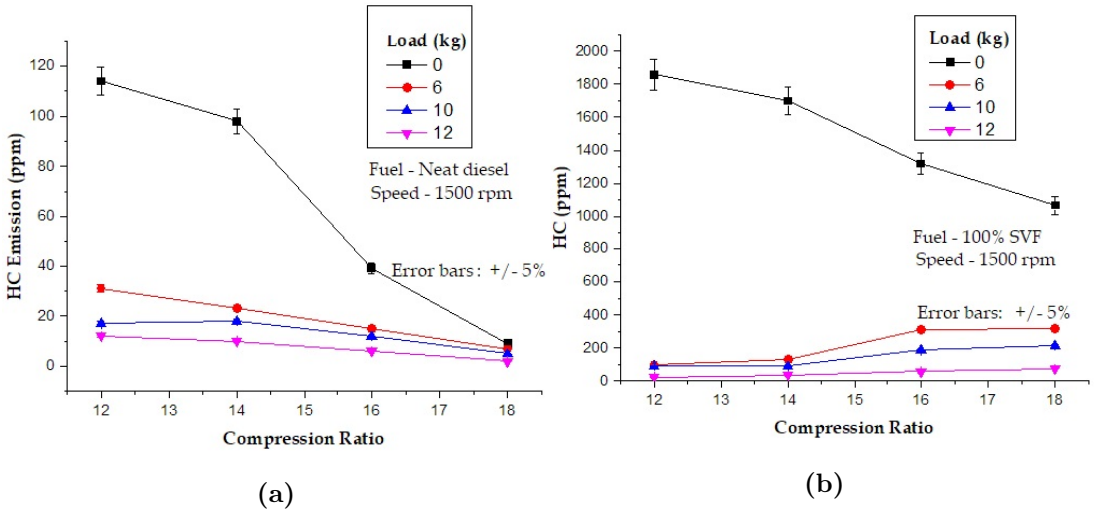

Figure 4.22: HC emission for varying loads at 1500 rpm for (a) neat diesel (b) syngas volume flowrate of 100%

CI engine was operated with neat diesel (ND), syngas volume flowrate (SVF) of 50% and 100% at CR of 18. Advance to CA 27.4° produced an increase of 2.5% and retarding to CA 20.8° caused an increase of 1.6% in HC emission for neat diesel. Advances to CA 25.2 and 27.4° had the effect of reducing emission by 2.8% and 7.1% respectively whilst retardation caused an increase of 4.1% for SVF of 100%. For SVF of 50%, advancing the injection timing to CA 27.4° and CA 25.2° bTDC reduced unburned HC emission by 4.5% and 1.8% respectively at speed of 1500 rpm. Retarding to CA 20.8° increased emission by 2.6%. For the IT of 27.4° bTDC the emissions for the engine when fuelled with neat diesel and SVF 100% is 58.54% and 54.7% respectively, marking the lowest values of emissions under these conditions and is attributable to longer duration of combustion assisted by high pressures and temperature leading to a more complete combustion process for both. Figure 4.23(b) shows the effect similar syngas-diesel blends and injection timing, had on the same emissions when CR was set at 12. For the dual-fuel mode of SVF 100% emissions decreased by 3.5% and 0.9% in the two advances and increased by 2.3% when retarded. The same trends is noted for SVF of 50% even recording much emission. The behaviour of the engine when fuelled with neat diesel is as other studies observed; with increases of emission when

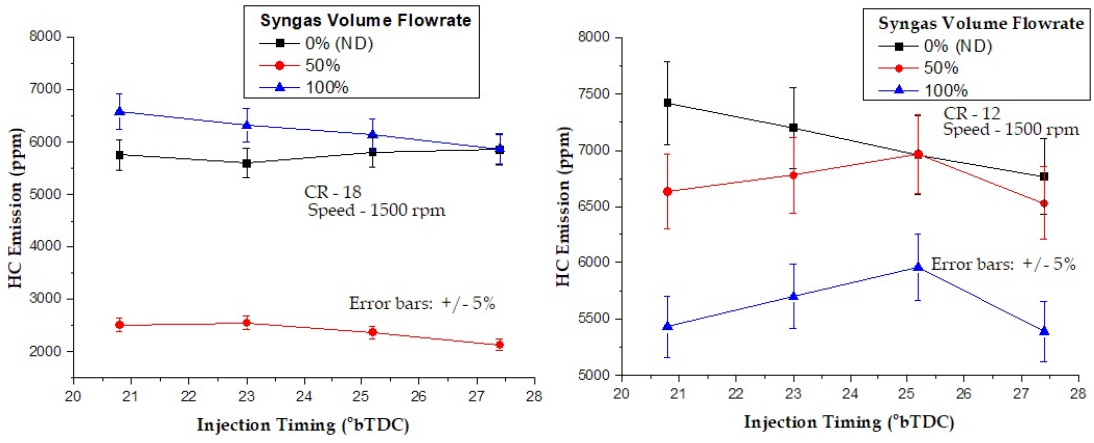

(a) **(b)**

Figure 4.23: HC emission with varying injection timing for compression ratios of (a) 18 (b) 12

4.5.4 Particulate Matter

IT is advanced to CA 25.2° and CA 27.4° bTDC by 0.5% and 1.8% respectively at CR 12. For the same fuel and IT conditions, the increase was by 2.1% and 2.54% at CR of 18. In the case of retardation increase is 0.7% and 1,6%. These results are because the engine other timings and supply are tuned for standard IT. The other results for dual-fuel mode could be attributed to the fact that advancing the injection timing caused an earlier start of combustion relative to the TDC. For that reason, time for combustion of the fuel-air mixture is increased, producing relatively higher temperatures and consequent complete combustion; in turn reducing the unburned HC emission. These findings, on the effects of IT adjustment on HC emission, correlated well with the findings reported by Mohammed et al. (2011); O.M.I. Nwafor (2012); Sayin and Canakci (2009). In addition, Sayin and Canakci (2009) observed that when injection timing was retarded by 6° (from 27° to 21°CA bTDC), the unburned HC increased by 51.2%. The above three studies also attributed the effect to the increased duration for combustion which led to better combustion.

Particulate matter (PM) sometimes referred to as soot or smoke, emitted from

compression ignition engines is mainly caused by incomplete combustion of hydrocarbon fuels (Liu et al., 2015). The formation of PM is favoured in the fuel-rich diesel spray and by relatively low flame temperatures (Bates and Dölle, 2017).

Figure 4.24(a) shows the variation of PM emission as the engine load is varied for dual-fuel engines running on different blends of syngas-diesel fuel at a constant speed of 1500 rpm and CR of 18. Adjusting the load from no-load to full load, PM emissions were observed to increase by 5% in neat diesel (ND) mode and 0.3% in dual fuel mode of syngas volume flowrate (SVF) of 100%.
Figure 4.24(b) shows the same variation of emission in similar fuel and load conditions with CR set at 16. The values obtained showed an increase of 11.2% in ND mode and 2.1% for 100% SVF in dual fuel mode when the load was increased from no-load to full load. At CR of 18 and full load, PM emission decreased by 33% when the fuel mode was changed from diesel to dual fuel for syngas volume flowrate (SVF) of 100%. These observations could be attributed to the reduced induction in fresh air charge into the combustion chamber, as usually happens in low engine speed conditions, resulting in a rich fuel zone. Liu et al. (2015) recorded similar results and also attributed it to the fact that, PM are mainly formed in the diesel rich areas, therefore the emitted particulate matter decreased when the syngas ratio is increased. The results also show that, PM emissions varied directly with applied engine load. This is attributed to more fuel being injected to the engine in response to the falling of the engine speed under increased load. With in-cylinder temperature and pressure not increased or airflow remaining constant, the flame propagation is slow leading to incomplete combustion. Figure 4.25(a) shows the effect on the PM emission from a dual-fuel CI engine of varying fuel injection timing when it is operated at a speed of 1500 rpm and CR 18. Values recorded indicate a decrease of 7% for ND and 1.9% for 100% SVF when engine IT was advanced to (CA) 27.4° bTDC and an increase of 0.4% and 2.7% respectively when retarded to 20.8° bTDC.

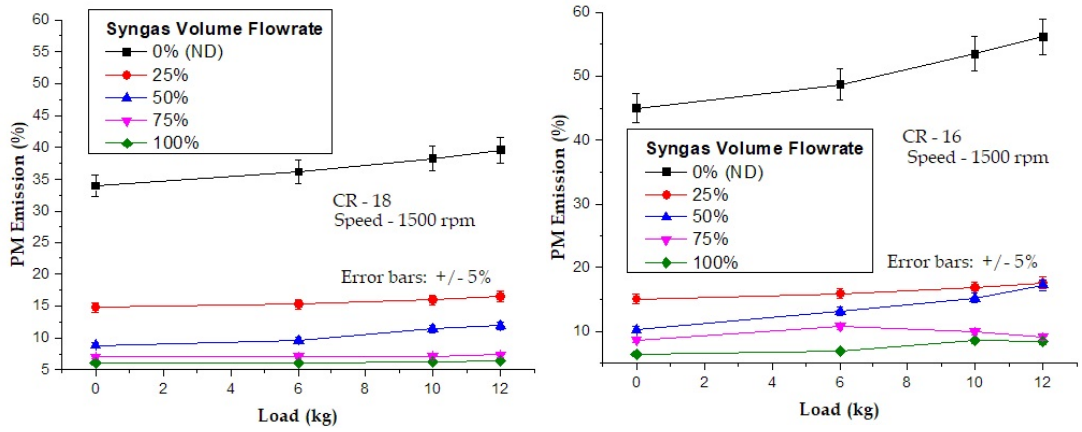

Figure 4.24: PM emission with engine load and syngas-diesel blends for compression ratios of (a) 18 (b) 16

.

This can be directly attributed to the extended period of combustion allowed when when an engine IT is advance. Figure 4.25(b) illustrates the effects on PM emission of also varying fuel IT, running the engine on the same speed of 1500 rpm but CR now set at 12. The results showed that PM emission decreased by up to 4.5% when operated with ND and by 3.5% for SVF of 100% for the same IT advance of 27.4° bTDC. The cause of this was the increased residence in the combustion chamber for the fuel-air resulting in complete combustion leading to reduced soot emission. A similar trend was observed by Wagemakers and Leermakers (2012) when reviewing Quin and Yao work who observed that; since advancing the amount of pilot diesel results in a better mixed diesel-air mixture due to the longer ignition delay (ID), lower PM emissions are realized with advanced diesel injection. Bates and Dölle (2017) obtained similar results and observed that at low levels of hydrogen (in syngas) there was a reduction in smoke emissions at part load. At higher loads and higher levels of hydrogen in syngas, it was pointed out that the smoke emission increased with the decrease of IT advance. Azimov et al. (2012) showed that at high diesel substitution levels, moderate load, and advanced diesel pilot IT, smoke increased.

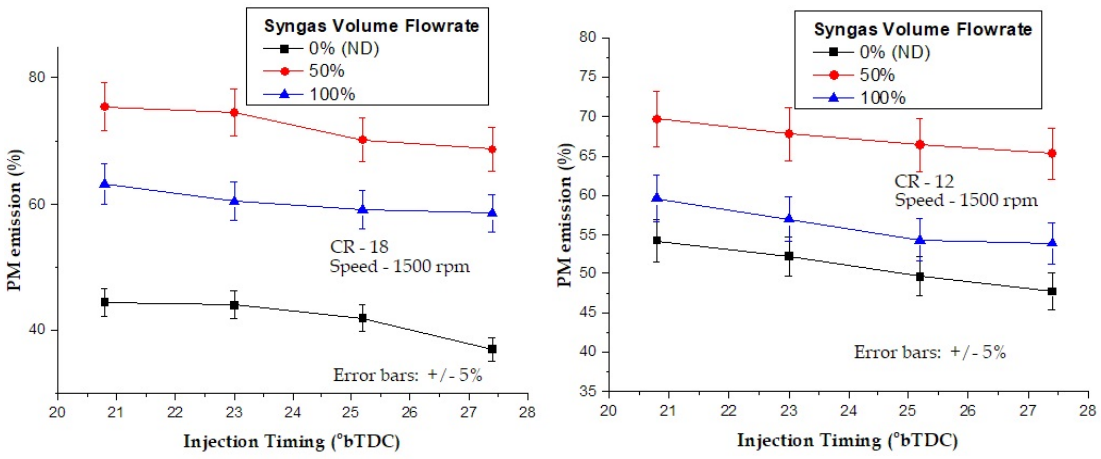

Figure 4.25: PM emission for varying injection timing for compression ratios of (a) 18 (b) 12

.

As seen in the results PM emission for neat diesel were 44% at CR 18 but raising to 52% when CR was adjusted to 12. Road (2012) made the same observation and reported that, smoke opacity for CI engine fuelled with neat diesel is inversely proportional to the compression ratio. The experiment demonstrated that for CR of 15, the value of opacity was above 60% and for a compression ratio of 17.5, its value decreased to 5.8% at the same engine load. Soni and Gupta (2016) in their numerical analysis of performance and emissions of dual-fuel CI engine obtained similar results and observed that, if mixing of fuel and air is good then 90% to 95% of carbon particles are converted into CO_2 during combustion. All these studies also attributed an increase of HC emission to poor combustion when fuel mixing is ineffectual as in low load and lower CRs.

4.5.5 Carbon Dioxide (CO_2)

Carbon dioxide (CO_2) is the most prominent greenhouse gas. Its presence in the exhausts of IC engine is largely an indication of complete combustion in hydrocarbon based fuels. The results obtain in the present study indicate a remarkable reduction in CO_2 emission when diesel fuel is substituted with various fraction

of syngas in syngas-blend. The test results presented here confirm that the use of syngas in dual fuel mode in the CI engine is a promising technique to reduce this greenhouse gas especially at high CRs and advance pilot fuel IT.

Figure 4.26 shows the effect of varying the compression ratio (CR) on CO_2 emitted from dual-fuel CI engine fuelled with varying blends of syngas-diesel when it was operated at a constant speed of 1500 rpm.

Values of CO_2 emission at CR of 12 decreased by 8.4% and at CR of 18 by 8.5% when ND was substituted with a syngas-diesel blend containing 100% syngas volume flowrate (SVF). The same effect was obtained for other CR fuel conditions, with SVF of 25%. 50% and 75% having emissions of 3.8%, 3.1% and 2.3% respectively to the high value of 9.6% obtained. The middle CRs of 14 and 16 had even sharper decrease of the emissions compared to what was recorded for CR 12. A number of researchers have also shown that CO_2 emissions decreased in dual fuel mode when compared with neat diesel fuel. These results could be attributed to the fact that, increasing the proportion of syngas in diesel-fuel blend amounted to replacing neat diesel fuel with a fuel that contains less carbon. An investigation conducted by Ahmed et al. (2018); O.M.I. Nwafor (2012) to establish the effect of varying proportions of syngas in blends of syngas-diesel on CO_2 emission from a dual fuel CI engine,

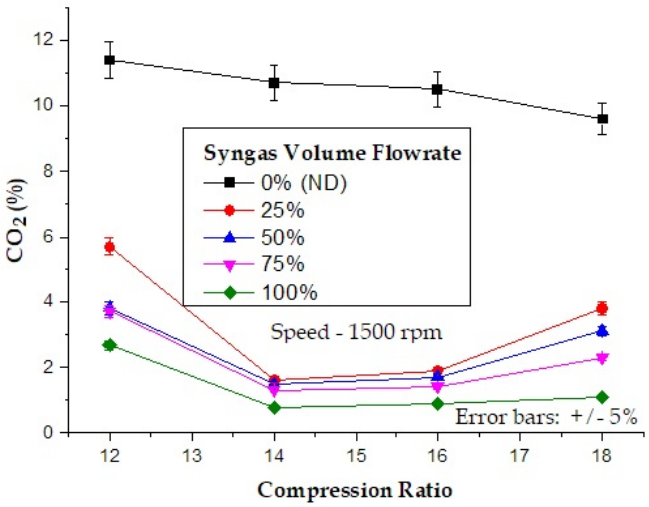

Figure 4.26: CO_2 emission for varying syngas volume flowrate.

found that less CO_2 emission was produced in dual fuel mode because of the lower carbon to hydrogen ratio on the blend.

Figure 4.27(a) shows the variation of CO_2 emission as the engine fuel injection timing (IT) was advanced or retarded with CR set at 18 and speed at 1500 rpm for syngas-diesel blends of neat diesel (ND), 50% and 100% SVF. The study observed that in advancing IT, a significant reduction in the emission was obtained in all dual fuel modes but increased for diesel mode. The reason is the same as stated before; in using blend of syngas-diesel, neat diesel has been substituted with fuel inherent less carbon. At SVF of 100% the value decreased by 0.16% at speed of 1500 rpm and CR of 18 when the engine was advanced to crank angle (CA) 27.4° bTDC. Retarding to CA 20.8° bTDC increased the value by 0.22%. Values in diesel mode showed an increase of 1.4% in advanced IT mode and a reduction of 1.8% for retarded IT. In standard IT combustion is more complete compared to the case of retardation which necessarily reduces duration of ignition, such that CO emission is suppressed for standard IT as CO_2 emission increase in exhaust gases. Figure 4.27(b), illustrates the variation of CO_2 emission in exhaust gases from a dual-fuel CI engine under similar fuel timing and speed conditions but CR set at 12.

Results obtained when CR was adjusted to 12, showed a 1.6% and 07% increase in emission for SVF 100% and neat diesel respectively when IT was advanced to CA 27.4° bTDC. With IT retardation a 0.41% and 0.2% increase of CO_2 emission when compared with values for CR 18. This study attributed the effect on emission caused by adjusting CR and IT, to the reduced temperatures and pressure at low CR, and increased combustion duration occasion by advance pilot fuel IT, which led to improved fuel combustion in the combustion chamber (CC) with the subsequent increase in CO_2 emission.

Bates and Dölle (2017) recorded similar observations and reported that emissions from dual fuel (syngas and diesel) CI engines are generally less than when running on diesel alone. Ahmed et al. (2018) observed that CO_2 emission showed an

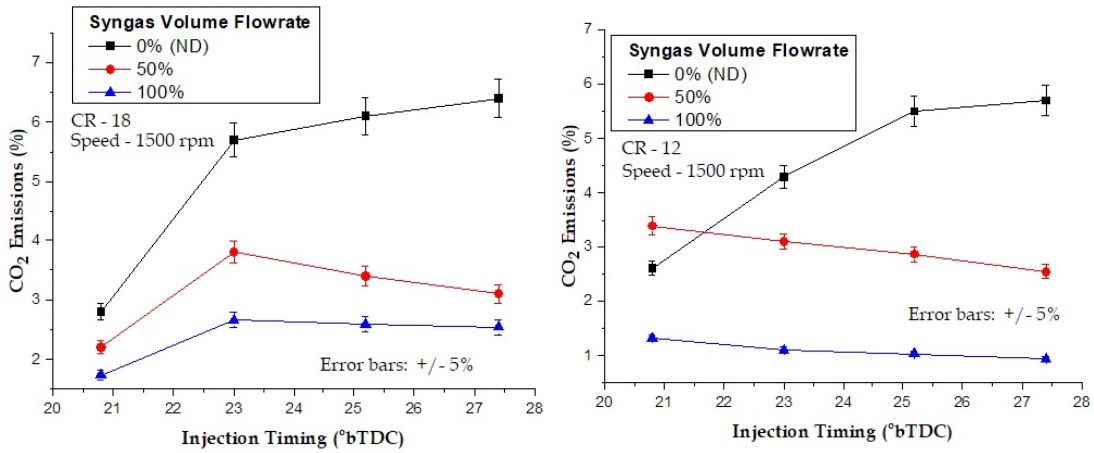

Figure 4.27: CO_2 emission with varying fuel injection timing for compression ratios of (a) 18 (b) 12

increasing trend when injection timing was advanced from 12 to 30° CA bTDC. Further, finding out that the rate of increase in CO_2 was lower when the injection timing was advanced from 12 to 18° CA bTDC than from 18 to 30° CA bTDC. Sayin and Canakci (2009) have reported that when IT was advanced from 27° to 33° CA bTDC, the level of CO_2 emission rose by 30.2% for dual-fuel at three-quarter load and speed of 1800 rpm. All these studies also attributed the results to the achievement of better combustion due to the availing of longer ignition time with the IT advancement.

4.5.6 Exhaust Gas Temperature

Exhaust gas temperature (EGT) is the temperature of the exhaust gases as they exited the combustion chamber (CC) and which were measured at the exhaust manifold. Exhaust gases are the waste product of combustion and are removed from engine when exhaust valves/ports opens while the combustion is still under high pressure. These gases passes through the exhaust manifold into muffler and silencer where they are expanded and decelerated to dampen noise. In the present engine, a calorimeter is fitted after manifold to extract heat from the gases (Heywood, 1988).

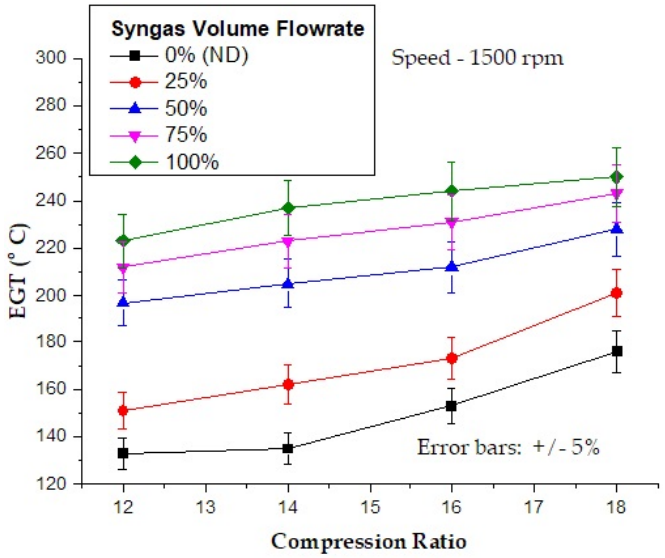

Figure 4.28: Variation of exhaust gas temperature with CR and syngas volume flowrate

The study of EGT is important for it indicates the state of engine combustion process. Incomplete combustion in engine due to too rich air-fuel mixture (much fuel and too little air) tend to cause high EGT, the same also happens with high loads and speeds on the engines.

Figure 4.28 shows the effect of compression ratio (CR) and syngas volume flowrate on exhaust gas temperature (EGT) at a constant engine speed of 1500 rpm and full load. There was an increase of 42% in EGT when fuel mode was changed from diesel to dual fuel for 100% syngas volume flowrate (SVF) at CR 18. This was attributed to the excess energy supplied to the engine as syngas and diesel fuels combined. Presence of slow combusting syngas may result in some unburned mixture entering the exhaust system where it combust causing high EGT. Hassan et al. (2011) experimented using a supercharged CI engine operated in dual fuel mode. In the study, higher EGT values for supercharged dual fuel were recorded. The results were attributed to the increased density of the air-fuel mixture entering the engine.

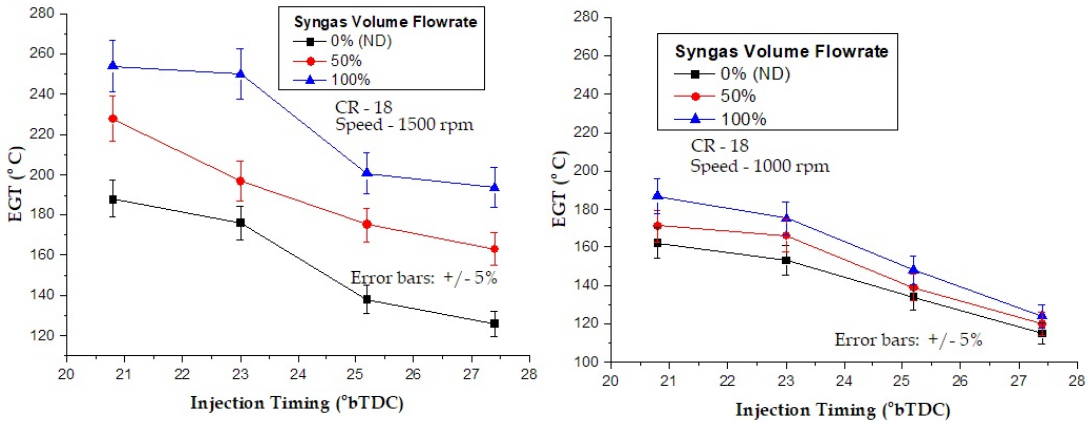

Figure 4.29: Variation of exhaust gas temperature with injection timing for speeds of (a) 1500 rpm (b) 1000 rpm

Figure 4.29(a) illustrates the variation of EGT when fuel injection timing (IT) was advanced to CA 27.4° and CA 25.2° or retarded to 20.8° at a speed of 1500 rpm and CR of 18. At standard IT, CR 18 and speed of 1500 rpm, EGT values recorded when the engine fuel IT was advanced to CA 27.4° for diesel mode showed decreases of 28.4% and 22.4% for dual fuel mode of 100% SVF. On retarding the IT, EGT increased by less than 1% in both fuel modes. Figure 4.29(b) illustrates the EGT variation with the same fuel and compression conditions maintained, while the engine speed is reduced to 1000 rpm. In diesel mode, EGT dropped by 24.8% and by 29% in 100% SVF when the engine was advanced to CA 27.4° at 1500 rpm and CR of 18. It was noted that advancing engine IT caused a decrease in EGT throughout, whilst retarding the IT produced increased temperature at both speeds. The cause of the effect was identified to be the prolonged time that an advance IT avails for the charge to mix, hence combustion was gradual, well-controlled and uniformly distributed, leading to reduced temperatures in the combustion chamber. This is attributed to the slow-burning syngas which acts as a diluent to diesel fuel in the mixture, causing the syngas-diesel blend to behave in a similar way like a lean mixture, where excess air tends to lower temperature in the CC.

O.M.I. Nwafor (2012) reported similar results, attributing the effect to the longer exposure of mixture to the state of ignition. The study also observed that; dual-fuel operation with advanced timing showed the highest exhaust temperatures at 3000 rpm. Further, the dual unit in standard timing produced the highest cylinder wall temperatures while the advanced system showed the lowest values at this speed. At an engine speed of 2400 rpm, there is no marked difference in the exhaust gas temperatures. However, the diesel fuel operation produces the lowest cylinder wall temperatures, whereas the standard unit showed the highest values.

4.6 Summary of the Results

The main objectives of this investigation was to run an engine without exhaust gas recirculation (EGR) and turbocharger, using blends of syngas-diesel (25%-100% SVF) in dual-fuel mode with controlled compression ration (CR), determined pilot fuel injection timing (IT), under medium-speed (1000 - 1500 rpm) and all-load (3 -11 kg) operating conditions to obtain rated output power of of 3.5 kW at reduced fuel consumption. Besides, reduce or eliminate altogether objectionable emission from its exhaust gases.

It has been noted, though engine power derated from under medium-speed, medium-full load conditions, it was feasible to increase the output power when a relatively high (100%) SVF was used. Further, advancing the pilot fuel IT effectively improve fuel economy. It was observed under these conditions, the engine BSFC could be improved by 7% and 13% when the engine was advanced to CA 25.2° and CA 27.4° respectively. , Under the same conditions CO, NO_x, CO_2, smoke and soot emissions were considerably reduced as the fuel IT advance was increased, however HC emission and EGT increased.

Therefore, operating a CI engine in dual fuel mode and advancing pilot fuel IT before the critical point might be a practical way to balance the requirements of power output, fuel consumption and emissions in the engine operation.

CHAPTER FIVE
CONCLUSIONS AND RECOMMENDATIONS

This chapter summarises the findings from the experimental investigation on combustion, performance and emission characteristics of a CI when operated in both diesel mode and varying syngas volume flowrates on dual fuel mode. Further, recommendations for future studies have been outlined in the areas where the present study did not venture due to certain limitations.

5.1 Conclusions

This study investigated the effects of blending diesel fuel with syngas, a gaseous fuel, on the combustion, performance and emissions of a CI engine. Tests were done on a CI engine fuelled with diesel blended with different volume fractions of syngas. The test results for engine operation with diesel and syngas-diesel blend were analysed and compared. The conclusions deduced from the tests are as follows:

- The in-cylinder pressure (CP) results obtained at the compression ratio (CR) of 18 and 1500 rpm showed a peak value of 32 bar for both diesel and dual-fuel of syngas volume flowrate (SVF) 100% at standard injection timing. Advancing injection timing (IT) to 25.175° increased CP to peak values of 34 bar for neat diesel (ND) and 36 bar for SVF of 100%. This result indicates that it is possible to improve the cylinder pressure by optimising syngas flowrate for a given engine and advancing IT to the optimum CA of 25.2° bTDC.

- Net heat release rate (HRR) in the substitution of 100% SVF was 41% higher than for SVF of 25% at CR of 18 and speed of 1500 rpm. Other results indicated an increase of HRR by 64.3% in diesel mode and by 39%

at the dual-fuel mode of SVF 100% when IT was advanced to 25.175°. This led to the conclusion that in dual fuel mode engines should be operated at SVF 100% levels of syngas volume flowrate and in advanced conditions to boost the work transferred to the piston

- The study showed that running the engine at its optimum operating conditions of CR of 18 and speed of 1500 rpm, it de-rated by about 32% for the dual-fuel mode of SVF 100% when compared with that of neat diesel mode. This is an indication of the poor state of fuel-energy conversion by the engine in the dual-fuel mode. This led to the conclusion that for CI engine to run in dual fuel mode some degree of modification must be effected.

- Results obtained in the present study showed that values of volumetric efficiency (VE) reduced by 17.5% when neat diesel was substituted with a blend of diesel and 100% SVF at 1500 rpm. This shows that VE suffers when syngas is premixed because it takes the volume usually occupied by fresh air. Since VE affects power generated in an engine, it is important to improve the air aspirated into the engine by replacing the naturally aspirated system with an artificially aspirated one.

- At CR 18 and 1500 rpm and in dual fuel mode of 100% SVF, CO increased by 4%, HC by 7.2% and PM decreased by 15.2% compared with diesel mode. When fuel IT was retarded to 20.8° and advanced to 27.4° the PM values obtained were higher in case of retardation but lower by 3.3% for SVF of 100% and by 15%, in diesel mode for advanced injection timing conditions. This led to the conclusion that CI engine emissions can be reduced by running the engine in dual fuel mode and by adjusting the CR and fuel IT appropriately.

- CO_2 emission values obtained for standard engine IT indicated up to 1.8% reduction in emission for diesel substitution with 100% SVF. In advancing IT to 27.4°, CO_2 emission decreased by 0.2% for SVF of 100%. This led to the conclusion that the use of syngas in a dual fuel mode and in advance fuel

IT for CI engine is a promising technique to reduce engine greenhouse-gas emissions especially at high loads.

- The effect of diesel substitution on exhaust gas temperature (EGT) showed an increase of 42% when fuel mode was changed from diesel to dual fuel at 100% SVF at CR 18. EGT values recorded when the engine IT was advanced to CA 27.4° for diesel mode showed a decrease of 28.4% and 22.4% for dual fuel mode of 100% SVF. Operating the CI engines in dual-fuel modes still caused a degree of heat losses through exhaust gases and therefore, it is desirable to fit an exhaust gas recirculation system in a dual-fuel engine.

- NO_x emission decreased by 2.5% when diesel fuel was substituted with SVF of 100% for compression ratio (CR) of 18 and by about 30% for CR of 12. Advancing injection timing reduced emissions by 3.6% in a dual-fuel mode of SVF 100% but significantly increased by 71.4% in diesel mode, with retardation causing a decrease of 7.3% in dual-fuel mode. This led to the conclusion that advancing and retardation of injection timing, adjusting CR and controlling the quantity of syngas in the syngas-diesel blend could be used to reduce NO_x emission in IC engines.

- The results obtained for BTE with a fuel IT advanced to 27.4° CA were 10% higher for engine fuelled by ND than when fuelled by syngas of 100% SVF-diesel blend. When CRs of 18 and 16 were analysed, BTE values for ND were 10% higher than for 100% SVF at CR 18 and 8% higher at CR 16 at 1500 rpm. The results, therefore, show that CR adjustment has much influence on the engine power output, especially in dual fuel mode and could be used to improve engine performance in that mode.

The results reported in this study confirm that the CI engine in dual fuel mode is a viable alternative to the traditional diesel engine, albeit minor adjustment to fuel injection timing and CR will be required in addition to supercharging of the engine.

5.2 Recommendations

The study of syngas application in the IC engine may be extended by carrying out further studies in syngas quality improvement, the effect of supercharging or turbocharging and exhaust gas recirculation (EGR) on combustion, performance and emission characteristics of an engine running on dual fuel mode.

- Syngas has a low heating value fuel gas compared to liquid fuels and gaseous fuels like CNG, will require its energy density to be boosted. One way of increasing LHV of the syngas is to increase H_2 content in its composition. The method proposed is to pass the syngas through a suitable catalyst to enrich it. This study recommends the expansion of the study to investigate a viable way to improve the LHV and energy density of the gas to alleviate engine de-rating when fuelled with syngas-diesel fuel blend.

- It has been shown that the cause of low power output in dual fuel CI engines with a pre-mix of syngas and air is its low volumetric efficiency caused by the syngas taking the space normally occupied by fresh air in engine operated with diesel. It is recommended that a turbocharger, or a supercharger be fitted as part of the air supply system modification in the research engine.

- The other method to improve the engine thermal efficiency and reduce NO_x emission without affecting significantly the CO and CO_2 emissions is retrofitting the exhaust system with an exhaust gas recirculation (EGR) facility. This will help to recover some heat from the exhaust gases which otherwise, will go to waste. It is recommended the EGR system be included in the dual-fuel CI engine.

- Results obtained under some conditions of diesel substitution with syngas volume flowrate (SVF) of 50% showed unexpected better engine performance and exhaust emissions than with SVF of 100%. The study recommends that further investigation be done for this unusual engine performance under these special conditions to use it to improve the engine

combustion, performance and emissions. The present was constraint by resources and required scope from studying the effect of chemical composition of syngas-diesel blends used on engine performance and emissions thus put off the study of the phenomenon.

REFERENCES

S. Acar and A. Ayanoglu. Determination of higher heating values (HHVs) of biomass fuels. *Energy Education Science and Technology Part A: Energy Science and Research*, 28(2):749–758, 2012. ISSN 1308772X.

M. A. Ahmed. Hydrogen Fueled Internal Combustion Engine : A Review. *International Journal of Innovative Technology and Research (IJITR)*, 4(4):3193–3198, 2016.

S. A. Ahmed, S. Zhou, Y. Zhu, and Y. Feng. Performance and emission characteristics analysis of dual fuel compression ignition engine using natural gas and diesel. *International Journal of Thermodynamics*, 21(1):16–25, 2018. ISSN 13019724. doi: 10.5541/ijot.316300.

M. S. Alam, A. T. Wijayanta, K. Nakaso, and J. Fukai. Syngas Production from Coal Gasification with CO_2 Rich Gas Mixtures. *Cleaner Combustion and Sustainable World Journal*, (819-0395):1103–1108, 2013. doi: 10.1007/978-3-642-30445-3.

R. Alvarez-Rodriguez, M. Bogataj, A. D. Bojarski, C. Clemente-Jul, P. Coca, A. D. Donato, Z. Kravanja, J. M. Lainez, C. R. A. Medina, and J. M. Nougues. Emerging Technologies on Syngas Purification: Process Intensification. In L. Puigjaner, editor, *Syngas from Waste Emerging Technologies*, pages 121–145. Springer-Verlag, London, first edition, 2012. ISBN 9781608052851. doi: 10.2174/97816080528511120101. URL http://www.eurekaselect.com/102081/volume/1.

G. T. Armstrong and T. L. Jobe. Heating Values of Natural Gas and Its Components. Technical Report August, U.S. Department of Commerce (National Bureau of Standard), Washington, DC, 1982.

M. Asaro and R. M. Smith. Coal to Liquids Technologies. *Encyclopedia*

of Sustainability Science and Technology, 3:389–442, 2013. doi: 10.1007/978-1-4419-0851-3.

U. Azimov, E. Tomita, N. Kawahara, and Y. Harada. Effect of syngas composition on combustion and exhaust emission characteristics in a pilot-ignited dual-fuel engine operated in PREMIER combustion mode. *International Journal of Hydrogen Energy*, 36(18):11985–11996, 2011. ISSN 03603199. doi: 10.1016/j.ijhydene.2011.04.192.

U. Azimov, E. Tomita, N. Kawahara, and S. S. Dol. Combustion Characteristics of Syngas and Natural Gas in Micro-pilot Ignited Dual-fuel Engine. *International Journal of Mechanical, Aerospace, Industrial, Mechatronic and Manufacturing Engineering*, 6(12):2863–2870, 2012.

M. Baratieri, P. Baggio, B. Bosio, M. Grigiante, and G. A. Longo. The use of biomass syngas in IC engines and CCGT plants: A comparative analysis. *Applied Thermal Engineering*, 29(16):3309–3318, 2009. ISSN 13594311. doi: 10.1016/j.applthermaleng.2009.05.003. URL http://dx.doi.org/10.1016/j.applthermaleng.2009.05.003.

J. Barbee, M. Davis, S. Davis, D. Gaddis, J. Harrison, M. Holtz, R. McElroy, J. Polizzi, and J. Willett. *Standards of the Tubular Exchanger Manufacturers Assoc.* New York, ninth edition, 2007.

R. P. Bates and K. Dölle. Syngas Use in Internal Combustion Engines - A Review. *Advances in Research*, 10(1):1–8, 2017. doi: 10.9734/AIR/2017/32896.

D. Bellman, C. Trecazzi, J. Katzer, G. Kawalkin, M. Eastman, and J. Strakey. Coal to liquids and gas. Technical report, The National Petroleum Council (NPC), Columbus, 2007.

P. R. Bevington and D. K. Robinson. *Data Reduction and Error Analysis for the Physical Sciences*. Kent A. Peterson, New York, third edition, 2003. ISBN 0-07-247227-8.

A. S. Bika. *Synthesis Gas Use in Internal Combustion Engines*. Ph.d, The University of Minnesota, 2010.

F. Binz and J. Binz. Operating instructions ecom-J2KNpro, 2015. ISSN 0543-1972.

M. Blesl and D. Bruchof. Syngas Production from Coal. *Iea ETSAP - Technology Brief*, (1):1–5, 2010.

S. Brusca, V. Chiodo, A. Galvagno, R. Lanzafame, and A. M. Cugno. Analysis of reforming gas combustion in Internal Combustion Engine. *Energy Procedia*, 45:899–908, 2014. ISSN 1876-6102. doi: 10.1016/j.egypro.2014.01.095. URL http://dx.doi.org/10.1016/j.egypro.2014.01.095.

K. Cheenkachorn, C. Poompipatpong, and C. G. Ho. Performance and emissions of a heavy-duty diesel engine fuelled with diesel and LNG (liquid natural gas). *Energy*, 53(May):52–57, 2013. ISSN 03605442. doi: 10.1016/j.energy.2013.02.027. URL http://dx.doi.org/10.1016/j.energy.2013.02.027.

A. Chrıbik, M. Poloni, and J. Lach. Effect of Gas Mixture Composition on the Parameters of an Internal Combustion Engine. *Acta Polytechnica*, 52(3):23–27, 2012.

L. L. Coq and D. Ashenafi. Syngas Treatment Unit for Small Scale Gasification-Application to IC Engine Gas Quality Requirement. *Journal of Applied Fluid Mechanics*, 5(January 2012):95–103, 2014. URL www.jafmonline.net.

R. P. Devi, S. Kamaraj, R. Angeeswaran, and S. Pugalendhi. Tar and Particulate Removal Methods for the Producer Gas Obtained from Biomass Gasification. *International Journal of Current Microbiology and Applied Sciences*, 6(10):269–284, 2017.

A. A. Dhavale, A. H. Kolekar, and K. M. Jadhav. An Experimental Investigation and Analysis for Engine Performance , Combustion and Emissions of Dual Fuel CI Engine. *International Engineering Research Journal (IERJ)*, (2):1215–1224, 2015.

A. E. Dhole, R. B. Yarasu, D. B. Lata, and A. Priyam. Effect on performance and emissions of a dual fuel diesel engine using hydrogen and producer gas as secondary fuels. *International Journal of Hydrogen Energy*, 39(15):8087–8097, 2014. ISSN 03603199. doi: 10.1016/j.ijhydene.2014.03.085. URL http://dx.doi.org/10.1016/j.ijhydene.2014.03.085.

J. Dirgo and D. Leith. Cyclone collection efficiency: comparison of experimental results with theoretical predictions. *Aerosol Science and Technology*, 4(4):401–415, 1985. ISSN 15217388. doi: 10.1080/02786828508959066.

A. Fallis. Future Transport fuels. *Journal of Chemical Information and Modeling*, 53(9):1689–1699, 2013. ISSN 1098-6596. doi: 10.1017/CBO9781107415324.004.

C. R. Ferguson and A. T. Kirkpatrick. *Internal Combustion Engines Applied Thermosciences*. John Wiley and Sons, Ltd, West Sussex, third edition, 2016. ISBN 9781118533314.

J. Fermoso, M. G. Plaza, B. Arias, C. Pevida, F. Rubiera, and J. J. Pis. Co-Gasification of Coal With Biomass and Petcoke in a High-Pressure Gasifier for Syngas Production. In *1st Spanish National Conference on Advances in Materials Recycling and Eco – Energy Madrid*, number SO1-5, pages 17–20, Madrid, 2009. Instituto Nacional del Carbón.

J. Fermoso, B. Arias, M. V. Gil, M. G. Plaza, C. Pevida, J. J. Pis, and F. Rubiera. Co-gasification of different rank coals with biomass and petroleum coke in a high-pressure reactor for H_2 -rich gas production. *Bioresource Technology*, 101 (9):3230–3235, 2010. ISSN 09608524. doi: 10.1016/j.biortech.2009.12.035.

R. Fernando. Developments in modelling and simulation of coal gasification. *IEA Clean Coal Centre*, (CCC/232):1–77, 2014.

J. Fo, B. Arias, M. Plaza, C. Pevida, F. Rubiera, J. Pis, F. García-Peña, and P. Casero. High-pressure co-gasification of coal with biomass and petroleum coke. *Fuel Processing Technology*, 2(90(7-8)):1–24, 2009.

J. S. Giraldo, D. J. Gotham, D. G. Nderitu, P. V. Preckel, and D. J. Mize.

Fundamentals of Nuclear Power. Technical Report December, State Utility Forecasting Group, West Lafayette, Indiana, 2012.

H. Guo, W. S. N. Neill, and B. Liko. The Combustion and Emissions Performance of a Syngas-Diesel Dual Fuel Compression Ignition Engine. In *ASME 2016 Internal Combustion Engine Division Fall Technical Conference*, number ICEF2016-9367, pages 1–10, Greenville, 2016. ResearchGate. doi: 10.1115/ICEF2016-9367.

F. Y. Hagos, A. Rashid, A. Aziz, and S. A. Sulaiman. Study of syngas combustion parameters effect on internal combustion engine. *Asian Journal of Scientific Research*, 6(2):187–196, 2013. ISSN 19921454. doi: 10.3923/ajsr.2013.187.196.

F. Y. Hagos, A. R. A. Aziz, and S. A. Sulaiman. Effect of Air-fuel Ratio on the Combustion Characteristics of Syngas (H_2:CO) in Direct-injection Spark-ignition Engine. *Energy Procedia*, 61(6 ICAE2014):2567–2571, 2014a. ISSN 1876-6102. doi: 10.1016/j.egypro.2014.12.047. URL http://dx.doi.org/10.1016/j.egypro.2014.12.047.

F. Y. Hagos, A. R. A. Aziz, and S. A. Sulaiman. Trends of syngas as a fuel in internal combustion engines. *Advances in Mechanical Engineering*, 2014 (January 2014):0–11, 2014b. ISSN 16878132. doi: 10.1155/2014/401587.

F. Y. Hagos, A. R. A. Aziz, and S. A. Sulaiman. Effect of injection timing on combustion, performance and emissions of lean-burn syngas (H_2/CO) in spark-ignition direct-injection engine. *International Journal of Engine Research*, 17 (9):921–933, 2016. ISSN 20413149. doi: 10.1177/1468087415623910.

V. Hariram and R. Vagesh Shangar. Influence of compression ratio on combustion and performance characteristics of direct injection compression ignition engine. *Alexandria Engineering Journal*, 54(4):807–814, 2015. ISSN 11100168. doi: 10.1016/j.aej.2015.06.007.

S. Hassan, Z. A. Zainal, and M. A. Miskam. Effects of advanced injection timing on performance and emission of a supercharged dual-fuel diesel engine fueled

by producer gas from downdraft gasifier. *Journal of Scientific and Industrial Research*, 70(3):220–224, 2011. ISSN 00224456.

J. B. Heywood. *Internal Combustion Engine Fundmentals*, volume 1. McGraw-Hill, Inc, New York, original edition, 1988. ISBN 0-07-028637-X. doi: 10.1017/CBO9781107415324.004.

N. Homdoung, N. Tippayawong, and D. Natthawud. Performance investigation of a modified small engine fueled with producer gas. *Maejo International Journal of Science and Technology*, 01(2):166–177, 2007. ISSN 19057873. doi: 10.14456/mijst.2015.2.

N. Homdoung, N. Tippayawong, and N. Dussadee. Prediction of small spark ignited engine performance using producer gas as fuel. *Case Studies in Thermal Engineering Journal*, 5:98–103, 2015. ISSN 2214-157X. doi: 10.1016/j.csite.2015.02.003. URL http://dx.doi.org/10.1016/j.csite.2015.02.003.

John R. Taylor. *An introduction to error analysis: The Study of Uncertainty in Physical Measurements*. University Science Books, Sausalito, second edition, 1997. ISBN 0-935702-75-X.

Y. Karagoz, T. Sandalcı, U. O. Koylu, and A. S. Dalkılıc. Effect of the use of natural gas – diesel fuel mixture on performance , emissions , and combustion characteristics of a compression ignition engine. *Advances in Mechanical Engineering*, 8(4):1–13, 2016. doi: 10.1177/1687814016643228.

K. Kolmetz and M. Widiawati. *Design Fin Fan Air Cooler Selection and Sizing (Engineering Design Guideline)*. KLM Technology Group, Johor Bahru, first edition, 2015.

N. Kousheshi, M. Yari, Amin Paykani, A. S. Mehr, and G. F. de la Fuente. Effect of Syngas Composition on the Combustion and Emissions Characteristics of a Syngas / Diesel. *Energies*, 13(212):1–2, 2020.

S. Kumar and S. K. Shukla. Performance of cyclone separator for syngas pro-

duction in downdraft gasifier. *Advances in Energy Research,*, 4(3):223–237, 2016.

S. Lal and S. K. Mohapatra. The effect of compression ratio on the performance and emission characteristics of a dual fuel diesel engine using biomass derived producer gas. *Applied Thermal Engineering*, 119(5 June 2017):63–72, 2017. doi: 10.1016/j.applthermaleng.2017.03.038.

L. C. Laurence and D. Ashenafi. Syngas Treatment Unit for Small Scale Gasification - Application to IC Engine Gas Quality Requirement. *Journal of Applied Fluid Mechanics*, 5(1):95–103, 2012.

M. Leahy, J. L. Barden, B. T. Murphy, N. Slater-thompson, and D. Peterson. International Energy Outlook 2013. Technical report, U.S. Energy Information Administration (EIA, Washington, 2013.

J. Lee. *A Study on Performance and Emissions of a 4-stroke IC Engine Operating on Landfill Gas with the Addition of H_2 , CO and Syngas*. PhD thesis, Columbia University in the City of New York, 2010.

Y. Liu, B. Xu, J. Jia, J. Wu, W. Shang, and Z. Ma. Effect of Injection Timing on Performance and Emissions of DI-diesel Engine Fueled with Isopropanol. In *International Conference on Electrical, Electronics and Mechatronics (ICEEM 2015)*, number Iceem, pages 133–137, Luoyang, 2015. Atlantis Press.

B. K. Mahgoub, S. A. Sulaiman, Z. A. A Karim, and F. Y. Hagos. Experimental study on the effect of varying syngas composition on the emissions of dual fuel CI engine operating at various engine speeds. *IOP Conference Series: Materials Science and Engineering*, 100(1):1–8, 2015a. ISSN 1757899X. doi: 10.1088/1757-899X/100/1/012006.

B. K. Mahgoub, S. Hassan, S. A. Sulaiman, R. Mamat, A. Abdul Adam, and F. Y. Hagos. Combustion and performance of syngas dual fueling in a CI engine with blended biodiesel as pilot fuel. *BioResources*, 12(3):5617–5631, 2017. ISSN 19302126. doi: 10.15376/biores.12.3.5617-5631.

B. K. M. Mahgoub, S. Hassan, and S. A. Sulaiman. Effect of Varying Engine Parameters and Syngas Composition on the Combustion Characteristics, Performance and Emission of Syngas: Diesel Duel Fuel Engine : A Review . *ARPN Journal of Engineering and Applied Sciences*, 10(17):7712–7718, 2015b.

B. K. M. Mahgoub, S. A. Sulaiman, and Z. A. A. Karim. Performance study of imitated syngas in a dual fuel compression ignition diesel engine. *International Journal of Automotive and Mechanical Engineering*, 11(1):2282–2293, 2015c. ISSN 21801606. doi: 10.15282/ijame.11.2015.11.0192.

N. R. Mate and D. Y. Dhande. A Study of the Two Wheeler Retarder Type Dynamometer System. *International Journal of Innovative Research in Science, Engineering and Technology*, 3(2):9057–9061, 2014.

S. E. Mohammed, M. B. Baharom, A. R. A. Aziz, and Firmansyah. The effects of fuel-injection timing at medium injection pressure on the engine characteristics and emissions of a CNG-DI engine fueled by a small amount of hydrogen in CNG. *International Journal of Hydrogen Energy*, 36(18):11997–12006, 2011. ISSN 03603199. doi: 10.1016/j.ijhydene.2011.05.110.

E. Monteiro, J. Sotton, M. Bellenoue, N. Afonso, and S. Malheiro. Experimental study of syngas combustion at engine-like conditions in a rapid compression machine. *Experimental Thermal and Fluid Science Journal*, 35:1473–1479, 2011. doi: 10.1016/j.expthermflusci.2011.06.006.

E. Monteiro, M. Bellenoue, J. Sottton, and A. Rouboa. Syngas Application to Spark Ignition Engine Working Simulations by Use of Rapid Compression Machine. *InTech Open Science*, pages 51–74, 2012.

R. Mukherjee. *Practical Thermal Design of air-cooled Heat Exchangers*. Begell House,, Wellingford, first edition, 2017.

S. S. Mulay, S. S. Mulay, and A. S. Mulay. User Manual for ICEngineSoft, 2014.

K. Murthy, N. Madhwesh, and B. R. Shrinivasarao. Influence of Injection Timing on the Performance of Dual Fuel Compression Ignition Engine with Exhaust

Gas Recirculation. *International Journal of Engineering Research and Development*, 1(11):36–42, 2012.

T. J. Mwiluka. *An assessment of coal from Mui basin as an alternative energy resource for Kenya*. Msc, University of Nairobi, 2009.

E. Núñez. *Bosch Automotive Handbook*. Bentley, Stuttgart, Germany, first edition, 2008.

O.M.I. Nwafor. Effects of Advanced Injection Timing on the Performance of Natural Gas in Diesel Engine. *Sadhana*, 25(4):11–20, 2012. ISSN 0960-1481. doi: 10.1016/S0960-1481(99)00132-9. URL http://www.sciencedirect.com/science/article/pii/S0960148199001329.

D. Owiro, G. Poquillon, K. S. Njonjo, and C. Oduor. Situational Analysis of Energy Industry, Policy and Strategy for Kenya. Technical report, Institute of Economic Affairs (IEA), Nairobi, 2015.

R. Patton, P. Steele, and F. Yu. Coal vs. charcoal-fueled diesel engines: A review. *Energy Sources, Part A: Recovery, Utilization and Environmental Effects*, 32 (4):315–322, 2010. ISSN 15567036. doi: 10.1080/15567030802612028.

B. E. Poling, J. M. Prausnitz, and J. P. O'Connell. *The Properties of Gases and Liquids*, volume 12. The McGraw-Hill Companies, Inc., New York, 5th edition, 2001. ISBN 0071499997. doi: 10.1063/1.3060771.

A. Pradhan, P. Baredar, Kumar, and Anil. Syngas as An Alternative Fuel Used in Internal Combustion Engines: A Review. *Journal of Pure and Applied Science and Technology*, 5(2):51–66, 2015.

V. Quaschning. *Renewable Energy and Climate Change*. John Wiley and Sons Ltd Chichester, Munich, 2nd edition, 2019.

S. M. Rahman, H. H. Masjuki, M. A. Kalam, A. Sanjid, and M. J. Abedin. Assessment of emission and performance of compression ignition engine with

varying injection timing. *Renewable and Sustainable Energy Reviews*, 35:221–230, 2014. ISSN 13640321. doi: 10.1016/j.rser.2014.03.049.

P. Raman and N. K. Ram. Performance analysis of an internal combustion engine operated on producer gas, in comparison with the performance of the natural gas and diesel engines. *Energy Procedia*, 63:317–333, 2013. ISSN 03605442. doi: 10.1016/j.energy.2013.10.033. URL http://dx.doi.org/10.1016/j.energy.2013.10.033.

T. B. Reed and A. Das. Handbook of biomass downdraft gasifier engine systems. Technical Report March, Solar Energy Research Institute, Golden, Colarado, 1988. URL http://www.osti.gov/servlets/purl/5206099/.

B. Road. Performance and Exhaust Gas Emissions Analysis of Direct Injection Cng-Diesel Dual Fuel Engine. *International Journal of Engineering Science and Technology (IJEST)*, 4(03):833–846, 2012.

E. Roberts. U . S . Energy : Present State and Future Perspective. *Science Education*, pages 1–62, 2013.

H. Rotich and J. Muia. Comprehensive Public Expenditure Review. Technical report, Government of Kenya, Nairobi, 2018.

H. Rotich and K. Thugge. Post-Election Economic and Fiscal Report 2018. Technical report, National Treasury, Kenya, Nairobi, 2018.

G. Ruoppolo, F. Miccio, P. Brachi, A. Picarelli, and R. Chirone. Fluidized Bed Gasification of Biomass and Biomass / Coal Pellets in Oxygen and Steam Atmosphere. *Chemical Engineering Transactions*, 32(23-5):595–600, 2013.

B. B. Sahoo, N. Sahoo, and U. K. Saha. Effect of H_2:CO ratio in syngas on the performance of a dual fuel diesel engine operation. *Applied Thermal Engineering*, 49:139–146, 2012. ISSN 13594311. doi: 10.1016/j.applthermaleng.2011.08.021.

S. K. Sansaniwal, M. A. Rosen, and S. K. Tyagi. Global challenges in the sustainable development of biomass gasification: An overview. *Renewable and Sustain-*

able Energy Reviews, 80(December):23–43, 2017. ISSN 18790690. doi: 10.1016/j.rser.2017.05.215. URL http://dx.doi.org/10.1016/j.rser.2017.05.215.

C. Sayin and M. Canakci. Effects of injection timing on the engine performance and exhaust emissions of a dual-fuel diesel engine. *Energy Conversion and Management*, 50(1):203–213, 2009. ISSN 0196-8904. doi: 10.1016/j.enconman.2008.06.007. URL http://dx.doi.org/10.1016/j.enconman.2008.06.007.

L. J. Shadle, D. A. Berry, and M. Syamlal. Coal Conversion Processes , Gasification. *Kirk - Othmer Encyclopedia of Chemical Technology*, (2):1–38, 2010. doi: 10.1002/0471238961.0701190913010801.a01.pub2.

Shital Sharadchandra Mulay, S. S. Mulay, and A. S. Mulay. Research Engine Test Set Up, 2014.

V. Shrivastava, A. K. Jha, A. K. Wamankar, and S. Murugan. Performance and Emission Studies of a CI Engine Coupled with Gasifier Running in Dual Fuel Mode Performance and Emission Studies of a CI Engine Coupled with Gasifier Running in Dual Fuel Mode. *Procedia Engineering*, 51(December 2013):600–608, 2014. ISSN 1877-7058. doi: 10.1016/j.proeng.2013.01.085. URL http://dx.doi.org/10.1016/j.proeng.2013.01.085.

D. Singh and N. D. Pal. Designing and Performance Evaluation of a Shell and Tube Heat Exchanger using ANSYS (Computational Fluid Dynamics). *International Journal of Scientific Engineering and Applied Science*, 2(3):427–446, 2016.

D. K. Soni and R. Gupta. Comparison of performance and emission characteristics of diesel and diesel-water blend under varying injection timings. *International Journal of Engineering, Science and Technology*, 7(4):49, 2016. ISSN 2141-2820. doi: 10.4314/ijest.v7i4.6.

A. Srivastava, R. Verma, V. Dubey, and P. Verma. Performance Analysis of Shell and Tube Type Heat Exchanger under the Effect of Varied Operating

Conditions. *IOSR Journal of Mechanical and Civil Engineering*, 11(3):8–17, 2014. URL www.iosrjournals.org.

Stellamaris N. Nzove. *Development and Evaluation of Performance of a Bench Scale Gasifier for Sub-bituminous Coal*. Msc, Jomo Kenyatta University of Agriculture and Technology, 2021.

S. Tomar, R. Mishra, S. Bisht, S. Kumar, A. Balyan, and G. Saxena. Optimisation of Connecting Rod Design to Achieve Vcr. *International Journal of Engineerin Research and Applications*, 3(6):281–286, 2013. doi: 10.1074/jbc.M008527200.

P. Tunå. *Generation of synthesis gas for fuels and chemicals production*. Ph.d, Lund University, 2013.

E. S. Udoetok. Thermal conductivity of binary mixtures of gases. *Frontiers in Heat and Mass Transfer*, 4(2):1–5, 2013. ISSN 21518629. doi: 10.5098/hmt.v4.2.3008.

S. V. B. Van Paasen and J. H. A. Kiel. Tar formation in a fluidised-bed gasifier: Impact of fuel properties and operating conditions. *Kardiologia Polska*, 67(6): 58, 2004. ISSN 00229032.

C. Vipavanich, S. Chuepeng, and S. Skullong. Heat release analysis and thermal efficiency of a single cylinder diesel dual fuel engine with gasoline port injection. *Case Studies in Thermal Engineering*, 12(February):143–148, 2018. ISSN 2214157X. doi: 10.1016/j.csite.2018.04.011.

A. Wagemakers and C. Leermakers. Review on the Effects of Dual-Fuel Operation, Using Diesel and Gaseous Fuels, on Emissions and Performance. *SAE International Journal of Engines*, 2012010869(2012-01-0869):1–18, 2012. ISSN 0148-7191. doi: 10.4271/2012-01-0869. URL http://papers.sae.org/2012-01-0869/.

APPENDICES

Appendix I: Compression Ignition Engine

A compression ignition (diesel) engine is a reciprocating-piston engine with internal (and thus heterogeneous) mixture formation and auto-ignition. During the compression stroke, intake air is compressed to 30 - 55 bar in naturally aspirated engines or 80 - 110 bar in supercharged engines, so that its temperature increases to 700 - 900°C. This temperature is sufficient to induce auto-ignition in the fuel injected into the cylinders shortly before the end of the compression stroke, as the piston approaches TDC. In heterogeneous processes the mixture formation is the most important factor in determining the quality of the combustion which then follows, and the efficiency with which the inducted combustion air is utilized, and thus in defining the available mean effective pressure levels.

Combustion Process

The start of injection (and thus the start of mixture formation) and the initiation of the exothermal reaction (start of ignition) are separated by a certain period, called ignition lag. The actual delay is defined by:

- the ignitability of the fuel (cetane number),
- the compression end pressure (compression ratio, boost factor),
- the compression end temperature (compression ratio, component temperatures,intercooling), and
- the fuel-management system.

The combustion process, which begins with the start of ignition, can be subdivided into three phases. In the “premixed flame” phase, the fuel is injected before the start of ignition and mixed with the air combusts. The injected-fuel, once ignition has started, combusts in a “diffusion flame”. That portion of the

combusted fuel which burns has a very rapid premixed flame and is primarily responsible for the pressure rise, and this is the primary cause of both combustion noise and oxides of nitrogen (NO_x). The slower-burning diffusion flame is the main source of particulates matter (PM) and unburned hydrocarbons (HC). The third phase (the post-injection one) is when the soot formed primarily during the second phase is oxidized. This phase is becoming increasingly significant in modern combustion processes. The heat release of a diesel engine depends on the combustion process itself, but also to a very large extent on the start of injection, the injection rate, and the maximum injection pressure. In direct-injection diesel engines, the number of orifices in the nozzle is another crucial factor. The injection to reduce combustion noise and ensure that injection for the main injection phase commences as early as possible. This reduces fuel consumption for given levels of nitrogen-oxide emissions (Núñez, 2008). Incomplete combustion leads to the emission of carbon monoxide, unburnt fuel, oil and soot. These incomplete combustion products comprise thousands of chemical components present in the gas and particulate phases. The concentration of a chemical species in engine exhaust is a function of several factors, including engine type, engine operating conditions, fuel and lubricating oil composition and emission control system (Rahman et al., 2014).

Mechanism of NO_X Formation:

The mechanism of formation and controlling its emission is that combustion is highly heterogeneous and transient in diesel engines. While NO and NO_2 are lumped together as NO_x, there are some distinctive differences between these two pollutants, NO is a colourless and odourless gas, while NO_2 is a red-brown gas with a pungent odour. Both gases are considered toxic, but NO_2 has a level of toxicity 5 times greater than that of NO. Although NO_2 is largely formed from oxidation of NO, attention has been given on how NO can be controlled before and after combustion (Sayin and Canakci, 2009). NO is formed during the post flame combustion process in a high-temperature region. The most widely accepted mechanism was suggested by Zeldovich (**?**). The principal source of NO

formation is the oxidation of the nitrogen present in atmospheric air. The nitric oxide formation chain reactions are initiated by atomic oxygen, which forms from the dissociation of oxygen molecules at the high temperatures reached during the combustion process.

Appendix II: Coal Gasification

All carbon-containing feedstocks such as coal, heavy oils or biomass that can be combusted can be gasified into synthesis gas. In the gasifier several reactions takeplace, but the overall reaction can be summarised by the reaction in Eq. A1.

$$C_aH_bO_cN_d + O_2/H_2O/N_2 \rightarrow CO + H_2 + C_xH_yO_z + CO_2 + H_2O + NH_3 + N_2 \quad \text{(A1)}$$

The solid carbon is partially oxidised with a gasification agent that can be oxygen (O_2), air, steam (H_2O) or a combination of them all. For most gasifiers, $C_xH_yO_z$ consists of mostly methane with some lower hydrocarbons such as ethane and ethylene. Depending on the feedstock used and the operating parameters, the gas can also contain heavier hydrocarbons such as benzene, toluene and naphthalenes. Hydrocarbons heavier than benzene are often referred to as tars. Gasification is a process that occurs in several steps: drying, pyrolysis, oxidation and reduction. The gasification reactions require heat, which must be supplied to the reactor to maintain the desired temperature. Heat can be supplied either directly by combusting a part of the fuel (autothermal) or indirectly (allothermal) (Tunå, 2013).

Classification of Gasifiers

There are three major types of gasifiers, distinguished by the way they convert the fuel. Most operate on coal or heavy oils, but most types can also operate on any carbon-containing feedstock such as biomass. They are: fixed bed, fluidised bed entrained flow, molten media and supercritical gasifiers.

Fixed bed gasifiers (sometimes denoted moving bed) are the most common type of gasifier worldwide due to the simplicity of the design. They are also more tolerant with regard to fuel particle size and moisture content than fluidised bed and entrained flow gasifiers. They can be used in a wide range of applications from small-scale biomass gasifiers to large-scale coal gasifiers. Fixed bed gasifiers have a 'fixed' bed of solid fuel that moves through the gasifier as the solid feedstock is converted into gas. They are divided into downdraft, updraft and crossdraft

gasifiers depending on how the gas flows relative to the bed (Shadle et al., 2010).

Fluidised beds have a more uniform temperature distribution in the reactor than fixed beds, with the result that there are no defined zones (such as drying). This necessitates more stringent pretreatment requirements for the moisture content of the feedstock. As the feedstock must fluidise, there are also more stringent pretreatment requirements regarding particle size. Fluidising bed gasifiers can be defined as having either a bubbling or a circulating fluidised bed, depending on how the bed moves in the reactor. In circulating fluidised bed (CFB) gasifiers the bed material circulates between the gasifier and a cyclone where ash and particles are separated from the producer gas and returned to the gasifier. The gasification agent is injected at the bottom of the reactor at high speed, causing the bed to lift.The bed in bubbling fluidised bed gasifiers (BFB) is much the same as in CFBs, except that there is no circulation to a cyclone (Ruoppolo et al., 2013).

Entrained flow gasifiers are high throughput reactors with low residence times and high temperatures. In an entrained flow gasifier a very fine powdered fuel is injected into the reactor vessel along with oxygen or oxygen and steam. A high temperature (1600–1900°C) is obtained and therefore short residence times are sufficient to achieve high carbon conversions (90–99%) allowing the reactors to have high throughput. In most cases the high-temperature results in a gas free from tars and hydrocarbons. The high performance of the entrained flow gasifier comes at the expense of fuel pretreatment requirements. A very fine powder is required (around 0.1 mm) for most gasifiers to allow fluidisation of the solid feedstock (Asaro and Smith, 2013).

The last type of gasifier is the molten media reactor in which the feedstock is dispersed in a molten carrier. The carrier generally provides heat for the gasification and can participate in the gasification if it contains catalytically active species such as nickel or iron. The major advantages of molten media reactors are the high heat transfer rates, as the molten media is the heat source, and the ability of the molten media to absorb contaminants in the feedstock, mainly sulphur

and alkalis. Molten media reactors can have a high temperature depending on the molten media and can accept most feedstocks. The disadvantage is that the processes must handle the molten media. For molten salts this can become very troublesome as the media are highly corrosive. Under supercritical conditions (T $>$ 374.8 °C, P $>$ 221 bar) water reacts with biomass to produce a gas rich in hydrogen and methane. The water self-dissociates to form both H_3O + and OH- ions that act as catalysts for converting the biomass into gas (Tunå, 2013).

Appendix III: Instruments Used in Engine Performance Analysis

3D-surface Diagrams for the Engine Performance

In this section, 3D-surface illustrations of the effect varying of load, syngas-diesel blend, compression ratio and pilot fuel injection timing has on brake specific fuel consumption (BSFC) and brake thermal efficiency (BTE) of dual fuel CI engine are depicted.

BSFC Effects

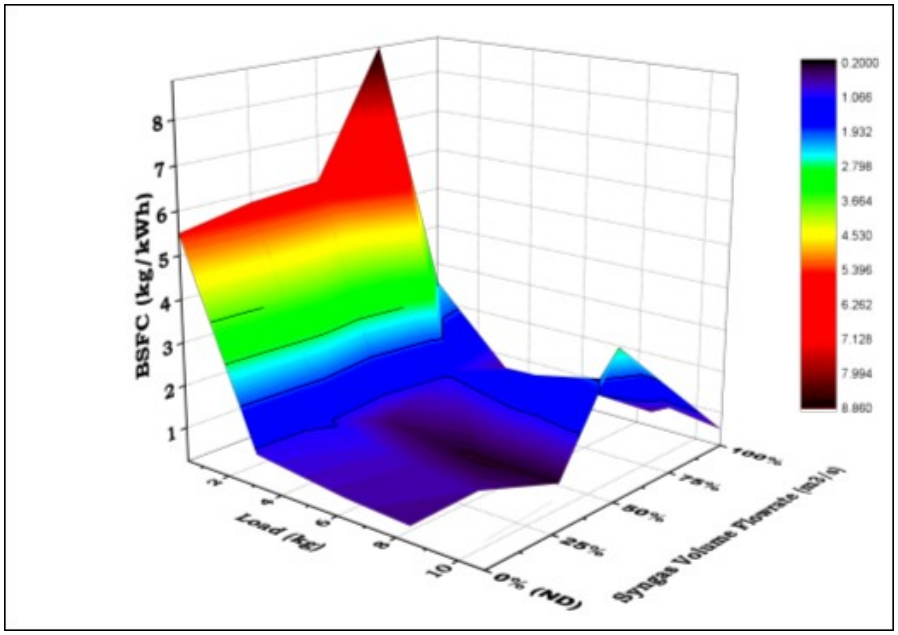

(a)

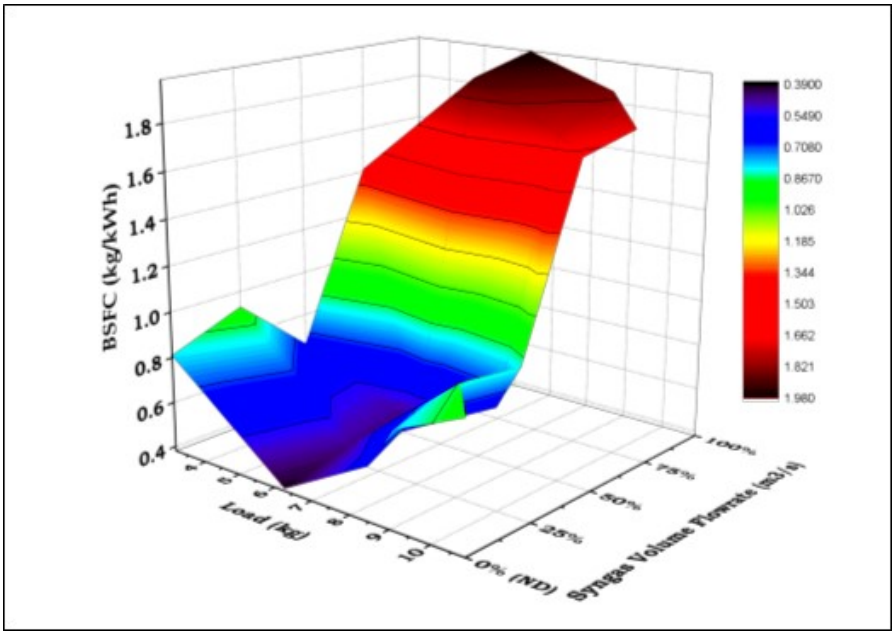

(b)

Figure A1: 3D-surface illustrations of Variation of BSFC with load for compression ratios of (a) 18 (b) 16

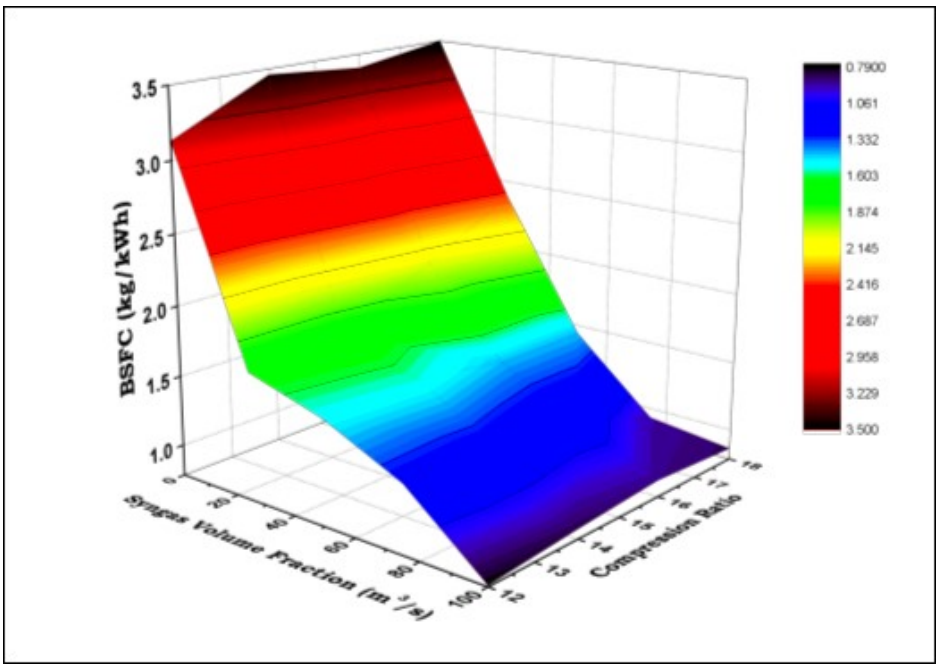

Figure A2: 3D-surface illustration of Variation of BSFC with syngas volume flowrate

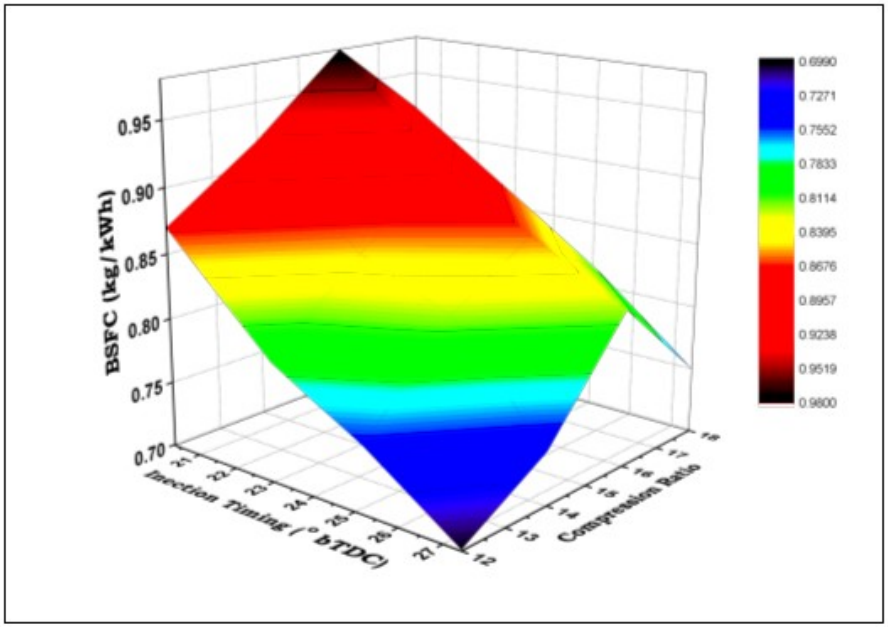

(a)

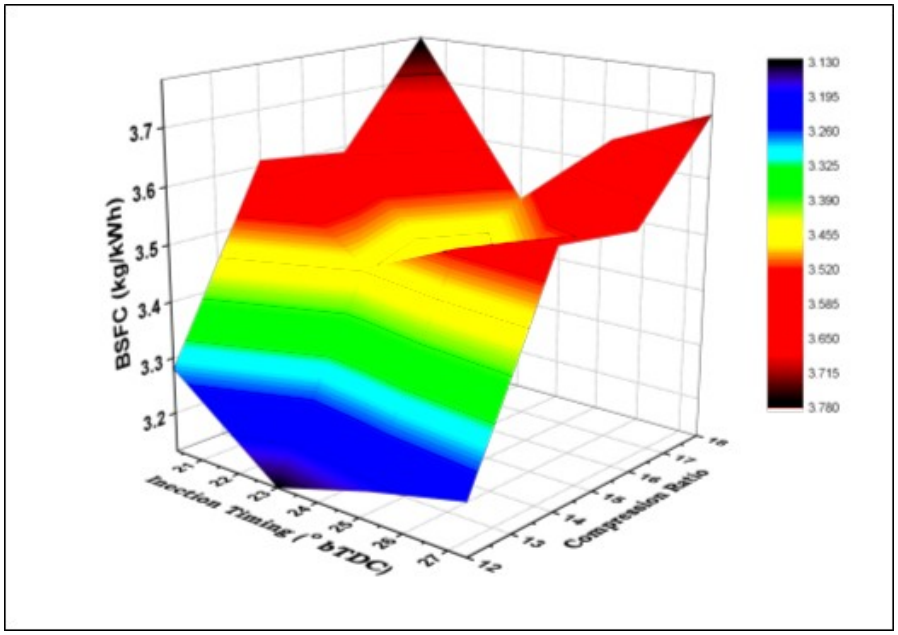

(b)

Figure A3: 3D-surface illustrations of Variation of BSFC with injection timing and CRs for (a) dual-fuel mode (b) diesel mode

BTE Effects

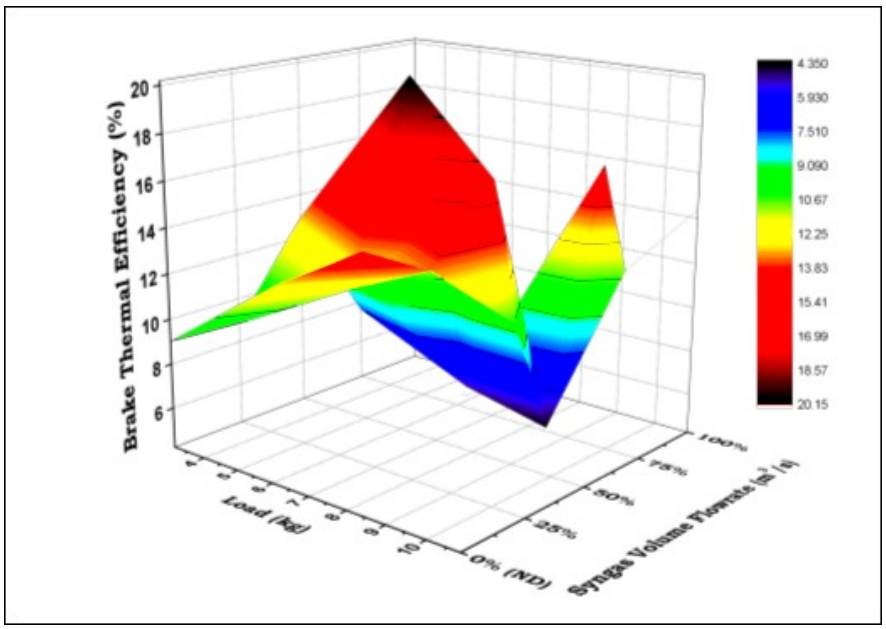

Figure A4: 3D-surface illustration of Variation of load and syngas volume flowrate with BTE (CR 18)

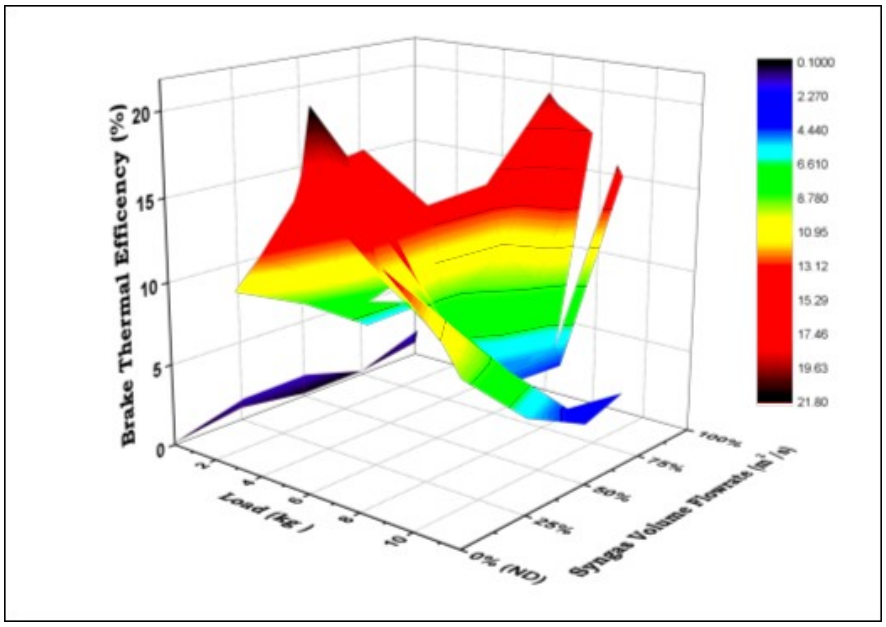

Figure A5: 3D-surface illustration of Variation of BTE with load and syngas volume flowrate (CR 16)

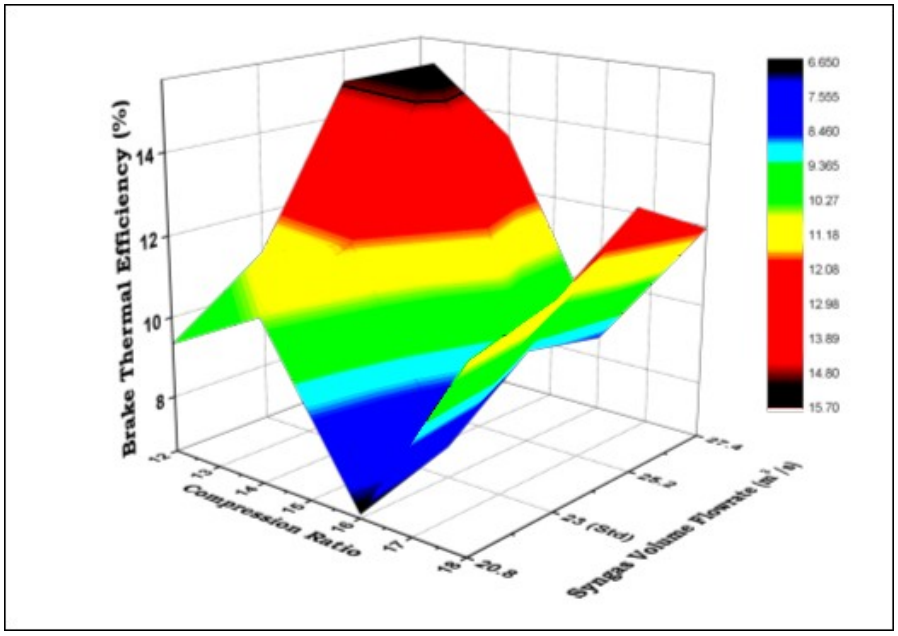

(a)

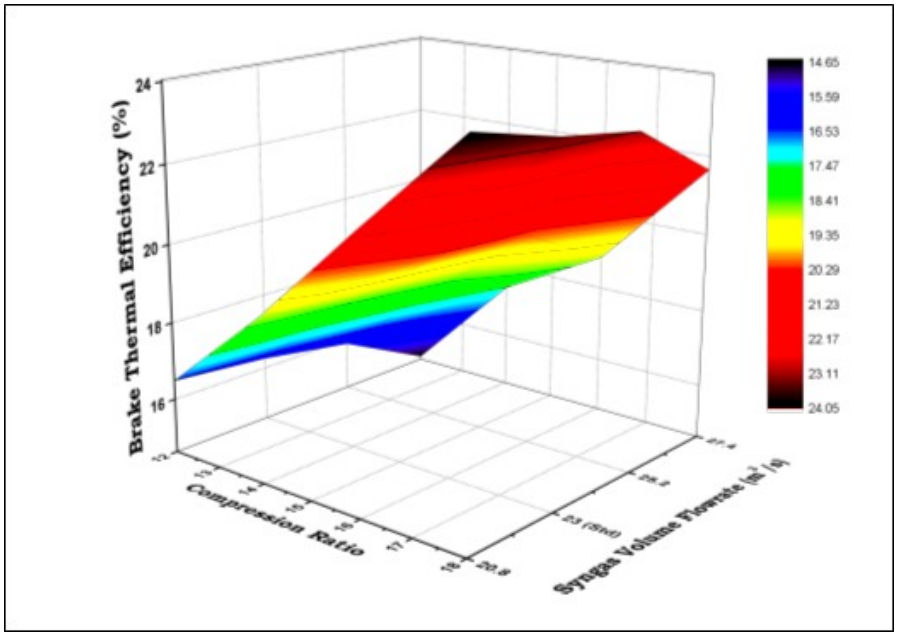

(b)

Figure A6: 3D-surface illustrations of Variation of BTE with injection timing and CR on BTE for (a) dual-fuel mode (b) diesel mode

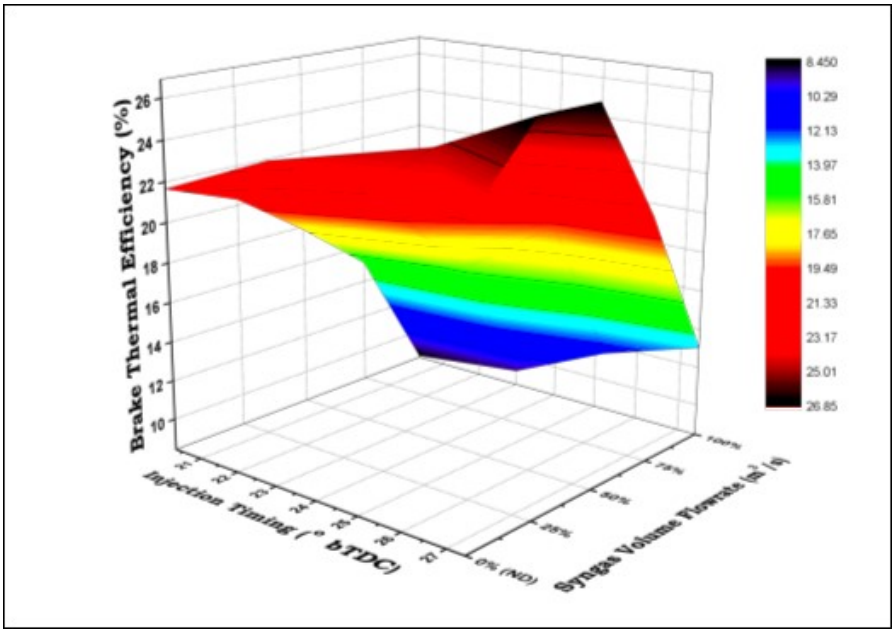

(a)

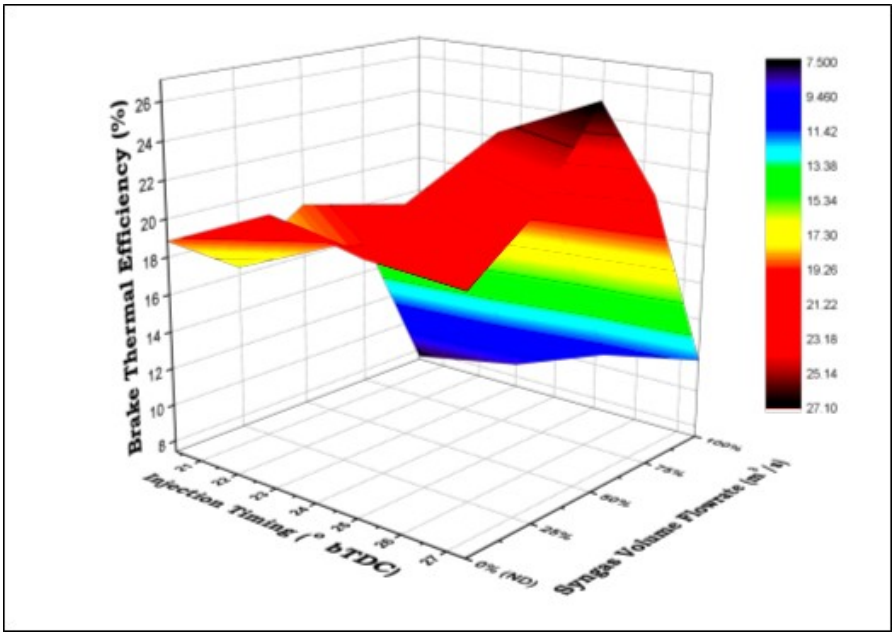

(b)

Figure A7: 3D-surface illustrations of Variation of BTE with injection timing for compression ratios of (a) 18 (b) 16

Equations Used in Engine Performance Analysis

Equations to analyse the engine perfomance are shown in Eqs. A2 to A9

Engine brake power:

$$BP = \frac{T \times 2\pi N}{60} \tag{A2}$$

where BP = brake power, T = torque indication in N.m, and N = revolution per minute.

Specific fuel consumption:

$$SFC = \frac{\dot{m}_f}{\dot{W}} \tag{A3}$$

where SFC = specific fuel consumption, $\dot{m}_f$ = rate of fuel flow into engine and $\dot{W}$ = engine power.

Brake specific fuel consumption:

$$BSFC = \frac{\dot{m}_f}{\dot{W}_b} \tag{A4}$$

where BSFC = brake specific fuel consumption, $\dot{m}_f$ = rate of fuel flow into engine and $\dot{W}_b$ = brake engine power.

Thermal efficiency:

$$\eta_{th} = \frac{\dot{W}}{\dot{m}_f \times CV} \tag{A5}$$

where η_{th} = thermal efficiency, $\dot{W}$ = engine power, $\dot{m}_f$ = rate of fuel flow into engine and CV = calorific value of fuel.

Brake thermal efficiency

$$\eta_{bth} = \frac{\dot{W}_b}{\dot{m}_f \times CV} \tag{A6}$$

where η_{bth} = brake thermal efficiency, $\dot{W}_b$ = brake power, $\dot{m}_f$ = rate of fuel flow into engine and CV = calorific value of fuel.

Brake thermal efficiency of an engine on dual fuel mode:

$$BTE = \frac{\text{Brake Power}}{\text{Power input from pilot diesel + Power input from the gas}} \tag{A7}$$

$$\eta_{bth} = \frac{\dot{\mathrm{W}}_b}{\dot{\mathrm{m}}_{fd} \times \mathrm{CV}_d + \dot{\mathrm{m}}_{fg} \times \mathrm{CV}_g} \tag{A8}$$

where BTE = η_{bth} = brake thermal efficiency, $\dot{\mathrm{W}}_b$ = brake power, $\dot{\mathrm{m}}_{fd}$ = rate of flow of diesel fuel into the engine, $\dot{\mathrm{m}}_{fg}$ = rate of flow of syngas fuel into the engine, CV_d = calorific value of diesel fuel and CV_g = calorific value of syngas fuel.

Diesel Substitution:

$$ds = \frac{\mathrm{D}_d - \mathrm{D}_{dg}}{\mathrm{D}_d} \times 100 \tag{A9}$$

where ds = diesel substitution, per cent, D_d = diesel consumption by the engine on single fuel mode, in kg/h, D_{dg} = diesel consumption by the engine on dual fuel mode, in kg/h.

Friction Power

Friction power (FP) is the heat from a fuel that is lost in friction, cooling and in exhaust in a second. It accounted for the difference between IP and BP as in Eq. A10.

$$\mathrm{FP} = \mathrm{IP} - \mathrm{BP} \tag{A10}$$

Notable, Homdoung *et al.* (Homdoung et al., 2015) have quoted Eqs. A11 to A16 to accurately predict friction losses in ICEs.

(i) Bearing friction,

$$\mathrm{fmep}_1 = 0.05464\left(\frac{\mathrm{B}}{\mathrm{S}}\right)\left(\frac{\mathrm{N}}{1000}\right) \tag{A11}$$

(ii) Piston and rings friction,

$$fmep_2 = 12.85\left(\frac{\mathrm{p}_s}{\mathrm{BS}}\right)\left(\frac{100\mathrm{U}_p}{1000}\right) \tag{A12}$$

where, p_s is piston skirt length.

(iii) Wall tension ring friction,

$$\text{fmep}_3 = 3.77\left(\frac{\text{Sn}_p}{\text{B}^2}\right) \tag{A13}$$

where, n_p is the number of piston rings.

(iv) Valve gear friction,

$$\text{fmep}_4 = 0.226\left(30 - \frac{4\text{N}}{1000}\right)\left(\frac{\text{GD}_{iv}}{\text{B}^2\text{S}}\right) \tag{A14}$$

where, G is the number of intake valves per cylinder and GD_{iv} is intake valve diameter.

(v) Pumping loss,

$$\text{fmep}_5 = 0.0275\left(\frac{\text{N}}{1000}\right)^{1.5} \tag{A15}$$

(vi) The combustion chamber and wall pumping loss,

$$\text{fmep}_6 = 0.0915\sqrt{\left(\frac{\text{imep}}{11.45}\right)}\left(\frac{\text{N}}{1000}\right)^{1.7} \tag{A16}$$

Appendix IV: Components Design Theory

Design consideration for the different components used in operating and modification of the dual fuel CI engine is shown here.

Cyclone Filter

The Cyclone-type filter is the most widely used technique to separate the syngas from the dust and ash entrained in the gas stream (Figure A8). The basic principle behind cyclone separators is to use centrifugal force to make it possible to separate dust particles from a gas stream. A cone section causes the vortex diameter to decrease until the gas reverses on itself and spins up the center to the outlet pipe or vortex finder. The shape of the cone induces the stream to spin, creating a vortex. Larger or denser particles are forced outward to the walls of the cyclone where the drag of the spinning air as well as the force of gravity causes them to fall down the sides of the cone into an outlet (Devi et al., 2017)

Heat Exchanger

There are different types of heat exchangers available in the market. Their applications being dependent on the nature of heating or cooling operations they are used for and volume and type of fluid handled. For this study an air cooled heat exchanger (ACHE) was selected.

Reasons for Using ACHE

Tomar et al. (2013) in their review of literature on HE's designs listed the following advantages of ACHE over the other type:

- location of the cooler- plant is independent of a source of water thereby making installation simpler since water piping and water pumps are eliminated.
- Air coolers are far more suitable in the environment- air used for cooling is simply allowed to mix with ambient air with negligible effect.

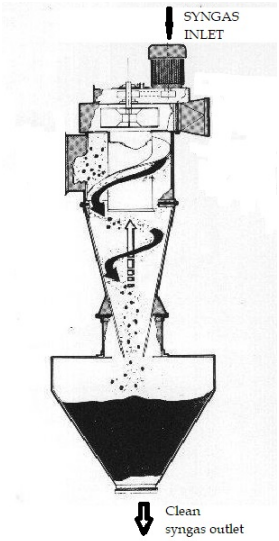

Figure A8: Cyclone filter for cleaning of syngas.

- ACHE cost and their maintenance costs are considerably lower as scaling, bio-fouling and sedimentation are eliminated.
- Their installation is simpler since water piping and water pumps are eliminated.

The following factors were considered when selecting a finned-type ACHE:

- Design temperature
- Corrosive properties of the air
- Temperature cycling frequency
- Cleaning method and frequency
- Type of fouling debris in the air
- Isolation of cooler
- Syngas outlet temperature required should be equal or slightly greater than the surrounding ambient air temperature.

Thermal properties of Gases

Standard tables of thermal properties of gases used in the design of the air cooled heat exchanger (ACHE) are shown in Figure A9(a, b, and c).

Operation of Mixing Unit

In operation, a syngas under pressure enters through the inlet pipe while air is supplied through an air inlet tube. The air enters the chamber channel in a swirling pattern. A slight reduction in pressure due to the expansion of the syngas-air within channel coupled with the high velocity swirling flow pattern produces a cooling effect which reduces the flow of heat out of the chamber

HEAT TRANSFER

Film coefficients for air and water (289 K and 101.3 kN/m^2)

Inside diameter of tube		Velocity		Mass velocity		Film coefficient of heat transfer h	
(mm)	(in)	(m/s)	(ft/s)	(kg/m^2 s)	(lb/ft^2 h)	(W/m^2 K) [Ref.18]	(Btu/h ft^2 °F) [Ref.18]
Air							
25	1.0	5	16.4	6.11	4530	31.2	5.5
		10	32.8	12.2	9050	50.0	8.8
		20	65.6	24.5	18,100	84.0	14.8
		40	131	48.9	36,200	146	25.7
		60	197	73.4	54,300	211	37.2
50	2.0	5	16.4	6.11	4530	23.8	4.2
		10	32.8	12.2	9050	44.9	7.9
		20	65.6	24.5	18,100	77.8	13.7
		40	131	48.9	36,200	127	22.4
		60	197	73.4	54,300	181	31.9
75	3.0	5	16.4	6.11	4530	21.6	3.8
		10	32.8	12.2	9050	39.7	7.0
		20	65.6	24.5	18,100	71.0	12.5
		40	131	48.9	36,200	119	21.0
		60	197	73.4	54,300	169	29.8
Water							
25	1.0	0.5	1.64	488	361,000	2160	380
		1.0	3.28	975	722,000	3750	660
		1.5	4.92	1460	1,080,000	5250	925
		2.0	6.55	1950	1,440,000	6520	1150
		2.5	8.18	2440	1,810,000	7780	1370
50	2.0	0.5	1.64	488	361,000	1870	330
		1.0	3.28	975	722,000	3270	575
		1.5	4.92	1460	1,080,000	4540	800
		2.0	6.55	1950	1,440,000	5590	985
		2.5	8.18	2440	1,810,000	6700	1180
75	3.0	0.5	1.64	488	361,000	1760	310
		1.0	3.28	975	722,000	3070	540
		1.5	4.92	1460	1,080,000	4200	740
		2.0	6.55	1950	1,440,000	5220	920
		2.5	8.18	2440	1,810,000	6220	1100

(a)

Properties of gases at 1 atm pressure

Temp. T, °C	Density ρ, kg/m^3	Specific Heat c_p, J/kg·K	Thermal Conductivity k, W/m·K	Thermal Diffusivity α, m^2/s	Dynamic Viscosity μ, kg/m·s	Kinematic Viscosity ν, m^2/s	Prandtl Number Pr
Carbon Dioxide, CO_2							
50	2.4035	746	0.01051	5.860 10^{-6}	1.129 10^{-5}	4.699 10^{-6}	0.8019
0	1.9635	811	0.01456	9.141 10^{-6}	1.375 10^{-5}	7.003 10^{-6}	0.7661
50	1.6597	866.6	0.01858	1.291 10^{-5}	1.612 10^{-5}	9.714 10^{-6}	0.7520
100	1.4373	914.8	0.02257	1.716 10^{-5}	1.841 10^{-5}	1.281 10^{-5}	0.7464
150	1.2675	957.4	0.02652	2.186 10^{-5}	2.063 10^{-5}	1.627 10^{-5}	0.7445
200	1.1336	995.2	0.03044	2.698 10^{-5}	2.276 10^{-5}	2.008 10^{-5}	0.7442
300	0.9358	1060	0.03814	3.847 10^{-5}	2.682 10^{-5}	2.866 10^{-5}	0.7450
400	0.7968	1112	0.04565	5.151 10^{-5}	3.061 10^{-5}	3.842 10^{-5}	0.7458
500	0.6937	1156	0.05293	6.600 10^{-5}	3.416 10^{-5}	4.924 10^{-5}	0.7460
1000	0.4213	1292	0.08491	1.560 10^{-4}	4.898 10^{-5}	1.162 10^{-4}	0.7455
1500	0.3025	1356	0.10688	2.606 10^{-4}	6.106 10^{-5}	2.019 10^{-4}	0.7745
2000	0.2359	1387	0.11522	3.521 10^{-4}	7.322 10^{-5}	3.103 10^{-4}	0.8815
Carbon Monoxide, CO							
50	1.5297	1081	0.01901	1.149 10^{-5}	1.378 10^{-5}	9.012 10^{-6}	0.7840
0	1.2497	1048	0.02278	1.739 10^{-5}	1.629 10^{-5}	1.303 10^{-5}	0.7499
50	1.0563	1039	0.02641	2.407 10^{-5}	1.863 10^{-5}	1.764 10^{-5}	0.7328
100	0.9148	1041	0.02992	3.142 10^{-5}	2.080 10^{-5}	2.274 10^{-5}	0.7239
150	0.8067	1049	0.03330	3.936 10^{-5}	2.283 10^{-5}	2.830 10^{-5}	0.7191
200	0.7214	1060	0.03656	4.782 10^{-5}	2.472 10^{-5}	3.426 10^{-5}	0.7164
300	0.5956	1085	0.04277	6.619 10^{-5}	2.812 10^{-5}	4.722 10^{-5}	0.7134
400	0.5071	1111	0.04860	8.628 10^{-5}	3.111 10^{-5}	6.136 10^{-5}	0.7111
500	0.4415	1135	0.05412	1.079 10^{-4}	3.379 10^{-5}	7.653 10^{-5}	0.7087
1000	0.2681	1226	0.07894	2.401 10^{-4}	4.557 10^{-5}	1.700 10^{-4}	0.7080
1500	0.1925	1279	0.10458	4.246 10^{-4}	6.321 10^{-5}	3.284 10^{-4}	0.7733
2000	0.1502	1309	0.13833	7.034 10^{-4}	9.826 10^{-5}	6.543 10^{-4}	0.9302
Methane, CH_4							
50	0.8761	2243	0.02367	1.204 10^{-5}	8.564 10^{-6}	9.774 10^{-6}	0.8116
0	0.7158	2217	0.03042	1.917 10^{-5}	1.028 10^{-5}	1.436 10^{-5}	0.7494
50	0.6050	2302	0.03766	2.704 10^{-5}	1.191 10^{-5}	1.969 10^{-5}	0.7282
100	0.5240	2443	0.04534	3.543 10^{-5}	1.345 10^{-5}	2.567 10^{-5}	0.7247
150	0.4620	2611	0.05344	4.431 10^{-5}	1.491 10^{-5}	3.227 10^{-5}	0.7284
200	0.4132	2791	0.06194	5.370 10^{-5}	1.630 10^{-5}	3.944 10^{-5}	0.7344
300	0.3411	3158	0.07996	7.422 10^{-5}	1.886 10^{-5}	5.529 10^{-5}	0.7450
400	0.2904	3510	0.09918	9.727 10^{-5}	2.119 10^{-5}	7.297 10^{-5}	0.7501
500	0.2529	3836	0.11933	1.230 10^{-4}	2.334 10^{-5}	9.228 10^{-5}	0.7502
1000	0.1536	5042	0.22562	2.914 10^{-4}	3.281 10^{-5}	2.136 10^{-4}	0.7331
1500	0.1103	5701	0.31857	5.068 10^{-4}	4.434 10^{-5}	4.022 10^{-4}	0.7936
2000	0.0860	6001	0.36750	7.120 10^{-4}	6.360 10^{-5}	7.395 10^{-4}	1.0386
Hydrogen, H_2							
50	0.11010	12635	0.1404	1.009 10^{-4}	7.293 10^{-6}	6.624 10^{-5}	0.6562
0	0.08995	13920	0.1652	1.319 10^{-4}	8.391 10^{-6}	9.329 10^{-5}	0.7071
50	0.07603	14349	0.1881	1.724 10^{-4}	9.427 10^{-6}	1.240 10^{-4}	0.7191
100	0.06584	14473	0.2095	2.199 10^{-4}	1.041 10^{-5}	1.582 10^{-4}	0.7196
150	0.05806	14492	0.2296	2.729 10^{-4}	1.136 10^{-5}	1.957 10^{-4}	0.7174
200	0.05193	14482	0.2486	3.306 10^{-4}	1.228 10^{-5}	2.365 10^{-4}	0.7155

(b)

Properties of gases at 1 atm pressure *(Concluded)*

Temp.	Density	Specific Heat	Thermal Conductivity	Thermal Diffusivity	Dynamic Viscosity	Kinematic Viscosity	Prandtl Number
T, °C	ρ, kg/m^3	c_p, J/kg·K	k, W/m·K	α, m^2/s	μ, kg/m·s	ν, m^2/s	Pr
300	0.04287	14481	0.2843	4.580×10^{-4}	1.403×10^{-5}	3.274×10^{-4}	0.7149
400	0.03650	14540	0.3180	5.992×10^{-4}	1.570×10^{-5}	4.302×10^{-4}	0.7179
500	0.03178	14653	0.3509	7.535×10^{-4}	1.730×10^{-5}	5.443×10^{-4}	0.7224
1000	0.01930	15577	0.5206	1.732×10^{-3}	2.455×10^{-5}	1.272×10^{-3}	0.7345
1500	0.01386	16553	0.6581	2.869×10^{-3}	3.099×10^{-5}	2.237×10^{-3}	0.7795
2000	0.01081	17400	0.5480	2.914×10^{-3}	3.690×10^{-5}	3.414×10^{-3}	1.1717
Nitrogen, N_2							
50	1.5299	957.3	0.02001	1.366×10^{-5}	1.390×10^{-5}	9.091×10^{-6}	0.6655
0	1.2498	1035	0.02384	1.843×10^{-5}	1.640×10^{-5}	1.312×10^{-5}	0.7121
50	1.0564	1042	0.02746	2.494×10^{-5}	1.874×10^{-5}	1.774×10^{-5}	0.7114
100	0.9149	1041	0.03090	3.244×10^{-5}	2.094×10^{-5}	2.289×10^{-5}	0.7056
150	0.8068	1043	0.03416	4.058×10^{-5}	2.300×10^{-5}	2.851×10^{-5}	0.7025
200	0.7215	1050	0.03727	4.921×10^{-5}	2.494×10^{-5}	3.457×10^{-5}	0.7025
300	0.5956	1070	0.04309	6.758×10^{-5}	2.849×10^{-5}	4.783×10^{-5}	0.7078
400	0.5072	1095	0.04848	8.727×10^{-5}	3.166×10^{-5}	6.242×10^{-5}	0.7153
500	0.4416	1120	0.05358	1.083×10^{-4}	3.451×10^{-5}	7.816×10^{-5}	0.7215
1000	0.2681	1213	0.07938	2.440×10^{-4}	4.594×10^{-5}	1.713×10^{-4}	0.7022
1500	0.1925	1266	0.11793	4.839×10^{-4}	5.562×10^{-5}	2.889×10^{-4}	0.5969
2000	0.1502	1297	0.18590	9.543×10^{-4}	6.426×10^{-5}	4.278×10^{-4}	0.4483
Oxygen, O_2							
50	1.7475	984.4	0.02067	1.201×10^{-5}	1.616×10^{-5}	9.246×10^{-6}	0.7694
0	1.4277	928.7	0.02472	1.865×10^{-5}	1.916×10^{-5}	1.342×10^{-5}	0.7198
50	1.2068	921.7	0.02867	2.577×10^{-5}	2.194×10^{-5}	1.818×10^{-5}	0.7053
100	1.0451	931.8	0.03254	3.342×10^{-5}	2.451×10^{-5}	2.346×10^{-5}	0.7019
150	0.9216	947.6	0.03637	4.164×10^{-5}	2.694×10^{-5}	2.923×10^{-5}	0.7019
200	0.8242	964.7	0.04014	5.048×10^{-5}	2.923×10^{-5}	3.546×10^{-5}	0.7025
300	0.6804	997.1	0.04751	7.003×10^{-5}	3.350×10^{-5}	4.923×10^{-5}	0.7030
400	0.5793	1025	0.05463	9.204×10^{-5}	3.744×10^{-5}	6.463×10^{-5}	0.7023
500	0.5044	1048	0.06148	1.163×10^{-4}	4.114×10^{-5}	8.156×10^{-5}	0.7010
1000	0.3063	1121	0.09198	2.678×10^{-4}	5.732×10^{-5}	1.871×10^{-4}	0.6986
1500	0.2199	1165	0.11901	4.643×10^{-4}	7.133×10^{-5}	3.243×10^{-4}	0.6985
2000	0.1716	1201	0.14705	7.139×10^{-4}	8.417×10^{-5}	4.907×10^{-4}	0.6873
Water Vapor, H_2O							
50	0.9839	1892	0.01353	7.271×10^{-6}	7.187×10^{-6}	7.305×10^{-6}	1.0047
0	0.8038	1874	0.01673	1.110×10^{-5}	8.956×10^{-6}	1.114×10^{-5}	1.0033
50	0.6794	1874	0.02032	1.596×10^{-5}	1.078×10^{-5}	1.587×10^{-5}	0.9944
100	0.5884	1887	0.02429	2.187×10^{-5}	1.265×10^{-5}	2.150×10^{-5}	0.9830
150	0.5189	1908	0.02861	2.890×10^{-5}	1.456×10^{-5}	2.806×10^{-5}	0.9712
200	0.4640	1935	0.03326	3.705×10^{-5}	1.650×10^{-5}	3.556×10^{-5}	0.9599
300	0.3831	1997	0.04345	5.680×10^{-5}	2.045×10^{-5}	5.340×10^{-5}	0.9401
400	0.3262	2066	0.05467	8.114×10^{-5}	2.446×10^{-5}	7.498×10^{-5}	0.9240
500	0.2840	2137	0.06677	1.100×10^{-4}	2.847×10^{-5}	1.002×10^{-4}	0.9108
1000	0.1725	2471	0.13623	3.196×10^{-4}	4.762×10^{-5}	2.761×10^{-4}	0.8639
1500	0.1238	2736	0.21301	6.288×10^{-4}	6.411×10^{-5}	5.177×10^{-4}	0.8233
2000	0.0966	2928	0.29183	1.032×10^{-3}	7.808×10^{-5}	8.084×10^{-4}	0.7833

Note: For ideal gases, the properties c_p, k, μ, and Pr are independent of pressure. The properties ρ, ν, and α at a pressure P (in atm) other than 1 atm are determined by multiplying the values of ρ at the given temperature by ρ and by dividing ν and α by P.

(c)

Figure A9: Thermal properties of syngas constituent gases. (Barbee et al., 2007)